

Washington University in St. Louis

Washington University Open Scholarship

All Theses and Dissertations (ETDs)

January 2009

Runx1 in Primitive Hematopoiesis and Characterization of Hematopoietic Stem Cells in a Mouse Chronic Inflammatory Arthritis Model

Yunglin Ma

Washington University in St. Louis

Follow this and additional works at: <https://openscholarship.wustl.edu/etd>

Recommended Citation

Ma, Yunglin, "Runx1 in Primitive Hematopoiesis and Characterization of Hematopoietic Stem Cells in a Mouse Chronic Inflammatory Arthritis Model" (2009). *All Theses and Dissertations (ETDs)*. 415.
<https://openscholarship.wustl.edu/etd/415>

This Dissertation is brought to you for free and open access by Washington University Open Scholarship. It has been accepted for inclusion in All Theses and Dissertations (ETDs) by an authorized administrator of Washington University Open Scholarship. For more information, please contact digital@wumail.wustl.edu.

WASHINGTON UNIVERSITY

Division of Biology and Biomedical Sciences

Program in Developmental Biology

Dissertation Examination Committee

Kyunghee Choi, Chair

David C. Beebe

Timothy A. Graubert

Daniel C. Link

Fanxin Long

Robert P. Mecham

Runx1 in Primitive Hematopoiesis and Characterization of Hematopoietic Stem
Cells in a Mouse Chronic Inflammatory Arthritis Model

by

Yunglin David Ma

A dissertation presented to the
Graduate School of Arts and Sciences
of Washington University in
partial fulfillment of the
requirements for the degree
of Doctor of Philosophy

August 2009

Saint Louis, Missouri

Acknowledgement

First of all, I would like to express my gratitude towards my mentor Dr. Kyunghye Choi (KC). This thesis would not have been accomplished without her supports, guidance, and encouragements throughout the course of my graduate studies. I am deeply inspired by her critical scientific thinking, enthusiasm about scientific research and positive attitude towards difficult tasks. KC encourages me to think creatively, and push myself to achieve more difficult goals. In short, she has made me a better scientist.

I would also like to thank the members of my thesis committees; Dr. David Beebe, Dr. Timothy Graubert, Dr. Daniel Link, Dr. Fanxin Long, and Dr. Robert Meham for their technical inputs in terms of suggestions, discussions, encouragements and collaborations. I am especially grateful to Dr. Robert Meham for serving as my thesis committee chair and all his helpful discussion, advice, meetings and supports.

In addition, I would like to thank all the current and previous lab members from Dr. Choi's group: Changwon Park, Qing Tan, Elizabeth Arentson, Kwadwo Oduro, Jesse Lugus, Fang Liu, Inyoung Kang, Junjie Yang, Wen-Jie Zhang, and Yun-Shin Chung for their suggestions, encouragement, and support. I especially want to thank Changwon Park for his frequent technical advice, suggestions, and encouragements throughout my graduate training. I have also received invaluable assistance from Qing and Elizabeth on many technical problems. Their expertise and help made my project possible and my life easier. Furthermore, collaborating with Kwadwo Oduro is also a pleasant experience. I

am honor to have the opportunities to work with and learn from these outstanding scientists in the Dr. Choi's lab.

Outside of Dr. Choi's lab, I would like to thank my friends and fellow graduate students; Shuo Luo, Haoyi Wang, Ta-Chih Hsiao, William Tu, Yen-Ching Yu, Gary Lee, and David Huang, for their support, advice, assistance, and friendship.

I would also like to acknowledge NIH Developmental Cardiology and Pulmonary Training Program and Kauffman Fellowship Pathway in Life Sciences Entrepreneurship for their financial support on my thesis research. Certainly, KC, Dr. Robert Mecham and Mr. Ken Harrington have helped me tremendously in applying for these financial supports.

I give my deepest appreciation to my parents, Joen-Shen Ma and Li-Wei Hsiou. Without their supports and unconditional love, I would never have made it through this journey. I am also very thankful for my brother, Yungcheng Ma. He has become my best friend who keep encouraging and supporting me and he help me think positively.

At last, I really appreciate the support from my wife, Hsinyu Michelle Lin. She is a wonderful companion who always stays by my side in any conditions. She brings all the joy to my life. I would never have made it trough this journey without her.

This dissertation is dedicated and in memory of my beloved grandmother, Yu-Hua Fan.

Table of Contents

Acknowledgments	ii
Table of Content	iv
List of Tables	vii
List of Figures	viii
Abstract of the Dissertation	xi
Curriculum Vitae	xiii
Chapter 1. <i>Runx1</i> in Primitive Hematopoiesis	1
1.1. Introduction	
Hematopoietic Development during Mouse Embryogenesis	3
<i>In vitro</i> Embryonic Stem Cell Differentiation Systems	8
TGF β Signaling in Embryonic Hematopoiesis	10
<i>Runx1</i> in Hematopoietic Development	13
Overall Goals of Chapter One	17
References	18
Figures.....	26
1.2. Results	
Primitive Erythropoiesis is Sensitive to RUNX1 Level.....	31
Abstract	32
Introduction	33
Materials and Methods	37
Results	44

Discussion	55
Acknowledgement	61
References	62
Figures	68

1.3. Conclusion and Future Directions

Summary of Chapter One.....	95
Possible Mechanisms for Runx1-Mediated Suppression of EryP Development	96
The Relationship between TGF β 1 and Runx1 in Primitive Hematopoiesis	99
References	101

Chapter 2. Characterization of Hematopoietic Stem Cells in a Mouse

Chronic Inflammatory Arthritis model	102
---	------------

2.1. Introduction

Hematopoietic Stem Cell Niche	104
The K/BxN Mouse Model of Inflammatory Arthritis	107
Overall Goals of Chapter Two	111
References	112

2.2. Results

Defects in osteoblast function but no changes in long term repopulating potential of hematopoietic stem cells in a mouse chronic inflammatory arthritis model	117
---	-----

Abstract	118
Introduction	119
Materials and Methods	121
Results	129
Discussion	139
Acknowledgement	144
References	145
Figures	148

2.3. Conclusion and Future Directions

Summary of Chapter Two	181
Hematopoietic Stem Cell Niche in KRNxG7 Mouse	182
References	187

List of Tables

Chapter 1

Table 1.2-1. Viability of progeny from intercrosses of *Runx1^{m/+}* mice 79

Table 1.2-2. Common erythroid genes were downregulated in *Runx1^{-/-}* and
iRUNX1+Dox EBs 80

Supplementary Table 1.2-1. Primer sequences for qRT-PCR 93

Chapter 2

Supplementary Table 2.2-1. Primer sequences used for qRT-PCR 179

List of Figures

Chapter 1

Figure 1.1-1. <i>In vitro</i> embryonic stem cell differentiation systems	26
Figure 1.1-2. A schematic diagram of TGF β superfamily ligands, their type I and type II receptors, and downstream SMAD molecules.....	28
Figure 1.2-1. Enforced RUNX1 expression during ES cell differentiation results in reduced EryP progenitors.....	68
Figure 1.2-2. <i>Runx1</i> null and <i>Runx1</i> mutations resulted in decreased number of EryP progenitors in yolk sac.....	70
Figure 1.2-3. <i>Gata1</i> and <i>Eklf</i> rescue decreased EryP progenitor formation in <i>Runx1</i> ^{-/-} and iRUNX1 EBs.....	72
Figure 1.2-4. TGF β 1 inhibits EryP progenitor formation and induces <i>Runx1</i> expression	74
Figure 1.2-5. <i>Alk5</i> deficiency generates increased EryP progenitors	77
Supplementary Figures 1.2-1. <i>Runx1</i> ^{-/-} EBs have reduced blast colonies and comparable FLK1 ⁺ differentiation kinetics compared to wild type EBs by FACS analysis.....	81
Supplementary Figures 1.2-2. <i>Runx1</i> ^{-/-} EB cells have no definitive hematopoietic colonies.....	83
Supplementary Figures 1.2-3. E10.5 <i>Runx1</i> ^{-/-} embryos have no gross abnormalities in blood cell generation.....	85
Supplementary Figures 1.2-4. Noggin, DAPT, and cyclopamine do not affect EryP progenitor formation and <i>Runx1</i> expression	87

Supplementary Figures 1.2-5. SB431542 treated EB cells generate increased EryP colonies.....	89
Supplementary Figures 1.2-6. <i>Gata1</i> and <i>Ekif</i> expressions were decreased in TGFβ1 treated EBs but increased in <i>Alk5</i> ^{-/-} EBs.....	91
Chapter 2	
Figure 2.2-1. Severe joint destruction and osteoporosis in KRN/G7 mice	148
Figure 2.2-2. Impaired bone formation rate in KRN/G7 mice.....	151
Figure 2.2-3. Characterization of mature cells and B cell development defect in KRNxG7 mice	153
Figure 2.2-4. Hematopoietic stem cells are not impaired in KRNxG7 mice	156
Figure 2.2-5. Characterization of HSCs and progenitors in KRNxG7 spleen ..	159
Supplementary Figures 2.2-1. <i>In vitro</i> osteoblasts differentiation from KRNxG7 bone marrow stromal cells is normal.....	161
Supplementary Figures 2.2-2. Marrow cellularity and KSL frequency are independent of harvesting method.....	163
Supplementary Figures 2.2-3. Depleted Lymphoid cells in KRNxG7 bone marrow.....	165
Supplementary Figures 2.2-4. BrdU analysis of progenitor populations.....	167
Supplementary Figures 2.2-5. Schema for Ki67/Hoechst analysis.....	169
Supplementary Figures 2.2-6. Expression of cell cycle Regulators in BM derived KSL cells.....	171
Supplementary Figures 2.2-7. Analyses for donor cell derived hematopoietic cell lineages in primary, secondary and tertiary recipients.....	173

Supplementary Figures 2.2-8. HSCs from 4 month old KRNxG7 mice are not compromised	175
Supplementary Figures 2.2-9. Splenomegaly in KRNxG7 mice	177

ABSTRACT OF THE DISSERTATION

Runx1 in Primitive Hematopoiesis and Characterization of Hematopoietic Stem Cells in a Mouse Chronic Inflammatory Arthritis Model

by

Yunglin David Ma

Doctor of Philosophy in Biology and Biomedical Sciences

Program in Developmental Biology

Washington University in St. Louis, 2009

Professor Kyunghee Choi, Chairperson

Hematopoietic cells are essential for growth and survival throughout adult life.

Two different aspects of hematopoiesis are addressed in this dissertation.

I. The regulation of primitive hematopoiesis by *Runx1* and TGF β signaling.

Primitive hematopoiesis, occurring exclusively in the yolk sac, is characterized by its transient nature. As the primitive hematopoiesis declines in the yolk sac, definitive hematopoietic progenitors generated in the yolk sac and/or embryo take over in blood cell production. Whether the transition from primitive to definitive hematopoietic program reflects a mere shift in hematopoietic sites or whether it is an actively regulated process is currently unknown. *Runx1* is necessary for the establishment of definitive hematopoiesis. Most studies on *Runx1* have focused on its role in generating hematopoietic stem cells. Intriguingly, *Runx1* expression can be detected in the yolk sac blood-islands where primitive erythroid (EryP) progenitors emerge. The function of *Runx1* in primitive hematopoiesis has not been carefully investigated. Herein, we determined if *Runx1* plays a role in primitive hematopoiesis

by utilizing *in vitro* embryonic stem (ES) cell differentiation system and by examining EryP development in *Runx1* mutant mice. We demonstrated that *Runx1* deficient mice contained a significantly reduced number of EryP progenitors compared to controls. Nonetheless, *Runx1* deficient mice survived until they required definitive hematopoietic cells. We demonstrated that a high level of enforced *Runx1* expression in the *in vitro* differentiation model of embryonic stem (ES) cells suppressed EryP progenitor generation. We also identified TGF β 1 as a cooperative signal of *Runx1* in negatively regulating EryP development. Our studies revealed an unexpected role of *Runx1* in both initiation and termination of primitive hematopoiesis.

II. The relationship between hematopoietic stem cells and bone marrow microenvironment.

There is an intricate relationship between hematopoiesis and bone homeostasis in normal physiological states during adulthood. By utilizing mice undergoing chronic inflammatory arthritis, we investigated the relationship between hematopoiesis and bone homeostasis in pathological conditions. We demonstrated that mice with chronic inflammatory arthritis are osteoporotic due to a severe defect in osteoblast function. Despite the defective osteoblast function, the hematopoietic stem cells from these mice exhibited normal properties in HSC frequency, cell cycling and long-term repopulating ability. Therefore, the bone forming capacity of osteoblasts is disassociated from their ability to maintain HSCs in a chronic inflammatory condition. These observations suggest other cell types, such as endothelial cells in the bone marrow, might serve as HSC niches under pathological conditions.

Curriculum Vitae

Yunqin David Ma

Washington University School of Medicine
Department of Pathology and Immunology
Campus Box 8118
660 South Euclid Ave
St. Louis, MO 63110
Phone: (314) 362-9045
Fax: (314) 362-8888
Email: yunqinma@wustl.edu

Place of Birth Taipei, Taiwan

EDUCATION

2003-present Developmental Biology Program, Department of Pathology and Immunology, Washington University School of Medicine, St. Louis, MO (Ph.D. candidate)
1999-2003 B.S. (Honors) Biochemistry and Molecular Biology, Purdue University, West Lafayette, IN

RESEARCH EXPERIENCE

2003-present Graduate Student, Laboratory of Dr. Kyunghye Choi, Developmental Biology Program, Department of Pathology and Immunology, Washington University School of Medicine, St. Louis, MO.
2000-2003 Undergraduate Research, Laboratory of Dr. Miriam S. Hasson, Structural Biology and Biochemistry, Purdue University, West Lafayette, IN.
2001 Summer Research Intern, Laboratory of Dr. Chien-Jen Chen, Graduate Institute of Epidemiology, National Taiwan University, Taiwan.

HONORS AND AWARDS

2005-2008 NIH Developmental Cardiology and Pulmonary Training Program (Grant Number: 5 T32 HL07873-08), Washington University, St. Louis, MO
2007 Kauffman Fellowship Pathway in Life Sciences Entrepreneurship, Washington University, St. Louis, MO
2001 Outstanding Achievement Award in Science, Purdue University, West Lafayette, IN

OTHER EXPERIENCES

- 2005-2008 Vice President and Treasurer, BioEntrepreneurship Core (BEC), Washington University, St. Louis, MO
- 2005 Teaching Assistant, Bio280: DNA science, course masters: Dr. Sarah Elgin and Dr. Mark Johnston, Washington University, St. Louis, MO
- 2003-2004 President, Taiwanese Graduate Student Association, Washington University, St. Louis, MO
- 1999-2001 President, Taiwan Student Association, Purdue University, West Lafayette, IN

PEER-REVIEWED PUBLICATIONS

Ma YD*, Park C*, Zhao H, Oduro KA, Tu X, Long F, Allen PM, Teitelbaum SL and Choi K. Defects in osteoblast function but no changes in long term repopulating potential of hematopoietic stem cells in a mouse chronic inflammatory arthritis model. **Blood**. (2009)

Lugus JJ, Park C, **Ma YD** and Choi K. Both primitive and definitive blood cells are derived from FLK1+ mesoderm. **Blood**. Oct 28. (2008)

Cheng YJ, Chien YC, Hildesheim A, Hsu MM, Chen IH, Chuang J, Chang J, **Ma YD**, Luo CT, Hsu WL, Hsu HH, Huang H, Chang JF, Chen CJ, Yang CS. No association between genetic polymorphisms of CYP1A1, GSTM1, GSTT1, GSTP1, NAT2, and nasopharyngeal carcinoma in Taiwan. **Cancer Epidemiol Biomarkers Prev**. Feb; 12(2):179-80 (2003).

SUBMITTED

Diao J, **Ma YD**, and Hasson MS. Open and Closed Conformations Reveal Induced Fit Movements in Butyrate kinase 2 Activation.

Ma YD, Arentson E, Dang J, Lenny N, Chang LW, Kim SI, Kyba M, Bresnick EH, Downing JR and Choi K. Cooperative Regulation of Primitive Erythropoiesis by *Runx1* and TGF β signaling.

INVITED BOOK CHAPTERS AND REVIEWS

Ma YD, Lugus JJ, Park C and Choi K. Differentiation of Embryonic Stem Cells into Blood. **Curr Prot Stem Cell Biol**. July; Chapter 1:Unit1F.4. (2008)

Park C, **Ma YD**, Choi K. Evidence for the hemangioblast. **Exp Hematol**. Sep; 33(9):965-70 (2005)

MEETING PRESENTATIONS

“The roles of *Runx1* and TGF β signaling in primitive hematopoiesis”
Developmental Biology Retreat. New Haven, MO. May 2009. Oral Presentation

“Hematopoietic Stem Cells and Bone Marrow Niche in Mouse Chronic
Inflammatory Arthritis Model” Developmental Biology Research Forum.
Washington University, MO. February 2009. Oral Presentation

Ma YD, Arentson E, Choi K. TGF β Signaling and *Runx1* in Primitive
Hematopoiesis. Immunology Program Retreat. Potosi, MO. September 2007.
Poster Presentation

Ma YD, Arentson E, Choi K. *Runx1* and TGF β Signaling in Yolk Sac
Hematopoiesis. Immunology Program Retreat. Potosi, MO. September 2006.
Poster Presentation

“TGF β 1 signaling in hematopoietic development” Developmental Biology
Research Forum. Washington University, MO. March 2006. Oral Presentation

Chapter 1

Runx1 in Primitive Hematopoiesis

Chapter 1.1

Introduction

Hematopoietic Development during Mouse Embryogenesis

The production of blood cells takes place in several distinct anatomical sites during mouse embryogenesis. The first blood cells to appear, known as primitive erythrocytes, are initially detectable in the extraembryonic yolk sac blood islands at embryonic day E7.5 of gestation and become extinct by E9.0. (Ferkowicz and Yoder, 2005). Meanwhile, the liver rudiment is colonized by hematopoietic stem cells by E10.5 and becomes the principal hematopoietic organ during fetal development (Houssaint, 1981). Beginning at birth, bone marrow (BM) is colonized by hematopoietic stem cells (HSCs) originating from the fetal liver. Thereafter, and continuing throughout adult life, all mature blood cells are produced in the bone marrow. The term primitive hematopoiesis is applied to the development of the initial yolk sac-derived erythroid cells, while definitive hematopoiesis refers to all blood cell lineages other than the primitive erythroid cells (Keller et al., 1999).

The blood islands are composed of both primitive erythroid cells (EryP) and endothelial cells, which constitute a small fraction of the whole yolk sac vascular system. The close developmental association of the hematopoietic and endothelial cell lineages within the yolk sac blood islands of the developing embryo has led to the hypothesis that they arise from a common precursor, termed the hemangioblast (Park et al., 2005; Sabin, 1920). Cell tracking studies indicate that hemangioblast development begins in the primitive streak, after which they migrate into the yolk sac blood islands (Huber et al., 2004). EryP cells are generated from a transient wave of progenitors, termed primitive erythroid

colony-forming cells (EryP-CFC), found exclusively in the yolk sac between E7.25 and E9.0 (Palis et al., 1999). Primitive erythrocytes (EryP) are larger than definitive erythrocytes (EryD). They are initially circulating as nucleated cells, and mainly express two embryonic forms of β -globin proteins ($\epsilon\gamma$ and βH1), as well as both embryonic and adult forms of α -globin proteins (ζ and α , respectively) (Kingsley et al., 2006). However, recent studies demonstrate that primitive erythrocytes undergo enucleation between E12.5 and 16.5, producing mature primitive erythrocytes that are comparable in size to definitive erythrocytes (Kingsley et al., 2004). In the fetal liver, hematopoietic progenitors generate definitive erythrocytes, as well as myeloid and lymphoid cells. Definitive erythroid cells are smaller than EryP, enucleated, and express a range of adult globin isoforms, namely $\alpha 1$, $\alpha 2$, $\beta 1$ and $\beta 2$ (Lensch and Daley, 2004; Palis et al., 1999).

Genetic knock-out mice have provided insight into the functions of various genes in the generation and maintenance of primitive erythroid cells. Deficiencies of *Scl*, *Lmo2*, or *Gata2* in mouse embryos result in mid-gestational embryonic lethality due to failure of or defective emergence of primitive hematopoiesis (Porcher et al., 1996; Robb et al., 1995; Shivdasani et al., 1995; Tsai et al., 1994; Warren et al., 1994; Yamada et al., 1998). The *Gata1* transcription factor has an essential role in the regulation of erythroid-specific genes in both primitive and definitive erythroid cells. *Gata1*-deficient mice and differentiated embryonic stem (ES) cells derived from *Gata1*-deficient mice cannot generate mature erythroid cells due to developmental arrest and cell death at the proerythroblast stage (Fujiwara et al., 1996; Pevny et al., 1991). Mice deficient in erythroid Kruppel-like

factor (*Eklf*) have severe defects in definitive hematopoiesis, and recent studies show that *Eklf* is also involved in primitive hematopoiesis (Basu et al., 2007; Hodge et al., 2006; Nuez et al., 1995; Perkins et al., 1995). However, some transcription factors have been shown to affect only definitive hematopoiesis without impacting primitive hematopoiesis. For example, mice lacking *c-myb* have normal primitive erythroid cells but die around day E15.0 with a severely anemic phenotype, due to a failure to generate definitive erythrocytes (Mucenski et al., 1991). Mice deficient in *PU.1* also show normal primitive hematopoiesis, but they display multiple defects in the development of lymphoid and myeloid cells, dying by day E18.5 (Scott et al., 1997). These results suggest that the molecular mechanisms governing primitive and definitive hematopoiesis might be differently regulated.

Generation of hematopoietic stem cells (HSCs) with the ability to produce all types of adult blood cells is the key feature of definitive hematopoiesis. The origins of the HSCs that initially colonize the fetal liver remain controversial. There are currently two major models concerning the source of HSCs. The first model is that the HSCs emerge from within the yolk sac and then migrate to the fetal liver, subsequently populating the bone marrow. The second model is that the HSCs that enable fetal liver hematopoiesis emerge from within the intraembryonic para-aortic-splanchnopleure (PAS)/aorta-gonad-mesonephros (AGM) region.

Support for the first model comes from studies showing that the yolk sac contains multiple definitive hematopoietic progenitors, including T cells, B cells, and myeloid cells, even before the embryonic circulation starts (Cumano et al.,

1993; Huang and Auerbach, 1993; Liu and Auerbach, 1991; Wong et al., 1986). Moreover, Lux et al. used *Ncx1*-null embryos, which lack a heartbeat and, thus, have no functional circulation, to demonstrate that *Ncx1*^{-/-} yolk sacs contain normal numbers of both primitive and definitive erythroid progenitors (Lux et al., 2008). There were few definitive erythroid progenitors found within the embryo proper of the *Ncx1*^{-/-} mice, supporting the hypothesis that all definitive hematopoietic progenitors are initially generated in the yolk sac and migrate out into other areas of the embryo with the onset of embryonic circulation. However, these studies did not demonstrate that cells arising from the yolk sac during early development have long-term repopulating ability, which is the key feature of HSCs. Interestingly, when Yoder et al. transplanted E9.0 or E10.0 yolk sac cells into neonatal mice to show that yolk sac cells contain long-term repopulating hematopoietic stem cells (Yoder and Hiatt, 1997; Yoder et al., 1997a; Yoder et al., 1997b). In contrast, transplantation of E10.0 yolk sac cells into adult recipients did not result in engraftment (Yoder and Hiatt, 1997). These observations suggest that hematopoietic stem cells do emerge from the yolk sac, they require an embryonic environment to develop and that the adult microenvironment may not support the differentiation of the HSCs generated from the yolk sac. Consistent with this interpretation, yolk sac-derived cells can reconstitute the adult hematopoietic system when precultured on AGM-derived stromal cells (Matsuoka et al., 2001). Recently, using a non-invasive, pulse-labeling technique, Samokhvalov et al. were able to demonstrate that yolk sac cells, marked during early embryogenesis, can contribute to adult HSC populations that persist for at

least 15 months after birth (Samokhvalov et al., 2007). These studies support the contention that HSCs arise from within the yolk sac.

There are also studies which support the model that HSCs that colonize the fetal liver originate from in the PAS/AGM region of the embryo (reviewed in Cumano and Godin, 2007). Godin et al. surgically removed the PAS/AGM regions from E8.5-E9.0 embryos and embedded them under the kidney capsules of SCID mice (Godin et al., 1993). Afterwards, they could detect serum immunoglobulin M (IgM), IgM-secreting plasma cells, and B cells of the B1a phenotype of donor origin 3-6 months after the engraftment. Furthermore, when culturing cells from the PAS/AGM region and from yolk sac isolated prior to the establishment of circulation, the PAS/AGM cells give rise to much higher numbers of myeloid and lymphoid cells than do the yolk sac cells (Cumano et al., 1996; Godin et al., 1995). More importantly, the AGM region contains spleen colony-forming cell (CFU-S) activity, which measures numbers of definitive hematopoietic progenitors, at a higher level than that what is seen in the extraembryonic yolk sac (Medvinsky et al., 1993). Importantly, the PAS region from precirculation stage or the AGM region from E10.0 embryos contain long-term repopulating HSCs but the yolk sacs do not (Cumano et al., 2001; Medvinsky and Dzierzak, 1996). It has been shown that HSCs emerge first from the dorsal aorta of the AGM region (E10.5), followed by emergence in the vitelline and umbilical arteries (de Bruijn et al., 2000). These studies demonstrated that HSCs emerge within the embryo proper, not from the yolk sac, to establish definitive hematopoiesis. In addition, several studies have suggested that HSCs may also emerge from the placenta

(Alvarez-Silva et al., 2003; Rhodes et al., 2008; Zeigler et al., 2006). Moreover, endothelial cells from all three tissues, AGM, yolk sac and placenta, have recently been proposed to be responsible for the generation of hematopoietic stem cells (Chen et al., 2009; Eilken et al., 2009; Lancrin et al., 2009; Zovein et al., 2008).

Intriguingly, when HSCs emerge and definitive hematopoiesis begins, primitive erythroid progenitors become extinct in aging yolk sac (Palis et al., 1999). This raises an interesting question as to what mechanism regulates the transition from primitive to definitive hematopoiesis. Whether the transition from the primitive to the definitive hematopoiesis reflects a mere shift in hematopoietic sites or whether it is an actively regulated process is currently unknown.

In vitro Embryonic Stem Cell Differentiation Systems

To understand the molecular mechanisms regulating early events in the developing embryo has been of great interest to investigators. Due to the nature of the rapid developmental sequence during embryogenesis, the difficulties of accessing embryonic tissues and to the limited availability of cells from early embryos, the usage of embryonic tissues and cells to study the molecular regulation of hematopoiesis in developing embryos has proven quite challenging. Moreover, genetic knock-outs of hematopoiesis-related genes result in embryonic lethality, precluding further analyses of tissues from knockout animals (Okuda et al., 1996; Pevny et al., 1991; Shivdasani et al., 1995; Tsai et al., 1994; Wang et al., 1996a). Therefore, *in vitro* studies of embryonic stem (ES) cell differentiation have been utilized as an alternative method to study early events of embryonic

hematopoietic development.

ES cells can divide and differentiate in liquid differentiating media readily to generate sphere-like, differentiated cells masses call embryoid bodies (EBs, Figure 1.1-1, reviewed in Choi, 2002; Keller et al., 1999). ES cells can also be differentiated on layers of stromal cells or in dishes coated with type IV collagen without forming the EB structure (Nishikawa et al., 1998). EBs contain cells of all three germ layers (mesoderm, endoderm, and ectoderm) and can be further differentiated into many different lineages including cardiac, smooth and skeletal muscle; neuronal; endothelial; and hematopoietic lineages (Choi, 2002; Keller et al., 1993; Vittet et al., 1996). Among these lineages, the hematopoietic cells have been the most extensively characterized.

Many molecular and cellular studies have revealed that the sequential development of early hematopoietic events in differentiated ES cells is similar to that found in the normal developing embryo (Faloon et al., 2000; Keller et al., 1993; Palis et al., 1999). For example, as in the developing embryo, the primitive erythroid progenitors emerge prior to definitive hematopoietic progenitors (Keller et al., 1993; Palis et al., 1999). Additionally, testing the effects of specific soluble factors or inhibitors in the ES-EB system enables investigators to develop further understanding about the roles of different signaling pathways in the development of various cell types of interest (Lee et al., 2008; Lengerke et al., 2008; Nostro et al., 2008). For these reasons, among others, the *in vitro* differentiation model of ES cells is a powerful system for studying early embryonic development.

Transforming Growth Factor beta (TGF β) Signaling in Embryonic Hematopoiesis

Numerous studies demonstrate that the transforming growth factor- β (TGF β) superfamily, including TGF β , bone morphogenetic protein (BMP), and activin, is critical for hematopoietic and vascular development (Larsson and Karlsson, 2005; Shi and Massague, 2003). Members of the TGF β superfamily bind to the transmembrane heterodimeric complexes of Type I and Type II serine/threonine kinase receptors to transduce their signals (Figure 1.1-2, Shi and Massague, 2003). Type II receptor kinases are constitutively active, while Type I receptors, also known as activin receptor-like kinases (ALKs), contain an inactive kinase domain (Shi and Massague, 2003). When the ligands bind to their cognate receptors as dimers, the constitutively active Type II receptor transphosphorylates and activates the kinase domain of type I receptors (Wrana et al., 1994). The phosphorylated type I receptor will then phosphorylate either SMAD1/SMAD5/SMAD8 or SMAD2/SMAD3, the receptor-specific SMADs (R-SMADs, Heldin et al., 1997). The phosphorylated R-SMADs will then partner with SMAD4, the common SMAD (Co-SMAD), and translocate into the nucleus where the SMAD complex interact with specific transcription factors to regulate the transcription of their target genes (Heldin et al., 1997). SMAD6 and SMAD7 are inhibitory SMADs (I-SMADs) and can inhibit the activated R-SMADs. SMAD6 preferentially inhibits the BMP SMADs (SMAD1/5/8) while SMAD7 blocks the activity of all R-SMADs (Hata et al., 1998; Hayashi et al., 1997; Ishisaki et al., 1999; Nakao et al., 1997).

There are three mammalian isoforms of TGF β s: TGF β 1, TGF β 2, and TGF β 3, of which TGF β 1 is the most abundant. During embryogenesis, as early as E7.5, TGF β 1 can be detected in blood islands in the yolk sac, in mesodermal cells of the allantois, and in the pro-angioblast progenitors within the cardiogenic mesoderm of the embryo (Akhurst et al., 1990). At later stages of the developing embryo, TGF β 1 expression is detectable in fetal liver, endothelial, epithelial, and osteogenic tissues (Akhurst et al., 1990; Lehnert and Akhurst, 1988). TGF β 1-deficient mice display severe defects in their yolk sacs, including abnormal vascular structures and in significantly reduced numbers of erythroid cells, leading to embryonic lethality in the period between E9.5-E11.5 (Dickson et al., 1995). Intriguingly, *Tgf β receptor II (TgfrII)* expression largely correlates with the expression patterns of *Tgf β 1* (Lawler et al., 1994), and a homozygous deficiency of *Tgf β rII* results in embryonic lethality with defects in yolk sac hematopoiesis and vasculogenesis, which are similar to the defects seen in homozygous *Tgf β 1* deficient mice (Oshima et al., 1996). Whether the primary cause of death of *Tgf β 1*^{-/-} or *TgfrII*^{-/-} mice is due to defects in vasculogenesis or in hematopoiesis is not clear.

Studies have shown that TGF β 1 can bind to its cognate receptors TGF β rI (ALK5) and TGF β rII to form a complex that activates the SMAD2/SMAD3 pathway (Heldin et al., 1997). In addition to signaling through ALK5, TGF β 1 can also bind to ALK1 and TGF β rII to form a complex which activates the SMAD1/5/8 pathway (Lux et al., 1999; Oh et al., 2000). Recent studies demonstrated that the expression patterns of ALK1 and ALK5 are mutually exclusive in blood vessels

(Seki et al., 2006). Specifically, ALK1 expression was detected in arterial endothelium, whereas ALK5 expression was detected in mesenchymal tissue and smooth muscle cells surrounding the aorta, but was undetectable in the endothelial cells (Seki et al., 2006). These findings suggest that ALK1 and ALK5 might possess distinct biological roles in the developing embryo. Both *Alk1* and *Alk5* knock-out mice die at similar mid-gestation stages, the period E9.5-E10.5, with severe defects in vascular development of the yolk sac and an absence of circulating red blood cells (Larsson et al., 2001; Oh et al., 2000; Seki et al., 2006). Intriguingly, in contrast to the severe anemia seen in the yolk sac and in the embryo proper of these mice, when *Alk5*^{-/-} yolk sac cells were assayed *in vitro*, a significant increase, relative to numbers in wild-type mice, of erythroid colony-forming cells was detected (CFU-Ery), whereas numbers of granulocyte-macrophage colony-forming cells (CFU-GM) and mixed colony-forming cells (CFU-Mix) appeared to be normal (Larsson et al., 2001). These studies suggest that TGF β signaling could have an inhibitory effect on the formation and/or proliferation of erythroid progenitors. Consistent with this observation, Park et al. showed that TGF β 1 inhibits BMP4 and VEGF-mediated hematopoietic induction in the ES-EB system (Park et al., 2004).

Moreover, inactivation of *Smad4* within *Flk1*-expressing cells, which can generate both primitive and definitive blood cells, results in a 50% reduction of various hematopoietic progenitors in the yolk sac (Park et al., 2006). *Smad2* knock-out embryos die during early embryonic development due to defective mesoderm formation, from which the hematopoietic lineages normally arise

(Nomura and Li, 1998; Waldrip et al., 1998; Weinstein et al., 1998). Inhibition of *Smad5* can neutralize the suppressive effects of TGF β on adult hematopoietic progenitors, so the data suggest that, apart from Smad2 and Smad3, Smad5 could also be a mediator of TGF β signaling in hematopoietic cells (Bruno et al., 1998). Deletion of *Smad5* in mice results in embryonic lethality around mid-gestation with reduced numbers of blood cells and defective vascular structure in the yolk sac, which is similar to what is observed in knock-out animals for the TGF β receptors (Chang et al., 1999; Yang et al., 1999). However, *in vitro* replating assays showed that yolk sacs from *Smad5*^{-/-} embryos had increased numbers of high-proliferative-potential colony-forming cells (HPP-CFCs) with enhanced replating potential, and also contained augmented hematopoietic progenitors (Liu et al., 2003). Intriguingly, differentiated ES cells derived from *Smad5*^{-/-} mice contained an elevated number of blast colony-forming cells (BL-CFCs), the *in vitro* equivalents of hemangioblasts, in contrast to reduced numbers of EryP progenitors (Liu et al., 2003). Collectively, these studies suggest that TGF β signaling has a regulatory role in hematopoietic development during embryogenesis, but the detailed mechanism of this regulation is not clear at this time.

Runx1 in Hematopoietic Development

Runx1, also known as *Aml1*, belongs to the core binding factor (CBF) transcription factor family, which consists of three DNA-binding CBF α subunits (*Runx1*, *Runx2*, and *Runx3*) and a common, non-DNA binding subunit, CBF β

(Speck and Gilliland, 2002). *Runx1* contains a highly conserved domain with homology to *Runt*, the *Drosophila* paired-rule gene and it binds to the TGT/CGGT DNA sequence (Daga et al., 1992; Meyers et al., 1993). RUNX1 heterodimerizes with its molecular partner, CBF β , through the *Runt* homology domain (RHD) to carry out its transcriptional activity (Meyers et al., 1993; Ogawa et al., 1993; Wang et al., 1993).

Runx1 and its partner, CBF β , are the most frequent targets of chromosome translocations in human acute myeloid leukemia (AML)(Liu et al., 1993; Miyoshi et al., 1991). The importance of *Runx1* in hematopoietic development was revealed from mouse knock-out studies. *Runx1*-null animals die between E12.5 and E13.5 due to lack of definitive hematopoiesis and hemorrhaging in the central nervous system (Okada et al., 1998; Okuda et al., 1996; Wang et al., 1996a). Definitive hematopoietic colonies cannot be identified in E10.5 or E11.5 *Runx1*^{-/-} yolk sacs, fetal liver, or *Runx1*^{-/-} EB cells (Wang et al., 1996a). Generation of chimeric animals by injecting *Runx1*^{-/-} ES cells into wild-type blastocysts demonstrated that *Runx1*^{-/-} ES cells were unable to produce any hematopoietic tissues while these cells can contribute to other non-hematopoietic organs (Okuda et al., 1996).

These studies indicate that the defects of the *Runx1* knock-out cells are specific to failures in the hematopoietic lineages, and not to defects in the fetal liver microenvironment. In addition, knock-out studies of CBF β show a parallel phenotype to *Runx1*-deficient mice, suggesting that CBF β is essential for RUNX1 function during early embryogenesis (Sasaki et al., 1996; Wang et al., 1996b).

To further understand the role of *Runx1* during early embryogenesis,

Runx1^{lacZ/+} mice and *in situ* hybridization were used. The expression of *Runx1* is first detectable in extraembryonic mesodermal cells at E7.25 and then in both primitive erythrocytes and endothelial cells of the yolk sac blood islands at E8.0-E8.5 (Lacaud et al., 2002; North et al., 1999). Between E8.5-E11.5, *Runx1* can be detected in endothelial cells and mesenchymal cells in the yolk sac, in the vitelline and umbilical arteries, and in the ventral aspect of the dorsal aorta in the AGM region where hematopoietic stem cells (HSCs) were first identified (North et al., 1999). Subsequent studies confirmed that *Runx1* is required for the emergence of HSCs during embryonic development (North et al., 1999; North et al., 2002; Yokomizo et al., 2001). Interestingly, E9.5-E11.5 *Runx1^{+/-}* embryos show significantly reduced numbers of definitive hematopoietic progenitors in their livers and yolk sacs, compared to wild-type controls (Cai et al., 2000; Mukoyama et al., 2000). Additionally, HSCs emerge prematurely in the E10.0 *Runx1^{+/-}* yolk sacs, and there was a premature termination of HSC activity in the *Runx1^{+/-}* AGM explants (Cai et al., 2000; North et al., 2002). These observations indicate that the degree of RUNX1 activity is critical for temporal and spatial regulation of the generation of HSCs during hematopoietic development. Although *Runx1* starts being expressed during the period when EryP progenitors are forming, what role *Runx1* plays in murine primitive hematopoiesis is currently unclear.

However, studies of *Runx1* in *Xenopus* and zebrafish indicate important roles of *Runx1* in primitive hematopoiesis in those animals. *Runx1* expression is among the earliest molecular markers for blood in *Xenopus*, and the introduction of the *Runt* domain from the *Xenopus Runx1* homologue, *Xaml*, into *Xenopus* embryos

results in the disruption of normal primitive hematopoiesis (Tracey et al., 1998). Studies in zebrafish also demonstrate that *Runx1* is involved in both primitive and definitive hematopoiesis (Kalev-Zylinska et al., 2002). These findings suggest that *Runx1* may also function in mouse primitive hematopoietic development.

Previous studies have also demonstrated that RUNX proteins, including RUNX1, RUNX2 and RUNX3, have cooperative interactions with TGF β superfamily signaling in several biological systems (Ito and Miyazono, 2003). Specifically, both *Runx1* and *Runx3* expression can be induced by TGF β 1, and they interact with FOXO3 to induce *Bim* expression to mediate apoptosis in hepatic (Willey and Howe, 2009) and gastric epithelial cells (Yano et al., 2006). Moreover, Runx2 can physically interact with BMPs-specific SMADs, including SMAD1 and SMAD5, to cooperatively induce osteoblast differentiation of mesenchymal progenitor cells (Lee et al., 2002; Lee et al., 2000; Zhang et al., 2000). Taken together, these studies suggest that there is, at the very least, possible crosstalk between *Runx1* and TGF β signaling.

Overall Goals of Chapter One

Hematopoietic development is composed of two waves of hematopoiesis: primitive and definitive. Primitive hematopoietic progenitors emerge exclusively and transiently in the yolk sac during embryogenesis. While primitive hematopoietic progenitors become distinct in aging yolk sac, definitive hematopoietic progenitors generated in the yolk sac and/or embryo take over blood cell production in later embryonic development and throughout adult life. *Runx1* is essential for the establishment of definitive hematopoiesis, but its expression is also detectable in the yolk sac blood islands, where primitive hematopoiesis occurs. Little is known about the role of *Runx1* in primitive hematopoiesis. Thus, the objective of this chapter was to elucidate the role of *Runx1* in primitive hematopoiesis, using *in vitro* ES cell differentiation systems and *Runx1* mutant mice. In addition, TGF β 1 has been suggested as a regulator of primitive hematopoiesis. TGF β signaling has been shown to function cooperatively with Runx family in other biological systems. Therefore, the question was explored of whether TGF β 1 and *Runx1* have a cooperative relationship in the regulation of primitive hematopoiesis.

References

- Akhurst, R. J., Lehnert, S. A., Faissner, A. and Duffie, E.** (1990). TGF beta in murine morphogenetic processes: the early embryo and cardiogenesis. *Development* **108**, 645-56.
- Alvarez-Silva, M., Belo-Diabangouaya, P., Salaun, J. and Dieterlen-Lievre, F.** (2003). Mouse placenta is a major hematopoietic organ. *Development* **130**, 5437-44.
- Basu, P., Lung, T. K., Lemsaddek, W., Sargent, T. G., Williams, D. C., Jr., Basu, M., Redmond, L. C., Lingrel, J. B., Haar, J. L. and Lloyd, J. A.** (2007). EKLF and KLF2 have compensatory roles in embryonic beta-globin gene expression and primitive erythropoiesis. *Blood* **110**, 3417-25.
- Bruno, E., Horrigan, S. K., Van Den Berg, D., Rozler, E., Fitting, P. R., Moss, S. T., Westbrook, C. and Hoffman, R.** (1998). The Smad5 gene is involved in the intracellular signaling pathways that mediate the inhibitory effects of transforming growth factor-beta on human hematopoiesis. *Blood* **91**, 1917-23.
- Cai, Z., de Bruijn, M., Ma, X., Dortland, B., Luteijn, T., Downing, R. J. and Dzierzak, E.** (2000). Haploinsufficiency of AML1 affects the temporal and spatial generation of hematopoietic stem cells in the mouse embryo. *Immunity* **13**, 423-31.
- Chang, H., Huylebroeck, D., Verschueren, K., Guo, Q., Matzuk, M. M. and Zwijsen, A.** (1999). Smad5 knockout mice die at mid-gestation due to multiple embryonic and extraembryonic defects. *Development* **126**, 1631-42.
- Chen, M. J., Yokomizo, T., Zeigler, B. M., Dzierzak, E. and Speck, N. A.** (2009). Runx1 is required for the endothelial to haematopoietic cell transition but not thereafter. *Nature* **457**, 887-91.
- Choi, K.** (2002). The hemangioblast: a common progenitor of hematopoietic and endothelial cells. *J Hematother Stem Cell Res* **11**, 91-101.
- Cumano, A., Dieterlen-Lievre, F. and Godin, I.** (1996). Lymphoid potential, probed before circulation in mouse, is restricted to caudal intraembryonic splanchnopleura. *Cell* **86**, 907-16.
- Cumano, A., Ferraz, J. C., Klaine, M., Di Santo, J. P. and Godin, I.** (2001). Intraembryonic, but not yolk sac hematopoietic precursors, isolated before circulation, provide long-term multilineage reconstitution. *Immunity* **15**, 477-85.
- Cumano, A., Furlonger, C. and Paige, C. J.** (1993). Differentiation and characterization of B-cell precursors detected in the yolk sac and embryo body of embryos beginning at the 10- to 12-somite stage. *Proc Natl Acad Sci U S A* **90**, 6429-33.
- Cumano, A. and Godin, I.** (2007). Ontogeny of the hematopoietic system. *Annu Rev Immunol* **25**, 745-85.
- Daga, A., Tighe, J. E. and Calabi, F.** (1992). Leukaemia/Drosophila homology. *Nature* **356**, 484.
- de Bruijn, M. F., Speck, N. A., Peeters, M. C. and Dzierzak, E.** (2000). Definitive hematopoietic stem cells first develop within the major arterial regions of the mouse embryo. *Embo J* **19**, 2465-74.
- Dickson, M. C., Martin, J. S., Cousins, F. M., Kulkarni, A. B., Karlsson, S. and Akhurst, R. J.** (1995). Defective haematopoiesis and vasculogenesis in transforming growth factor-beta 1 knock out mice. *Development* **121**, 1845-54.
- Eilken, H. M., Nishikawa, S. and Schroeder, T.** (2009). Continuous single-cell imaging of blood generation from haemogenic endothelium. *Nature* **457**, 896-900.

Faloon, P., Arentson, E., Kazarov, A., Deng, C. X., Porcher, C., Orkin, S. and Choi, K. (2000). Basic fibroblast growth factor positively regulates hematopoietic development. *Development* **127**, 1931-41.

Ferkowicz, M. J. and Yoder, M. C. (2005). Blood island formation: longstanding observations and modern interpretations. *Exp Hematol* **33**, 1041-7.

Fujiwara, Y., Browne, C. P., Cunniff, K., Goff, S. C. and Orkin, S. H. (1996). Arrested development of embryonic red cell precursors in mouse embryos lacking transcription factor GATA-1. *Proc Natl Acad Sci U S A* **93**, 12355-8.

Godin, I., Dieterlen-Lievre, F. and Cumano, A. (1995). Emergence of multipotent hemopoietic cells in the yolk sac and paraaortic splanchnopleura in mouse embryos, beginning at 8.5 days postcoitus. *Proc Natl Acad Sci U S A* **92**, 773-7.

Godin, I. E., Garcia-Porrero, J. A., Coutinho, A., Dieterlen-Lievre, F. and Marcos, M. A. (1993). Para-aortic splanchnopleura from early mouse embryos contains B1a cell progenitors. *Nature* **364**, 67-70.

Hata, A., Lagna, G., Massague, J. and Hemmati-Brivanlou, A. (1998). Smad6 inhibits BMP/Smad1 signaling by specifically competing with the Smad4 tumor suppressor. *Genes Dev* **12**, 186-97.

Hayashi, H., Abdollah, S., Qiu, Y., Cai, J., Xu, Y. Y., Grinnell, B. W., Richardson, M. A., Topper, J. N., Gimbrone, M. A., Jr., Wrana, J. L. et al. (1997). The MAD-related protein Smad7 associates with the TGFbeta receptor and functions as an antagonist of TGFbeta signaling. *Cell* **89**, 1165-73.

Heldin, C. H., Miyazono, K. and ten Dijke, P. (1997). TGF-beta signalling from cell membrane to nucleus through SMAD proteins. *Nature* **390**, 465-71.

Hodge, D., Coghill, E., Keys, J., Maguire, T., Hartmann, B., McDowall, A., Weiss, M., Grimmond, S. and Perkins, A. (2006). A global role for EKLF in definitive and primitive erythropoiesis. *Blood* **107**, 3359-70.

Houssaint, E. (1981). Differentiation of the mouse hepatic primordium. II. Extrinsic origin of the haemopoietic cell line. *Cell Differ* **10**, 243-52.

Huang, H. and Auerbach, R. (1993). Identification and characterization of hematopoietic stem cells from the yolk sac of the early mouse embryo. *Proc Natl Acad Sci U S A* **90**, 10110-4.

Huber, T. L., Kouskoff, V., Fehling, H. J., Palis, J. and Keller, G. (2004). Haemangioblast commitment is initiated in the primitive streak of the mouse embryo. *Nature* **432**, 625-30.

Ishisaki, A., Yamato, K., Hashimoto, S., Nakao, A., Tamaki, K., Nonaka, K., ten Dijke, P., Sugino, H. and Nishihara, T. (1999). Differential inhibition of Smad6 and Smad7 on bone morphogenetic protein- and activin-mediated growth arrest and apoptosis in B cells. *J Biol Chem* **274**, 13637-42.

Ito, Y. and Miyazono, K. (2003). RUNX transcription factors as key targets of TGF-beta superfamily signaling. *Curr Opin Genet Dev* **13**, 43-7.

Kalev-Zylinska, M. L., Horsfield, J. A., Flores, M. V., Postlethwait, J. H., Vitas, M. R., Baas, A. M., Crosier, P. S. and Crosier, K. E. (2002). Runx1 is required for zebrafish blood and vessel development and expression of a human RUNX1-CBF2T1 transgene advances a model for studies of leukemogenesis. *Development* **129**, 2015-30.

Keller, G., Kennedy, M., Papayannopoulou, T. and Wiles, M. V. (1993). Hematopoietic commitment during embryonic stem cell differentiation in culture. *Mol*

Cell Biol **13**, 473-86.

Keller, G., Lacaud, G. and Robertson, S. (1999). Development of the hematopoietic system in the mouse. *Exp Hematol* **27**, 777-87.

Kingsley, P. D., Malik, J., Emerson, R. L., Bushnell, T. P., McGrath, K. E., Bloedorn, L. A., Bulger, M. and Palis, J. (2006). "Maturational" globin switching in primary primitive erythroid cells. *Blood* **107**, 1665-72.

Kingsley, P. D., Malik, J., Fantauzzo, K. A. and Palis, J. (2004). Yolk sac-derived primitive erythroblasts enucleate during mammalian embryogenesis. *Blood* **104**, 19-25.

Lacaud, G., Gore, L., Kennedy, M., Kouskoff, V., Kingsley, P., Hogan, C., Carlsson, L., Speck, N., Palis, J. and Keller, G. (2002). Runx1 is essential for hematopoietic commitment at the hemangioblast stage of development in vitro. *Blood* **100**, 458-66.

Lancrin, C., Sroczynska, P., Stephenson, C., Allen, T., Kouskoff, V. and Lacaud, G. (2009). The haemangioblast generates haematopoietic cells through a haemogenic endothelium stage. *Nature* **457**, 892-5.

Larsson, J., Goumans, M. J., Sjostrand, L. J., van Rooijen, M. A., Ward, D., Leveen, P., Xu, X., ten Dijke, P., Mummery, C. L. and Karlsson, S. (2001). Abnormal angiogenesis but intact hematopoietic potential in TGF-beta type I receptor-deficient mice. *Embo J* **20**, 1663-73.

Larsson, J. and Karlsson, S. (2005). The role of Smad signaling in hematopoiesis. *Oncogene* **24**, 5676-92.

Lawler, S., Candia, A. F., Ebner, R., Shum, L., Lopez, A. R., Moses, H. L., Wright, C. V. and Derynck, R. (1994). The murine type II TGF-beta receptor has a coincident embryonic expression and binding preference for TGF-beta 1. *Development* **120**, 165-75.

Lee, D., Park, C., Lee, H., Lugus, J. J., Kim, S. H., Arentson, E., Chung, Y. S., Gomez, G., Kyba, M., Lin, S. et al. (2008). ER71 acts downstream of BMP, Notch, and Wnt signaling in blood and vessel progenitor specification. *Cell Stem Cell* **2**, 497-507.

Lee, K. S., Hong, S. H. and Bae, S. C. (2002). Both the Smad and p38 MAPK pathways play a crucial role in Runx2 expression following induction by transforming growth factor-beta and bone morphogenetic protein. *Oncogene* **21**, 7156-63.

Lee, K. S., Kim, H. J., Li, Q. L., Chi, X. Z., Ueta, C., Komori, T., Wozney, J. M., Kim, E. G., Choi, J. Y., Ryoo, H. M. et al. (2000). Runx2 is a common target of transforming growth factor beta1 and bone morphogenetic protein 2, and cooperation between Runx2 and Smad5 induces osteoblast-specific gene expression in the pluripotent mesenchymal precursor cell line C2C12. *Mol Cell Biol* **20**, 8783-92.

Lehnert, S. A. and Akhurst, R. J. (1988). Embryonic expression pattern of TGF beta type-1 RNA suggests both paracrine and autocrine mechanisms of action. *Development* **104**, 263-73.

Lengerke, C., Schmitt, S., Bowman, T. V., Jang, I. H., Maouche-Chretien, L., McKinney-Freeman, S., Davidson, A. J., Hammerschmidt, M., Rentzsch, F., Green, J. B. et al. (2008). BMP and Wnt specify hematopoietic fate by activation of the Cdx-Hox pathway. *Cell Stem Cell* **2**, 72-82.

Lensch, M. W. and Daley, G. Q. (2004). Origins of mammalian hematopoiesis: in vivo paradigms and in vitro models. *Curr Top Dev Biol* **60**, 127-96.

Liu, B., Sun, Y., Jiang, F., Zhang, S., Wu, Y., Lan, Y., Yang, X. and Mao, N. (2003). Disruption of Smad5 gene leads to enhanced proliferation of high-proliferative potential precursors during embryonic hematopoiesis. *Blood* **101**, 124-33.

- Liu, C. P. and Auerbach, R.** (1991). In vitro development of murine T cells from prethymic and pre-liver embryonic yolk sac hematopoietic stem cells. *Development* **113**, 1315-23.
- Liu, P., Tarle, S. A., Hajra, A., Claxton, D. F., Marlton, P., Freedman, M., Siciliano, M. J. and Collins, F. S.** (1993). Fusion between transcription factor CBF beta/PEBP2 beta and a myosin heavy chain in acute myeloid leukemia. *Science* **261**, 1041-4.
- Lux, A., Attisano, L. and Marchuk, D. A.** (1999). Assignment of transforming growth factor beta1 and beta3 and a third new ligand to the type I receptor ALK-1. *J Biol Chem* **274**, 9984-92.
- Lux, C. T., Yoshimoto, M., McGrath, K., Conway, S. J., Palis, J. and Yoder, M. C.** (2008). All primitive and definitive hematopoietic progenitor cells emerging before E10 in the mouse embryo are products of the yolk sac. *Blood* **111**, 3435-8.
- Matsuoka, S., Tsuji, K., Hisakawa, H., Xu, M., Ebihara, Y., Ishii, T., Sugiyama, D., Manabe, A., Tanaka, R., Ikeda, Y. et al.** (2001). Generation of definitive hematopoietic stem cells from murine early yolk sac and para-aortic splanchnopleures by aorta-gonad-mesonephros region-derived stromal cells. *Blood* **98**, 6-12.
- Medvinsky, A. and Dzierzak, E.** (1996). Definitive hematopoiesis is autonomously initiated by the AGM region. *Cell* **86**, 897-906.
- Medvinsky, A. L., Samoylina, N. L., Muller, A. M. and Dzierzak, E. A.** (1993). An early pre-liver intraembryonic source of CFU-S in the developing mouse. *Nature* **364**, 64-7.
- Meyers, S., Downing, J. R. and Hiebert, S. W.** (1993). Identification of AML-1 and the (8;21) translocation protein (AML-1/ETO) as sequence-specific DNA-binding proteins: the runt homology domain is required for DNA binding and protein-protein interactions. *Mol Cell Biol* **13**, 6336-45.
- Miyoshi, H., Shimizu, K., Kozu, T., Maseki, N., Kaneko, Y. and Ohki, M.** (1991). t(8;21) breakpoints on chromosome 21 in acute myeloid leukemia are clustered within a limited region of a single gene, AML1. *Proc Natl Acad Sci U S A* **88**, 10431-4.
- Mucenski, M. L., McLain, K., Kier, A. B., Swerdlow, S. H., Schreiner, C. M., Miller, T. A., Pietryga, D. W., Scott, W. J., Jr. and Potter, S. S.** (1991). A functional c-myb gene is required for normal murine fetal hepatic hematopoiesis. *Cell* **65**, 677-89.
- Mukoyama, Y., Chiba, N., Hara, T., Okada, H., Ito, Y., Kanamaru, R., Miyajima, A., Satake, M. and Watanabe, T.** (2000). The AML1 transcription factor functions to develop and maintain hematogenic precursor cells in the embryonic aorta-gonad-mesonephros region. *Dev Biol* **220**, 27-36.
- Nakao, A., Afrakhte, M., Moren, A., Nakayama, T., Christian, J. L., Heuchel, R., Itoh, S., Kawabata, M., Heldin, N. E., Heldin, C. H. et al.** (1997). Identification of Smad7, a TGFbeta-inducible antagonist of TGF-beta signalling. *Nature* **389**, 631-5.
- Nishikawa, S. I., Nishikawa, S., Hirashima, M., Matsuyoshi, N. and Kodama, H.** (1998). Progressive lineage analysis by cell sorting and culture identifies FLK1+VE-cadherin+ cells at a diverging point of endothelial and hemopoietic lineages. *Development* **125**, 1747-57.
- Nomura, M. and Li, E.** (1998). Smad2 role in mesoderm formation, left-right patterning and craniofacial development. *Nature* **393**, 786-90.
- North, T., Gu, T. L., Stacy, T., Wang, Q., Howard, L., Binder, M., Marin-Padilla, M. and Speck, N. A.** (1999). Cbfa2 is required for the formation of intra-aortic

- hematopoietic clusters. *Development* **126**, 2563-75.
- North, T. E., de Bruijn, M. F., Stacy, T., Talebian, L., Lind, E., Robin, C., Binder, M., Dzierzak, E. and Speck, N. A.** (2002). Runx1 expression marks long-term repopulating hematopoietic stem cells in the midgestation mouse embryo. *Immunity* **16**, 661-72.
- Nostro, M. C., Cheng, X., Keller, G. M. and Gadue, P.** (2008). Wnt, activin, and BMP signaling regulate distinct stages in the developmental pathway from embryonic stem cells to blood. *Cell Stem Cell* **2**, 60-71.
- Nuez, B., Michalovich, D., Bygrave, A., Ploemacher, R. and Grosveld, F.** (1995). Defective haematopoiesis in fetal liver resulting from inactivation of the EKLf gene. *Nature* **375**, 316-8.
- Ogawa, E., Maruyama, M., Kagoshima, H., Inuzuka, M., Lu, J., Satake, M., Shigesada, K. and Ito, Y.** (1993). PEBP2/PEA2 represents a family of transcription factors homologous to the products of the *Drosophila* runt gene and the human AML1 gene. *Proc Natl Acad Sci U S A* **90**, 6859-63.
- Oh, S. P., Seki, T., Goss, K. A., Imamura, T., Yi, Y., Donahoe, P. K., Li, L., Miyazono, K., ten Dijke, P., Kim, S. et al.** (2000). Activin receptor-like kinase 1 modulates transforming growth factor-beta 1 signaling in the regulation of angiogenesis. *Proc Natl Acad Sci U S A* **97**, 2626-31.
- Okada, H., Watanabe, T., Niki, M., Takano, H., Chiba, N., Yanai, N., Tani, K., Hibino, H., Asano, S., Mucenski, M. L. et al.** (1998). AML1(-/-) embryos do not express certain hematopoiesis-related gene transcripts including those of the PU.1 gene. *Oncogene* **17**, 2287-93.
- Okuda, T., van Deursen, J., Hiebert, S. W., Grosveld, G. and Downing, J. R.** (1996). AML1, the target of multiple chromosomal translocations in human leukemia, is essential for normal fetal liver hematopoiesis. *Cell* **84**, 321-30.
- Oshima, M., Oshima, H. and Taketo, M. M.** (1996). TGF-beta receptor type II deficiency results in defects of yolk sac hematopoiesis and vasculogenesis. *Dev Biol* **179**, 297-302.
- Palis, J., Robertson, S., Kennedy, M., Wall, C. and Keller, G.** (1999). Development of erythroid and myeloid progenitors in the yolk sac and embryo proper of the mouse. *Development* **126**, 5073-84.
- Park, C., Afrikanova, I., Chung, Y. S., Zhang, W. J., Arentson, E., Fong Gh, G., Rosendahl, A. and Choi, K.** (2004). A hierarchical order of factors in the generation of FLK1- and SCL-expressing hematopoietic and endothelial progenitors from embryonic stem cells. *Development* **131**, 2749-62.
- Park, C., Lavine, K., Mishina, Y., Deng, C. X., Ornitz, D. M. and Choi, K.** (2006). Bone morphogenetic protein receptor 1A signaling is dispensable for hematopoietic development but essential for vessel and atrioventricular endocardial cushion formation. *Development* **133**, 3473-84.
- Park, C., Ma, Y. D. and Choi, K.** (2005). Evidence for the hemangioblast. *Exp Hematol* **33**, 965-70.
- Perkins, A. C., Sharpe, A. H. and Orkin, S. H.** (1995). Lethal beta-thalassaemia in mice lacking the erythroid CACCC-transcription factor EKLf. *Nature* **375**, 318-22.
- Pevny, L., Simon, M. C., Robertson, E., Klein, W. H., Tsai, S. F., D'Agati, V., Orkin, S. H. and Costantini, F.** (1991). Erythroid differentiation in chimaeric mice blocked by a

targeted mutation in the gene for transcription factor GATA-1. *Nature* **349**, 257-60.

Porcher, C., Swat, W., Rockwell, K., Fujiwara, Y., Alt, F. W. and Orkin, S. H. (1996). The T cell leukemia oncoprotein SCL/tal-1 is essential for development of all hematopoietic lineages. *Cell* **86**, 47-57.

Rhodes, K. E., Gekas, C., Wang, Y., Lux, C. T., Francis, C. S., Chan, D. N., Conway, S., Orkin, S. H., Yoder, M. C. and Mikkola, H. K. (2008). The emergence of hematopoietic stem cells is initiated in the placental vasculature in the absence of circulation. *Cell Stem Cell* **2**, 252-63.

Robb, L., Lyons, I., Li, R., Hartley, L., Kontgen, F., Harvey, R. P., Metcalf, D. and Begley, C. G. (1995). Absence of yolk sac hematopoiesis from mice with a targeted disruption of the scl gene. *Proc Natl Acad Sci U S A* **92**, 7075-9.

Sabin, F. R. (1920). Studies on the origin of blood vessels and of red corpuscles as seen in the living blastoderm of the chick during the second day of incubation.

Samokhvalov, I. M., Samokhvalova, N. I. and Nishikawa, S. (2007). Cell tracing shows the contribution of the yolk sac to adult haematopoiesis. *Nature* **446**, 1056-61.

Sasaki, K., Yagi, H., Bronson, R. T., Tominaga, K., Matsunashi, T., Deguchi, K., Tani, Y., Kishimoto, T. and Komori, T. (1996). Absence of fetal liver hematopoiesis in mice deficient in transcriptional coactivator core binding factor beta. *Proc Natl Acad Sci U S A* **93**, 12359-63.

Scott, E. W., Fisher, R. C., Olson, M. C., Kehrli, E. W., Simon, M. C. and Singh, H. (1997). PU.1 functions in a cell-autonomous manner to control the differentiation of multipotential lymphoid-myeloid progenitors. *Immunity* **6**, 437-47.

Seki, T., Hong, K. H. and Oh, S. P. (2006). Nonoverlapping expression patterns of ALK1 and ALK5 reveal distinct roles of each receptor in vascular development. *Lab Invest* **86**, 116-29.

Shi, Y. and Massague, J. (2003). Mechanisms of TGF-beta signaling from cell membrane to the nucleus. *Cell* **113**, 685-700.

Shivdasani, R. A., Mayer, E. L. and Orkin, S. H. (1995). Absence of blood formation in mice lacking the T-cell leukaemia oncoprotein tal-1/SCL. *Nature* **373**, 432-4.

Speck, N. A. and Gilliland, D. G. (2002). Core-binding factors in haematopoiesis and leukaemia. *Nat Rev Cancer* **2**, 502-13.

Tracey, W. D., Jr., Pepling, M. E., Horb, M. E., Thomsen, G. H. and Gergen, J. P. (1998). A *Xenopus* homologue of aml-1 reveals unexpected patterning mechanisms leading to the formation of embryonic blood. *Development* **125**, 1371-80.

Tsai, F. Y., Keller, G., Kuo, F. C., Weiss, M., Chen, J., Rosenblatt, M., Alt, F. W. and Orkin, S. H. (1994). An early haematopoietic defect in mice lacking the transcription factor GATA-2. *Nature* **371**, 221-6.

Vittet, D., Prandini, M. H., Berthier, R., Schweitzer, A., Martin-Sisteron, H., Uzan, G. and Dejana, E. (1996). Embryonic stem cells differentiate in vitro to endothelial cells through successive maturation steps. *Blood* **88**, 3424-31.

Waldrip, W. R., Bikoff, E. K., Hoodless, P. A., Wrana, J. L. and Robertson, E. J. (1998). Smad2 signaling in extraembryonic tissues determines anterior-posterior polarity of the early mouse embryo. *Cell* **92**, 797-808.

Wang, Q., Stacy, T., Binder, M., Marin-Padilla, M., Sharpe, A. H. and Speck, N. A. (1996a). Disruption of the Cbfa2 gene causes necrosis and hemorrhaging in the central nervous system and blocks definitive hematopoiesis. *Proc Natl Acad Sci U S A* **93**,

3444-9.

Wang, Q., Stacy, T., Miller, J. D., Lewis, A. F., Gu, T. L., Huang, X., Bushweller, J. H., Bories, J. C., Alt, F. W., Ryan, G. et al. (1996b). The CBFbeta subunit is essential for CBFalpha2 (AML1) function in vivo. *Cell* **87**, 697-708.

Wang, S., Wang, Q., Crute, B. E., Melnikova, I. N., Keller, S. R. and Speck, N. A. (1993). Cloning and characterization of subunits of the T-cell receptor and murine leukemia virus enhancer core-binding factor. *Mol Cell Biol* **13**, 3324-39.

Warren, A. J., Colledge, W. H., Carlton, M. B., Evans, M. J., Smith, A. J. and Rabbitts, T. H. (1994). The oncogenic cysteine-rich LIM domain protein rbtn2 is essential for erythroid development. *Cell* **78**, 45-57.

Weinstein, M., Yang, X., Li, C., Xu, X., Gotay, J. and Deng, C. X. (1998). Failure of egg cylinder elongation and mesoderm induction in mouse embryos lacking the tumor suppressor smad2. *Proc Natl Acad Sci U S A* **95**, 9378-83.

Willey, G. M. and Howe, P. H. (2009). Runx1 is a co-activator with FOXO3 to mediate Transforming Growth Factor {beta} (TGF {beta})-induced Bim transcription in hepatic cells. *J Biol Chem*.

Wong, P. M., Chung, S. W., Chui, D. H. and Eaves, C. J. (1986). Properties of the earliest clonogenic hemopoietic precursors to appear in the developing murine yolk sac. *Proc Natl Acad Sci U S A* **83**, 3851-4.

Wrana, J. L., Attisano, L., Wieser, R., Ventura, F. and Massague, J. (1994). Mechanism of activation of the TGF-beta receptor. *Nature* **370**, 341-7.

Yamada, Y., Warren, A. J., Dobson, C., Forster, A., Pannell, R. and Rabbitts, T. H. (1998). The T cell leukemia LIM protein Lmo2 is necessary for adult mouse hematopoiesis. *Proc Natl Acad Sci U S A* **95**, 3890-5.

Yang, X., Castilla, L. H., Xu, X., Li, C., Gotay, J., Weinstein, M., Liu, P. P. and Deng, C. X. (1999). Angiogenesis defects and mesenchymal apoptosis in mice lacking SMAD5. *Development* **126**, 1571-80.

Yano, T., Ito, K., Fukamachi, H., Chi, X. Z., Wee, H. J., Inoue, K., Ida, H., Bouillet, P., Strasser, A., Bae, S. C. et al. (2006). The RUNX3 tumor suppressor upregulates Bim in gastric epithelial cells undergoing transforming growth factor beta-induced apoptosis. *Mol Cell Biol* **26**, 4474-88.

Yoder, M. C. and Hiatt, K. (1997). Engraftment of embryonic hematopoietic cells in conditioned newborn recipients. *Blood* **89**, 2176-83.

Yoder, M. C., Hiatt, K., Dutt, P., Mukherjee, P., Bodine, D. M. and Orlic, D. (1997a). Characterization of definitive lymphohematopoietic stem cells in the day 9 murine yolk sac. *Immunity* **7**, 335-44.

Yoder, M. C., Hiatt, K. and Mukherjee, P. (1997b). In vivo repopulating hematopoietic stem cells are present in the murine yolk sac at day 9.0 postcoitus. *Proc Natl Acad Sci U S A* **94**, 6776-80.

Yokomizo, T., Ogawa, M., Osato, M., Kanno, T., Yoshida, H., Fujimoto, T., Fraser, S., Nishikawa, S., Okada, H., Satake, M. et al. (2001). Requirement of Runx1/AML1/PEBP2alphaB for the generation of haematopoietic cells from endothelial cells. *Genes Cells* **6**, 13-23.

Zeigler, B. M., Sugiyama, D., Chen, M., Guo, Y., Downs, K. M. and Speck, N. A. (2006). The allantois and chorion, when isolated before circulation or chorio-allantoic fusion, have hematopoietic potential. *Development* **133**, 4183-92.

Zhang, Y. W., Yasui, N., Ito, K., Huang, G., Fujii, M., Hanai, J., Nogami, H., Ochi, T., Miyazono, K. and Ito, Y. (2000). A RUNX2/PEBP2alpha A/CBFA1 mutation displaying impaired transactivation and Smad interaction in cleidocranial dysplasia. *Proc Natl Acad Sci U S A* **97**, 10549-54.

Zovein, A. C., Hofmann, J. J., Lynch, M., French, W. J., Turlo, K. A., Yang, Y., Becker, M. S., Zanetta, L., Dejana, E., Gasson, J. C. et al. (2008). Fate tracing reveals the endothelial origin of hematopoietic stem cells. *Cell Stem Cell* **3**, 625-36.

Figure 1.1-1.

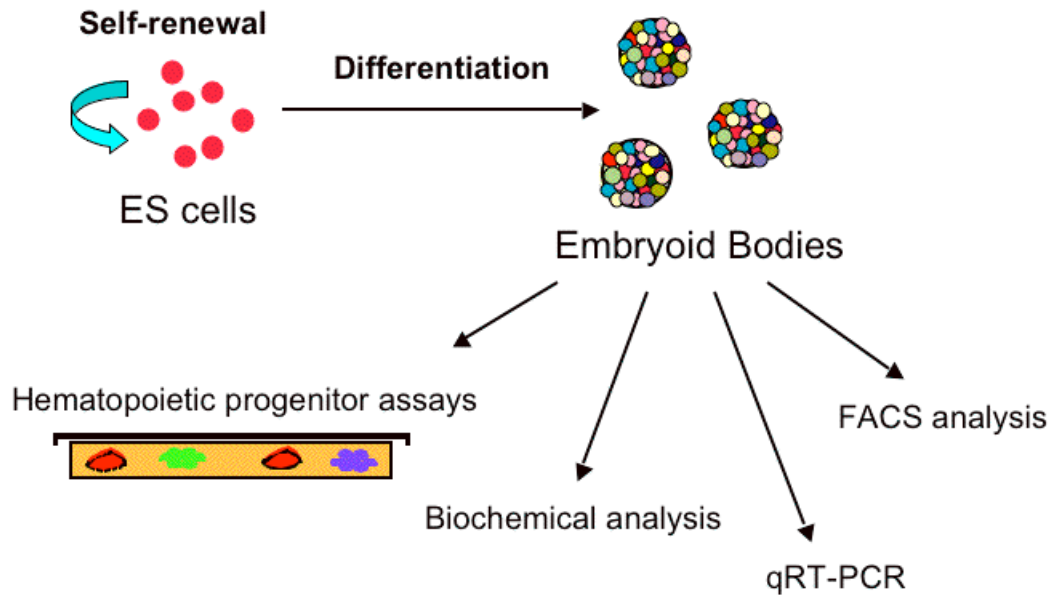


Figure 1.1-1. *In vitro* embryonic stem cell differentiation systems.

Schematic diagram of *in vitro* ES cell differentiation systems. ES cells can be differentiated *in vitro* and give rise to differentiated cell masses called embryoid bodies (EBs). EBs are composed of multiple cell types, as indicated by different colors. Many cellular and molecular analyses can be performed on EBs such as hematopoietic colony assay, biochemical analysis, quantitative reverse transcription polymerase chain reaction (qRT-PCR), or flow cytometry (FACS analysis).

Figure 1.1-2.

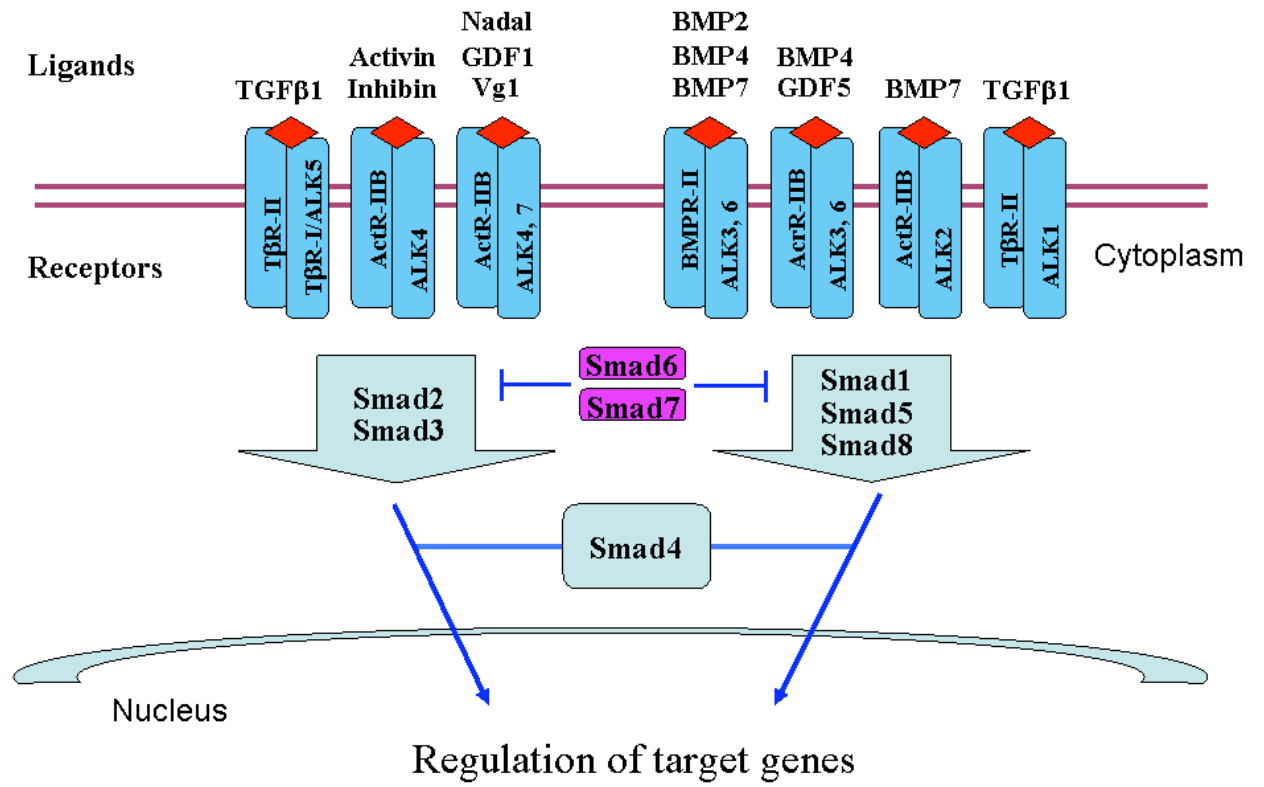


Figure 1.1-2. A schematic diagram of TGF β superfamily ligands, their type I and type II receptors, and downstream SMAD molecules (modified from Shi and Massague, 2003).

Members of the TGF β superfamily bind to the transmembrane heterodimeric complexes of Type I and Type II serine/threonine kinase receptors to transduce their signals. Type II receptor kinases are constitutively active, while Type I receptors, also known as activin receptor-like kinases (ALKs), contain an inactive kinase domain. When the ligands bind to their cognate receptors as dimers, the constitutively active Type II receptor transphosphorylates and activates the kinase domain of type I receptors. The phosphorylated type I receptor will then phosphorylate either SMAD1/SMAD5/SMAD8 or SMAD2/SMAD3, the receptor-specific SMADs (R-SMADs). The phosphorylated R-SMADs will then partner with SMAD4, the common SMAD (Co-SMAD), and translocate into the nucleus where the SMAD complex interact with specific transcription factors to regulate the transcription of their target genes. SMAD6 and SMAD7 are inhibitory (I-SMADs) and can inhibit the activated R-SMADs.

Chapter 1.2

Results

This chapter represents a submitted manuscript.

Primitive Erythropoiesis is Sensitive to RUNX1 Level

Yunglin D. Ma^{1,2}, Elizabeth Arentson¹, Jinjun Dang³, Noel Lenny³, Li-Wei Chang¹,
Shin-Il Kim⁴, Michael Kyba⁵, Emery H. Bresnick⁴, James R. Downing³ and
Kyunghee Choi^{1,2#}

¹Department of Pathology and Immunology, ²Developmental Biology Program
Washington University School of Medicine, St. Louis, MO

³Department of Pathology, St Jude Children's Research Hospital, Memphis, TN

⁴Department of Pharmacology, University of Wisconsin School of Medicine and
Public Health, Madison, WI

#Corresponding author, kchoi@wustl.edu

Key words: *Runx1*, *Gata1*, *Eklf*, TGF β signaling, primitive erythropoiesis, yolk sac
hematopoiesis

Abstract

Primitive hematopoiesis, also known as primitive erythropoiesis, occurs exclusively in the yolk sac and is characterized by its transient nature. Primitive erythroid (EryP) progenitors emerge from the yolk sac by the end of gastrulation, undergo extensive proliferation and differentiation and become extinct by embryonic day 9. By this time, definitive hematopoietic progenitors generated in the yolk sac and/or embryo produce blood cells that represent definitive hematopoiesis. *Runx1* is critical for the emergence of definitive hematopoiesis. Herein, we determined the role of *Runx1* in primitive hematopoiesis. We demonstrate that a high level of enforced *Runx1* expression in the *in vitro* differentiation model of embryonic stem (ES) cells suppressed EryP progenitor generation. Unexpectedly, both *Runx1* null ES and yolk sacs produced a greatly reduced number of EryP progenitors. Furthermore, *Runx1* DNA and CBF β binding were required for optimal EryP generation from the yolk sac. In both *Runx1* null and overexpression ES systems, the reduction in EryP progenitor formation coincided with down regulation of *Gata1* and *Eklf*. Introduction of *Gata1* or *Eklf* partially rescued EryP defects seen in *Runx1* null or overexpression system. TGF β 1 treatment led to *Runx1* upregulation and suppression of EryP formation. *Alk5*, a type-I TGF β 1 receptor, was highly expressed in EryP cells and *Alk5* deficient ES cells generated a higher EryP progenitor number. Collectively, we demonstrate that optimal EryP production is sensitive to *Runx1* expression level.

Introduction

During mouse development, hematopoietic cells are generated from several distinct anatomic sites: yolk sac, embryonic blood vessels including the aorta-gonad-mesonephros region, fetal liver and bone marrow. The first emerging mature hematopoietic cells, designated as primitive erythrocytes (EryP), are exclusively produced in the yolk sac. The primitive erythropoiesis is quickly replaced by adult type hematopoiesis, termed “definitive”. While EryP is believed to develop from mesodermal progenitors, definitive hematopoiesis is established by hematopoietic stem cells (HSCs). Whether HSCs originate from the yolk sac, aorta/genital ridge/mesonephros (AGM) or placenta is an actively investigated area (Cumano et al., 2001; de Bruijn et al., 2000; Lux et al., 2008; Rhodes et al., 2008; Samokhvalov et al., 2007).

EryP cells are characterized by the expression of embryonic globin genes. EryP progenitors in the yolk sac can be detected as early as embryonic day (E) 7.5, undergo extensive proliferation and differentiation in a synchronous manner and become extinct by E9.0 (Palis et al., 1999). Recent studies have established that EryP cells also enucleate, similar to adult globin expressing definitive erythroid (EryD) cells, during maturation in circulation (Fraser et al., 2007; Kingsley et al., 2004). It is possible that EryP extinction merely reflects the hematopoietic site shift from the yolk sac to other organs, such that EryP progenitors are no longer produced from aging yolk sacs. However, as definitive hematopoiesis ensues concomitant to the cessation of primitive hematopoiesis in the yolk sac (Kingsley

et al., 2006; Palis et al., 1999), it is possible that transition from primitive to definitive hematopoiesis could be an active process, which is molecularly regulated.

Runx1, also known as *AML1*, is the most frequent target of chromosome translocations in human acute myeloid leukemia (AML)(Miyoshi et al., 1991). *Runx1* belongs to the core binding factor (CBF) transcription factor family. This family contains a common non-DNA binding CBF β subunit and three CBF α members, *Runx1*, 2 and 3 (Speck and Gilliland, 2002). The mammalian RUNX proteins contain a highly conserved Runt domain, which functions in DNA binding, CBF β subunit interactions, and ATP binding (Crute et al., 1996). By applying site-directed mutagenesis, Nagata and Werner have identified specific amino acids for the DNA-binding and heterodimerization of the Runt domain of RUNX1 (Nagata and Werner, 2001). Previous studies have demonstrated that *Runx1*^{-/-} animals die between E11.5 and E13.5 and display lack of definitive hematopoiesis and hemorrhage in the central nervous system (Okuda et al., 1996; Wang et al., 1996). The chimeric animals generated between *Runx1*^{-/-} ES cells and wild-type blastocysts showed no contribution of *Runx1*^{-/-} ES cells to any hematopoietic tissues despite their contributions to other tissues (Okuda et al., 1996). Importantly, *Runx1* deficient embryos failed to generate hematopoietic clusters, which arise from the ventral side of the dorsal aorta in the AGM region (North et al., 1999). Collectively, these studies have demonstrated that *Runx1* is essential for the emergence of definitive hematopoiesis.

Accumulating studies indicate that the TGF β superfamily of growth factors is critical for hematopoietic and vascular development (Larsson and Karlsson, 2005). During early embryonic development, TGF β 1 expression can be detected in the yolk sac blood islands, the mesodermal cells of the allantois, and the cardiac mesoderm of the embryo (Akhurst et al., 1990). Upon binding type II receptor, TGF β induces heteromeric receptor complex formation with type I transmembrane serine-threonine kinases. Activated type I receptors, Alk1 and Alk5, phosphorylate cytoplasmic receptor-associated SMAD proteins (R-SMADs), SMAD1/5/8 and SMAD2/3, respectively (Shi and Massague, 2003). Both *Tgf β 1* and *Tgf β 11* deficient mice, which die around E10.5, display anemia with severe reductions of mature erythrocytes and defective angiogenesis in the yolk sac (Dickson et al., 1995; Oshima et al., 1996). While *Alk5*^{-/-} mice are also anemic, they have an increased number of presumably definitive erythroid progenitors, indicating that hematopoietic deficiency seen in these mice are indirect due to vascular defects (Larsson et al., 2001). We previously reported that TGF β 1 could inhibit BMP4 and VEGF mediated hematopoietic induction from *in vitro* differentiating ES cells (Park et al., 2004). These studies suggest that TGF β 1 signaling is involved in hematopoietic and vascular development and implies that TGF β 1 through ALK5 could inhibit the growth and differentiation of erythroid progenitors.

By utilizing various *Runx1* mutant mice as well as an *in vitro* differentiation model

of ES cells, we investigated whether *Runx1*, an essential gene for the generation of definitive hematopoiesis, could modulate primitive hematopoiesis. Our studies demonstrate that *Runx1* plays a critical role in EryP development. First, *Runx1* deficient animals generated greatly reduced number of EryP progenitors. Both DNA binding and CBF β interaction of RUNX1 were required for EryP progenitor development. Second, a high dosage of RUNX1 during EB differentiation could suppress EryP progenitor formation. We also show that TGF β 1 could upregulate *Runx1* expression and suppressed EryP progenitor formation. *Alk5*, a type-I TGF β 1 receptor, was highly expressed in EryP cells and *Alk5* deficient ES cells generated a higher EryP progenitor number. Collectively, *Runx1* level could be important for optimal primitive erythropoiesis.

Materials and Methods

Cell culture and hematopoietic progenitor assays

We received the *Runx1* cDNA (full length mouse *Runx1b* encoding amino acid residues 1-451), J1, *Runx1*^{+/-}, and *Runx1*^{-/-} ES cells from Dr. Nancy Speck, the *Alk1*^{+/-} and *Alk1*^{-/-} ES cells from Dr. Paul Oh, the *Alk5*^{+/+} and *Alk5*^{-/-} ES cells from Dr. Stefan Carlson, and the *Tgfβ1*^{+/-} and *Tgfβ1*^{-/-} ES cells from Dr. Ashok Kulkarni. The inducible RUNX1 ES (iRUNX1) cell was generated as described previously (Kyba et al., 2002; Lugus et al., 2007).

Embryonic stem cell culture and *in vitro* ES differentiation were performed as described previously (Ma et al., 2008; Park et al., 2004; Zhang et al., 2005).

Exogenous RUNX1 was induced in iRUNX1 EB cells with 1.0 µg/ml or indicated concentration of doxycycline (Dox; Sigma). The following factors were used in differentiation: BMP4 (5 ng/ml; R&D Systems), VEGF₁₆₅ (10 ng/ml; R&D Systems), TGFβ1 (10 ng/ml; R&D Systems), SB431542 (2 µM; TOCRIS bioscience), Noggin (50 ng/ml; R&D Systems), DAPT (2 µM added 2 times/day; R&D Systems), and Cyclopamine (3 µM; TRC-Canada).

EryP colonies were generated by harvesting EB cells on the indicated day of differentiation, dissociating them in trypsin, passaging them through a 20G needle 5-7 times, and plating them in methylcellulose containing 10% plasma-derived serum (PDS, Animal Technologies, Inc. Texas), 12.5 µg/ml ascorbic acid, 5% protein-free hybridoma medium (PFHM-II; Gibco), L-glutamine (2 mM),

transferrin (300 µg/ml; Boehringer Mannheim), MTG (4.5×10^{-4} M), and Epo (2 units/ml; Amgen). EryP colonies were counted 4-5 days after replating.

Definitive erythroid and myeloid colony assays, day 6 EB cells were replated in methylcellulose containing 10% plasma-derived serum (PDS, Animal Technologies, Inc. Texas), 12.5 µg/ml ascorbic acid, 5% protein-free hybridoma medium (PFHM-II; Gibco), L-glutamine (2 mM), transferrin (200 µg/ml; Boehringer Mannheim), MTG (4.5×10^{-4} M), and Epo (2 units/ml; Amgen), together with the following cytokines: kit ligand (KL 1% conditioned media), IL-3 (1% conditioned media), IL-1 (5 ng/ml), IL-6 (5 ng/ml), IL-11 (5 ng/ml), G-SCF (2 ng/ml), M-CSF (5 ng/ml) and GM-CSF (3 ng/ml). Blast colonies were generated by replating day 2.75 EB cells in the presence of VEGF (5 ng/ml), kit ligand (1% conditioned media), and D4T endothelial cell conditioned media (25%). Blast colonies and hematopoietic colonies were counted 5-8 days after replating.

Biochemical analysis of iRUNX1 cells

To determine the induction of RUNX1 protein in iRUNX1 cells, ES cells were differentiated in serum with the indicated amount of Dox added on day 3 and harvested on day 4. Subsequent steps to detect the inducible RUNX1 were performed as previously described (Park et al., 2004). For generation of the iRUNX1 ES cells, FLAG tag was added to the N-terminus of RUNX1. The FLAG tag antibody (Sigma) was used to detect the induction of exogenous RUNX1.

Generation of Runx1 mutant knock-in mice

Mouse Runx1 cDNA was digested with SacII and ClaI to obtain a 1.2-kb fragment of partial coding sequence containing 62bp of exon 4 and exons 5-8 and was cloned into pBluescript II. The rabbit β globin polyadenylation (pA) cassette was inserted to the Runx1 cDNA. A neomycin-positive selection cassette, expressed under the control of the herpes simplex virus thymidine kinase promoter with a 5' SacII site, was then inserted in reverse orientation downstream of the pA cassette. Site-directed mutagenesis was performed to introduce mutations into the Runx1 cDNA using a QuickChange site-directed mutagenesis kit (Stratagene, La Jolla, CA) and mutagenic primers for F146S (5'-GAGCGGTAGAGGCAAGAGCTCCACTCTGACCATCACCGTCT-3'), T149A (5'-AGGCAAGAGCTTCACTCTGGCCATCACCGTCTTTACAAATC-3'), and R174Q (5'-CACAGTGGACGGCCCCCAAGAACCCCGAAGACATC-3'). Next, the partial Runx1 cDNA-PA-neo was removed by digestion with SacII and cloned into a unique SacII site in AML-SS-12, which contained a 10-kb SacI-SpeI fragment of mouse genomic DNA flanking Runx1 exon 4 and a diphtheria toxin-negative selection cassette that was cloned into the vector pBluescript II SK (Okuda et al., 1996). The presence of each point mutation and the exon 4-8 sequences in the targeting construct were confirmed by sequence analysis.

The resulting targeting vector was linearized with NotI, and 25 μ g was transfected into the 129/SVEV ES cells (Specialty Media, Phillipsburg, NJ) by electroporation. Homologous recombinant clones were identified by Southern

blot analysis. Blastocyst injection and breeding of chimeras were performed as described previously (Lorsbach et al., 2004).

Yolk sac isolation

Runx1^{+/-}, *Runx1*^{+/F146S}, *Runx1*^{+/T149A}, and *Runx1*^{+/T174Q} mice were used for timed mating. Yolk sacs were isolated at the indicated times and somite pairs were counted. Yolk sacs were incubated in collagenase (Sigma) with 20% FCS in PBS for 1.5-2 hours at 37°C, passaged through a 20G needle 4-6 times, and washed with 10% FCS in PBS twice. The single-cell suspensions of yolk sacs were subjected to hematopoietic replating as described above. Hematopoietic colonies were counted 4-7 days after replating.

Retrovirus production and infection of differentiated ES cells

Retroviral infection using the Phoenix packaging cell line was described previously (Grignani et al., 1998). Briefly, Phoenix packaging cells were maintained in DMEM with 10% FCS and 1% L-Glutamine. On day 0, 3x10⁵ cells were plated in one well of a gelatinized 6-well plate. On day 1, Phoenix cells were transfected with 3 µg of MSCV-IRES-GFP (control), MSCV-RUNX1-IRES-GFP, MSCV-GATA1-IRES-GFP, or MSCV-EKLF-IRES-GFP using FuGene 6 (Roche). The medium was changed 18-24 hours later. The transfected cells were then grown at 32°C for 24 hours, and the medium containing viral particles was collected and filtered through a 0.45 µm filter before use. *Runx1*^{-/-} and iRUNX1 ES cells were differentiated on OP9 cells for 3 days and infected with MSCV-

IRES-GFP (control), MSCV-RUNX1-IRES-GFP, MSCV-GATA1-IRES-GFP, or MSCV-EKLF-IRES-GFP viral supernatants in the presence of polybrene (7.5 µg/ml). Dox (1.0 µg/ml) was added to iRUNX1 cells on day 3 of differentiation. The cells were collected on day 4 by dissociation in trypsin for EryP replating.

Gene expression analysis

RNA preparation and cDNA generation were described previously (Lugus et al., 2007; Park et al., 2004). qRT-PCR reactions were performed in duplicate or triplicate. Primer sequences utilized in this study are described in Supplementary Table 1.

GeneChip analysis

J1, *Runx1*^{-/-}, iRUNX1, and iRUNX1+Dox EB cells were differentiated in serum. Dox was added on day 3 of EB formation, and cells were collected on day 4. Total RNA was purified using TRIzol (Invitrogen, CA), following the manufacturer's protocol. Aliquots of 3 µg of total RNA were subjected to GeneChip® Mouse Genome 430 2.0 Array (Affymetrix). GeneChip results were analyzed in dChip (Li and Wong, 2001; Zhong et al., 2003). Differences of gene expression were determined by applying a 90% confidence interval of >1.4-fold and above and using a baseline to experimental intensity difference of >100.

Flow cytometry

FACS analysis has been described previously (Ma et al., 2008; Park et al., 2004). Briefly, EBs were collected and dissociated in 7.5 mM EDTA in PBS for 1 minute at 37°C. Cells were immediately resuspended in washing/staining buffer (4% FSC in PBS) and passaged through a 20G needle 5-7 times. 5×10^5 cells were incubated with anti-Flk-1-phycoerythrin (Flk-1-PE, Pharmingen, 1:200 dilution) for 15 minutes at 4°C in the dark, washed three times, and analyzed using a Becton-Dickinson FACS Caliber. FACS data was analyzed with CellQuest software (Becton-Dickinson). For Ter119 detection in E10.5 embryos, embryo proper and yolk sacs were incubated for 90 minutes at 37°C in 0.1% collagenase (Sigma-Aldrich, St Louis, MO) with 20% fetal bovine serum in phosphate-buffered saline (PBS), and were separated into single-cell suspension by passing through 20-gauge syringes. The resulting suspension cells were stained with FITC-conjugated Ter119 antibodies (eBioscience, San Diego, CA), and analyzed by FACS. The absolute Ter119+ cell number is equal to the total cell number from the embryo proper or the yolk sac multiplied by the percentage of Ter119+ cells analyzed by FACS.

Yolk sac benzidine staining

Yolk sacs were fixed in 1 mL 0.2% benzidine solution, which was prepared by dissolving 100mg of bezidine dihydrochloride (Sigma) in 50mL of 0.5% acetic acid at room temperature for 15 minutes. Next, 20 μ l of 30% H₂O₂ was added to the tissue and incubated for 5-15 minutes at room temperature. Stained yolk sacs were photographed by light microscopy.

Statistics

The results of hematopoietic replating, qRT-PCR, FACS analysis were analyzed by Student's t test. $P < 0.05$ was considered statistically significant.

Results

Enforced RUNX1 expression in EBs suppresses primitive erythroid progenitor formation

To assess if *Runx1* has a role in EryP development, we first examined EryP formation and *Runx1* expression during ES differentiation. Specifically, A2Lox ES cells, a derivative of E14Tg2a ES cells (Iacovino et al., 2009) were differentiated in serum-containing media. These *in vitro* differentiated ES cells, termed embryoid bodies (EB), were analyzed from day 0 to 7 for EryP progenitors and *Runx1* expression. As in the developing embryo, EryP progenitors appeared within a very short window of time in the ES/EB system. EryP progenitors were not detected until day 3 of differentiation, rapidly increased by day 4, and sharply diminished thereafter (Figure 1.2-1A). Thus, EryP progenitor formation and/or proliferation occur between days 3 and 4 during EB development. In EBs, *Runx1* expression was detected starting from day 3, rapidly increased and reached a plateau after day 4 (Figure 1.2-1B). Initial analyses suggested that the onset of *Runx1* expression coincided with the EryP emergence and that high levels of *Runx1* expression were sustained when EryP progenitors were no longer produced in later time points (\geq days 5) during EB development.

To evaluate the role of *Runx1* in primitive erythropoiesis, we employed an inducible ES cell system (Kyba et al., 2002). To this end, we generated inducible RUNX1 (iRUNX1) ES cells by targeting the tet-responsive locus of A2Lox ES cells with the full length mouse *Runx1* cDNA (amino acid residues 1-451), which

was fused to a FLAG tag at the 5' end (Figure 1.2-1C). After the correct targeting event was validated by a tet-responsive locus/cDNA vector-specific PCR (not shown), inducible *Runx1* expression was verified by adding doxycycline (Dox) to differentiating ES cells. Specifically, iRUNX1 ES cells were differentiated in serum and treated with various concentrations of Dox on day 3, at which time point, EryP progenitors are rapidly emerging. Day 4 EB cells were harvested and subjected to Western blot analyses using anti-FLAG tag antibody. Exogenous RUNX1 was detectable in day 4 EBs with Dox concentrations as low as 0.03 $\mu\text{g/ml}$ (Figure 1.2-1D). The protein analyses were corroborated by qRT-PCR of *Runx1* expression, which showed that Dox-treated iRUNX1 EB cells had approximately 3- fold (0.01 $\mu\text{g/ml}$ Dox) to 11-fold (≥ 1 $\mu\text{g/ml}$ Dox) induction of *Runx1* mRNA expression compared to non-induced cells (Figure 1.2-1E). To determine the effect of enforced *Runx1* expression on EryP, iRUNX1 ES cells were differentiated in serum. Exogenous RUNX1 was induced from day 3 by adding Dox, and day 4 EB cells were subjected to EryP replating. The number of EryP colonies generated was significantly decreased by about 50%-70% when Dox (≥ 1 $\mu\text{g/ml}$) was added to EBs compared to -Dox controls or when Dox was added at low concentrations (≤ 0.03 $\mu\text{g/ml}$) (Figure 1.2-1F, not shown). No notable differences were observed in proliferation and/or apoptosis between Dox treated versus non-treated EB cells, as judged by Annexin V staining or viable cell count (not shown). Our result showed that high level of *Runx1* expression between days 3 and day 4 during EB differentiation has suppressive effect on primitive erythroid progenitor formation.

***Runx1* is required for optimal primitive hematopoiesis**

Previous studies suggested that *Runx1* null mice did not have defects in primitive erythropoiesis. However, quantitative analyses on EryP were not performed in these studies (Okuda et al., 1996; Wang et al., 1996). In light of the findings that EryP progenitor formation was sensitive to awe determined if EryP progenitor number or the kinetics of EryP development could be altered in the absence of *Runx1*. To this end, *Runx1*^{+/+}, *Runx1*^{+/-}, and *Runx1*^{-/-} ES cells were differentiated in serum, collected from day 3 to day 7, and subjected to EryP replating. Unexpectedly, we saw a great reduction in EryP colony number from *Runx1*^{-/-} EB cells at all time points (Figure 1.2-2A). When day 2.75 EB cells were collected and subjected to blast colony replating (Faloon et al., 2000), we observed a significantly reduced number of blast colonies, compared to *Runx1*^{+/-} and *Runx1*^{+/+} controls (Supplementary Figure 1.2-1A). However, we did not detect any changes in the frequency or kinetic changes in FLK-1 expression in EB development (Supplementary Figure 1.2-1B). This suggested that *Runx1* is required downstream of *Flk1* mesoderm. To verify the essential role of *Runx1* in definitive hematopoiesis, *Runx1*^{+/+}, *Runx1*^{+/-}, and *Runx1*^{-/-} ES cells were differentiated in serum for six days, and day 6 EBs were subjected to definitive and myeloid progenitor replatings. No hematopoietic colonies were generated from *Runx1*^{-/-} EBs (Supplementary Figure 1.2-2A, B). This result is consistent with the phenotype of the *Runx1* knock-out embryos that have no definitive

hematopoiesis (Okuda et al., 1996; Wang et al., 1996). Collectively, *Runx1* clearly plays a role in regulating normal primitive hematopoiesis.

To further investigate the role of Runx1 in primitive hematopoiesis, we examined EryP from *Runx1*^{-/-} yolk sacs. *Runx1*^{+/-} mice were generated as previously described and were used for establishing timed matings (Okuda et al., 1996). Consistent with previous studies, E9.5-E10.5 *Runx1*^{-/-} embryos did not display any overt phenotypic defects and were similar in gross morphology to +/- or wild type controls (Supplementary Figure 1.2-3A and not shown). Moreover, E10.5 *Runx1*^{-/-} embryos showed similar benzidine staining pattern compared to +/- or +/+ embryos (Supplementary Figure 1.2-3B). Ter119⁺ cells were readily present within E10.5 *Runx1*^{-/-} embryos, although the absolute number of Ter119⁺ cells was slightly less compared to +/- or +/+ embryos (Supplementary Figure 1.2-3C). Despite the seemingly normal presence of EryP cells, when E8.5 *Runx1* +/+, +/- and -/- embryos were analyzed, a significantly reduced number of primitive erythroid colonies was obtained from E8.5 *Runx1*^{-/-} yolk sacs compared to littermate controls (Figure 1.2-2B). No definitive erythroid or myeloid colonies were generated when *Runx1*^{-/-} yolk sacs from later time points were analyzed, confirming that Runx1 was required for definitive hematopoietic development (data not shown). This suggests that even though the generation of EryP progenitor was greatly compromised in *Runx1*^{-/-} embryos, the remaining EryP progenitors generated were sufficient for maintaining and providing the integrity of the developing embryo until definitive hematopoiesis is required.

DNA binding and CBF β interaction of Runx1 is required for normal primitive hematopoiesis

DNA binding and CBF β interaction are critical for proper RUNX1 function. Based on the current structural and biochemical studies, mutations of the Runt domain can be classified into three groups: mutations that interrupt DNA binding ability (i.e. R174Q), mutations that disrupt CBF β binding (i.e. T149A), and mutations that cause incorrect folding of the Runt domain (i.e. F146S), resulting in the loss of DNA and CBF β binding (Matheny et al., 2007; Nagata and Werner, 2001). To determine whether RUNX1 DNA or CBF β binding is required for primitive hematopoiesis, we examined F146S, T149A and R174Q Runx1 knock-in mutant mice. When heterozygous mutant mice were brother-sister mated and the resulting pups analyzed at P21, we did not detect any live homozygous animals for F146S, T149A, or R174Q *Runx1* mutant alleles (Table 1). Next, heterozygous mutant mice were used for timed matings, and E8.5 yolk sacs of these mutant embryos were subjected to EryP replating. Somite pairs were counted while dissecting the embryos to ensure that they were at similar developmental stages. The number of EryP colonies obtained from *Runx1*^{F146S/F146S} homozygous mutant animals was significantly less, compared to their littermate controls (Figure 1.2-2C). The reduction level in the number of EryP colonies from the *Runx1*^{F146S/F146S} yolk sacs was similar to that from the *Runx1*^{-/-} yolk sacs. *Runx1*^{T149/T149} or the *Runx1*^{R174Q/R174Q} yolk sacs also produced less EryP progenitors, however, the number of EryP colonies generated from these animals was higher than that from

the *Runx1*^{F146S/F146S} or *Runx1*^{-/-} yolk sacs (Figure 1.2-2D, E). The results demonstrate that the ability of Runx1 to interact with CBF β and bind DNA are required for its normal role in primitive hematopoiesis, suggesting that components of the Runx1 transcriptional network are important for the normal development, proliferation and survival of primitive erythroid cells.

Common erythroid genes are downregulated in *Runx1* deficient as well as in RUNX1 enforced EBs

To understand molecular mechanisms by which *Runx1* regulates primitive hematopoiesis, we performed global gene expression analyses of *in vitro* differentiated *Runx1*^{+/+}, *Runx1*^{-/-} and iRUNX1 \pm Dox EBs. Dox was treated from days 3-4 at 1 μ g/ml. RNA samples were subjected to Affymetrix GeneChip[®] Mouse Genome 430 2.0 microarray analyses. GeneChip results were analyzed using dChip. We identified that 296 genes were reduced in the *Runx1*^{-/-} EBs, compared to *Runx1*^{+/+} EBs, by more than 1.4 fold and that 1219 genes were decreased in Dox treated iRUNX1 EBs compared to -Dox controls. Among the down-regulated genes in *Runx1*^{-/-} and RUNX1 enforced EBs, hematopoietic-related genes were selected and listed in Table 2.

Upon examining the gene expression profile, we noticed several patterns associated with *Runx1* deficiency and *Runx1* overexpression. First, there were genes that were downregulated in Dox treated cells but not in *Runx1*^{-/-} EBs. These included *Lmo2* and *Scf*. Recently, *Scf* has been reported to be upstream

of *Runx1* (Landry et al., 2008; Nottingham et al., 2007). Second, we found genes that were downregulated in both *Runx1*^{-/-} and enforced RUNX1 EB cells. These included *Hbb-y* and *Hba-a1* as well as several transcription factors including *Gata1*, *Eklf* and *cMyb*. This category of genes could be *Runx1* dosage sensitive downstream targets. Third, several genes, including *Eraf* and glycoprotein A (*Gypa*), were greatly downregulated in *Runx1*^{-/-} EBs, while no significant changes were observed in Dox treated iRUNX1 EB cells.

To confirm gene chip analyses, we analyzed day 4 EB cells from *Runx1*^{+/+}, *Runx1*^{-/-} and iRunx1±Dox by qRT-PCR analyses. Such analyses confirmed that *Gata1*, *Eklf* and *cMyb* were downregulated in *Runx1*^{-/-} as well as *Runx1* overexpressed EBs (Figure 1.2-3A, B). The results were consistent with the interpretation that *Runx1* deficiency or enforced RUNX1 results in down-regulation of *Gata1* and *Eklf* expression, which in turn affects optimal EryP progenitor formation.

To establish that *Runx1* is upstream of *Gata1* and/or *Eklf* in EryP development, we first determined whether *Runx1* could rescue EryP defects in *Runx1*^{-/-} ES cells. Specifically, *Runx1*^{-/-} ES cells were differentiated on OP9 cells for 3 days and then infected with MSCV-RUNX1 virus for an additional day. Day 4 differentiated cells were harvested and analyzed for EryP. *Runx1*^{-/-} cells infected with MSCV-RUNX1 virus generated an increased number of EryP colonies compared to *Runx1*^{-/-} cells infected with GFP control virus (Figure 1.2-3C). Next,

we tested whether *Gata1* and/or *Eklf* could rescue EryP defects observed in *Runx1*^{-/-} or Dox treated iRunx1 EB cells. To this end, *Runx1*^{-/-} and iRUNX1 ES cells were differentiated on OP9 cells for 3 days, infected with MSCV-GATA1 and/or the MSCV-EKLF virus for an additional day. Dox was added to iRUNX1 differentiating ES cells on day 3. Day 4 differentiated cells were harvested and analyzed for EryP. *Runx1*^{-/-} differentiated cells that were infected with MSCV-GATA1 or with MSCV-EKLF virus generated an increased number of EryP colonies compared to control retrovirus-infected cells (Figure 1.2-3C). Moreover, MSCV-GATA1 or the MSCV-EKLF virus also partially rescued EryP defects observed in Dox treated iRUNX1 cells (Figure 1.2-3D). We did not observe any obvious additive effects between *Gata1* and *Eklf*.

TGFβ1 suppresses primitive hematopoiesis

We previously demonstrated an inhibitory role for TGFβ1 in hematopoietic development in the ES/EB system (Park et al., 2004). To further elucidate signaling pathways that might regulate EryP generation, we tested various pharmacological inhibitors known to affect hematopoietic differentiation in the ES/EB system. As the window of time between days 3 and 4 is critical for EryP progenitor formation and/or expansion, we added various inhibitors on day 3 and analyzed day 4 EBs for EryP colonies. Of the factors tested, TGFβ1 inhibited EryP progenitor formation. Meanwhile, inhibition of BMP (noggin), Notch (DAPT, gamma-secretase inhibitor N-S-phenyl-glycine-t-butylester) or Hedgehog (cyclopamine) signaling did not affect the number of EryP colonies formed

(Figure 1.2-4A and Supplementary Figure 1.2-4A). As the inhibitory effect of TGF β 1 on EryP could be serum dependent, we also performed ES differentiation in serum free conditions by adding BMP4 and VEGF (Park et al., 2004). TGF β 1 inhibitory role was also observed in serum free conditions (Figure 1.2-4C). Importantly, *Runx1* expression was increased when TGF β 1 was added to the culture (Figure 1.2-4B and 1.2-4D). *Runx1* expression was increased even greater in serum free conditions (Figure 1.2-4D). We did not observe substantial changes of *Runx1* expression among other inhibitor treated EBs (Supplementary Figure 1.2-4B).

To determine if the potential inverse relationship between TGF β 1 and *Runx1* expression in EryP formation was relevant, we next analyzed *Tgf β 1*^{-/-} ES cells. As serum might contain TGF β 1, we applied serum free conditions in generating EryP by adding BMP-4 and VEGF. In serum free conditions, day 5 EB cells generated prominent number of EryP colonies (Figure 1.2-4E). *Tgf β 1*^{-/-} ES cells generated a greater number of EryP colonies compared to +/+ or +/- ES cells (Figure 1.2-4E and not shown). Importantly, *Runx1* expression levels in day 4 or 5 *Tgf β 1*^{-/-} EB cells were significantly lower compared to *Tgf β 1*^{+/-} EB cells (Figure 1.2-4F).

TGF β 1 suppresses primitive erythropoiesis through ALK5

TGF β 1 can bind either type I receptor, ALK1 or ALK5, to activate down-stream SMAD1/5/8 or SMAD2/3, respectively (Goumans et al., 2002; Lux et al., 1999;

Oh et al., 2000; Shi and Massague, 2003). In order to determine which type I TGF β 1 receptor is responsible for the suppression of EryP, we first examined *Alk1* and *Alk5* expression levels in maturing EryP cells. Specifically, wild-type ES cells were differentiated in serum, and day 4 EB cells were subjected to EryP replating. EryP colonies were collected two and three days after replating and subjected to qRT-PCR analysis. Gene expression analyses of day 2 and day 3 EryP cells demonstrated that *Alk5*, not *Alk1*, was highly expressed in differentiating EryP cells (Figure 1.2-5A).

Next, we used the ES/EB system of *Alk1* and *Alk5* null ES cell lines to further dissect the axis of the TGF β 1 signaling in primitive hematopoiesis (Larsson et al., 2001; Oh et al., 2000). Specifically, we differentiated *Alk1*^{-/-} and *Alk5*^{-/-} ES cells, along with their controls, in serum for 4 days, and EB cells were subjected to EryP replating. As shown in Figure 1.2-5B, *Alk5*^{-/-} EBs generated a significantly higher number of EryP colonies compared to *Alk5*^{+/+} EBs. However, the number of EryP colonies generated from *Alk1*^{+/-} vs *Alk1*^{-/-} was similar (Figure 1.2-5B). To further examine the TGF β 1-ALK5 axis in EryP development, we treated wild-type EBs in serum with SB431542 on day 3 (Inman et al., 2002), which inhibits the interaction between TGF β 1 and ALK5, not ALK1. SB431542 treated EBs generated more EryP colonies than non-treated EBs (Supplementary Figure 1.2-5). To eliminate the possibility that TGF β 1 could use additional receptors in EryP suppression, we used serum-free differentiation conditions to test whether EryP colony numbers could be further decreased with TGF β 1 treatment in *Alk5*^{-/-} EBs.

We subjected *Alk1^{+/-}*, *Alk1^{-/-}*, *Alk5^{+/+}*, and *Alk5^{-/-}* ES cells to serum-free differentiation with BMP4 and VEGF. TGFβ1 was added on day 3, and day 4 EB cells were analyzed for EryP colony formation. The results showed that *Alk5^{-/-}* EBs had similar EryP colonies regardless of TGFβ1 treatment, whereas *Alk1^{-/-}* EBs generated less number of EryP colonies when treated with TGFβ1 (Figure 1.2-5C). *Runx1* was expressed at much lower levels in day 4 *Alk5^{-/-}* EBs compared to *Alk5^{+/+}* EBs (Figure 1.2-5D). In addition, *Runx1* expression levels were similar in *Alk1^{-/-}* and controls. However, both *Gata1* and *Eklf* were downregulated by TGFβ1, but upregulated in *Alk5^{-/-}* EBs (Supplementary Figure 1.2-6A, B). Collectively, these data indicated that TGFβ1 through ALK5, rather than through ALK1, could modulate *Runx1* expression to suppress EryP progenitor development and/or proliferation.

Discussion

The expression of *Runx1* is among the earliest molecular markers for blood formation in *Xenopus*, and expression of a truncated Xaml protein can inhibit primitive hematopoiesis (Tracey et al., 1998). Studies in zebrafish demonstrate that *runx1* is involved in both primitive and definitive hematopoiesis (Kalev-Zylinska et al., 2002). In mice, *Runx1* expression can be first detected in extraembryonic mesodermal cells at E7.25 and in primitive erythrocytes of the yolk sac blood islands at E8.0-E8.5 (Lacaud et al., 2002; North et al., 1999). Herein, we demonstrate that yolk sacs from *Runx1* mutant mice (*Runx1*^{-/-}), harboring homozygous deletion of the Runt domain encoding exon 4, have defects in primitive hematopoiesis. The defect was at the progenitor level, as the number of EryP progenitors was greatly decreased in these mice. However, we could still detect Ter119⁺ cells in yolk sacs from the *Runx1*^{-/-} embryos at E10.5, at a level, which was similar to that of wild type controls. Benzidine staining levels were also comparable between wild type and *Runx1*^{-/-} embryos at E10.5. Although we have not examined mature EryP cell morphology, Yokomizo et al. recently showed that circulating primitive erythrocytes from *Runx1*^{-/-} embryos, which also delete exon 4, were morphologically defective (Yokomizo et al., 2008). We suggest that the residual EryP precursors present in *Runx1*^{-/-} embryos could still produce mature primitive erythroid cells, which could deliver adequate oxygen to sustain the survival of the knockout embryos during the early embryogenesis. In adult, only a small fraction of hematopoietic stem cells (HSCs) generate mature blood cells at a given time. Thus, to guarantee production of

EryP cells, it is possible that developing embryos reserve a large number of EryP progenitors, which exceed the amount that the embryo actually requires. Future studies to determine whether all EryP progenitors participate in generating mature EryP cells are warranted. Alternatively, Yokomizo et al. showed that the number of EryP progenitors present within the *Runx1*^{-/-} embryos, was similar to that from +/- control embryos (Yokomizo et al., 2008). As the authors in this study used the whole embryo for EryP replating, this study suggests an intra-embryonic generation of EryP progenitors in the absence of *Runx1*. Previous studies support the notion that Runx1 dosage could modulate hematopoietic progenitor production from different embryonic tissues. Specifically, the spatial and temporal appearance of hematopoietic stem cells (HSCs) in the yolk sac and AGM is sensitive to Runx1 dosage, as HSCs appear prematurely in the E10 *Runx1*^{+/-} yolk sac and there was a premature termination of HSC activity in the *Runx1*^{+/-} AGM explant culture (Cai et al., 2000). Studies on whether AGM can generate EryP progenitors when Runx1 mediated definitive hematopoietic program is absent are warranted.

Intriguingly, in contrast to *Runx1*^{-/-} mice, which delete exon 4, that we used in this study, another Runx1 mutant mouse line (North et al., 1999), which harbors *lacZ* in place of exon 7 and 8, or *Runx1*^{LacZ/LacZ} ES cells do not appear to have EryP defects (Lacaud et al., 2002). This suggests that a functional Runt domain is critical for primitive EryP development. Indeed, by utilizing *Runx1* mutant mice homozygous for DNA, CBFβ as well as DNA and CBFβ-binding domain, we

show that both DNA and CBF β binding are required for optimal EryP development.

While EryP progenitors in the yolk sac were sub-optimally generated in the absence of *Runx1*, we also found that a high level of *Runx1* expression in the ES/EB system was able to repress EryP progenitor formation and/or expansion. *Runx1* can either activate or repress target genes by interacting with co-activator or co-repressor, respectively (Kitabayashi et al., 1998; Lutterbach et al., 2000). Although we could not determine the interaction between RUNX1 and mSin3A co-repressor in the ES/EB system (data not shown), we cannot rule out the possibility that such RUNX1 suppression of EryP was due to RUNX1 interaction with other co-repressors. Currently available studies support the notion that *Runx1* dosage is critical for proper hematopoiesis. As discussed, hematopoietic stem cell and hematopoietic progenitor generation were sensitive to Runx1 dosage (Cai et al., 2000; Mukoyama et al., 2000; North et al., 2002). Additionally, an extra copy of *Runx1* on chromosome 21 could potentially be responsible for predisposing Down's syndrome children to increased risk of developing leukemia (Dufresne-Zacharia et al., 1994; Gurbuxani et al., 2004).

We provide evidence that *Gata1* and *Eklf* are genetically downstream of *Runx1* in EryP development. Both genes were downregulated by enforced Runx1 expression and in *Runx1*^{-/-} EBs compared to wild type controls. Moreover, both *Gata1* and *Eklf* could partially rescue EryP defects seen in induced *Runx1* and

Runx1^{-/-} ES cells. *Gata1* plays a critical role in the regulation of erythroid-specific genes in both primitive and definitive erythroid cells. *Gata1* is highly expressed in both primitive and definitive erythroid progenitors (Whitelaw et al., 1990). *Gata1* knockout ES cells fail to generate EryP progenitors. EryD progenitors fail to mature in the absence of GATA1 (Weiss et al., 1994). *Gata1* knockout ES cells contribute to all non-hematopoietic tissues but fail to give rise to mature red blood cell in chimaeric mice (Pevny et al., 1991). Moreover, GATA1 has been shown to bind to the promoters of many erythroid cell-specific genes including the β globin locus control region (β LCR) (Cantor and Orkin, 2002; Palstra et al., 2008; Vakoc et al., 2005). *Eklf* was originally thought to mainly regulate the adult β -globin genes. However, recent studies have shown that EKLF also regulates embryonic globin expression (Basu et al., 2007; Hodge et al., 2006). *Eklf*^{-/-} embryos have nucleated primitive erythroid cells with an abnormal morphology (Drissen et al., 2005). In *Runx1*^{-/-} EBs, embryonic globin expression was significantly lower compared to wild-type controls. However, we failed to show direct binding of RUNX1 to the *Gata1*, *Eklf*, or β LCR region by chromatin immuno-precipitation (ChIP) analysis (data not shown). We conclude that low embryonic globin expressions in induced *Runx1* and *Runx1*^{-/-} EBs could be due to the suboptimal expression of *Gata1* and *Eklf*.

TGF β 1^{-/-}, *Tgf β RII*^{-/-}, and *Alk5*^{-/-} mice all display anemia and severe defects in angiogenesis in the yolk sac (Dickson et al., 1995; Larsson et al., 2001; Oshima et al., 1996). Despite the severe anemia, *Alk5*^{-/-} yolk sacs contained a higher

number of erythroid progenitors, demonstrating that anemia seen in these mice is secondary to the angiogenic defects. Intriguingly, *TGFβ1*^{-/-} yolk sacs appeared to contain significant numbers of circulating non-hemoglobinized blood cells (Dickson et al., 1995). Herein, we demonstrate that TGFβ1 could up-regulate *Runx1* and suppress EryP progenitor formation. We determined that ALK5 is the major TGFβ type I receptor in primitive erythroid cells. Both *TGFβ1*^{-/-} and *Alk5*^{-/-} ES cells generated a higher number of EryP colonies. It is worth pointing out that the increase in *Runx1* expression level by TGFβ1 treatment in serum was at best 1.5-2 fold. In our studies, TGFβ1 suppressed a broader range of hematopoietic-related transcriptional factors, such as *Scl*, *Gata1*, *Eklf*, *c-myb* and *Lmo2*.

Therefore, we suggest that TGFβ1 could inhibit EryP development through many genetic pathways, one of which could be *Runx1*. Alternatively, previous studies have established that TGFβ growth factors can modulate RUNX protein stability and/or activity. Specifically, TGFβ/BMP-activated Smads can interact with RUNX and stimulate transcription of RUNX target genes (Hanai et al., 1999; Ito, 2004; Miyazono et al., 2004). Moreover, BMP induces differentiation of mesenchymal cells into osteoblasts by upregulating the expression of *Runx2* and its interaction with BMP-activated SMADs (Ito and Miyazono, 2003; Lee et al., 2000; Zhang et al., 2000). In hepatic cells (Wildey and Howe, 2009), TGFβ induces *Runx1*, which in turn interacts with FOXO3 to upregulate *Bim* expression to mediate apoptosis. Finally, TGFβ/BMP activate a stress-activated protein kinase p38 (SAPKs) (Gallea et al., 2001; Hanafusa et al., 1999). Both the Smad and MAPK pathways are essential components of the TGFβ superfamily signaling during osteoblast

differentiation (Derynck et al., 2001; Fujii et al., 1999; Gallea et al., 2001; Nishimura et al., 1998; Yamamoto et al., 1997) and for *Runx2* induction (Lee et al., 2002). We suggest that such interaction between TGF β 1 and *Runx1* also regulates primitive hematopoiesis. Collectively, our studies demonstrate that *Runx1* dosage is critical for optimal EryP progenitor generation. Potentially, TGF β 1 family of factors could be upstream, which can modulate *Runx1* levels or activity to achieve optimal primitive hematopoiesis.

Acknowledgments

We would like to thank Drs. Nancy Speck for *Runx1*^{-/-} ES cells, Paul Oh for *Alk1*^{-/-} ES cells, Stefan Carlson for *Alk5*^{-/-} ES cells and Ashok Kulkarni for *Tgfβ1*^{-/-} ES cells. We are also very thankful to Dr. John D. Crispino and Dr. James J. Bieker for providing us with *Gata1* and *Eklf* cDNA, respectively. We would like to thank Choi lab members for critically reading the manuscript. This work was supported by grants from the NIH Developmental Cardiology and Pulmonary Training Grant 5T32HL07873-08 (Y.D.M.), Washington University Kauffman Fellowship Pathway in Life Sciences Entrepreneurship predoctoral fellowship (Y.D.M.) and the NIH HL55337 and HL63736 (K.C.).

References

- Akhurst, R. J., Lehnert, S. A., Faissner, A. and Duffie, E.** (1990). TGF beta in murine morphogenetic processes: the early embryo and cardiogenesis. *Development* **108**, 645-56.
- Basu, P., Lung, T. K., Lemsaddek, W., Sargent, T. G., Williams, D. C., Jr., Basu, M., Redmond, L. C., Lingrel, J. B., Haar, J. L. and Lloyd, J. A.** (2007). EKLF and KLF2 have compensatory roles in embryonic beta-globin gene expression and primitive erythropoiesis. *Blood* **110**, 3417-25.
- Cai, Z., de Bruijn, M., Ma, X., Dortland, B., Luteijn, T., Downing, R. J. and Dzierzak, E.** (2000). Haploinsufficiency of AML1 affects the temporal and spatial generation of hematopoietic stem cells in the mouse embryo. *Immunity* **13**, 423-31.
- Cantor, A. B. and Orkin, S. H.** (2002). Transcriptional regulation of erythropoiesis: an affair involving multiple partners. *Oncogene* **21**, 3368-76.
- Crute, B. E., Lewis, A. F., Wu, Z., Bushweller, J. H. and Speck, N. A.** (1996). Biochemical and biophysical properties of the core-binding factor alpha2 (AML1) DNA-binding domain. *J Biol Chem* **271**, 26251-60.
- Cumano, A., Ferraz, J. C., Klaine, M., Di Santo, J. P. and Godin, I.** (2001). Intraembryonic, but not yolk sac hematopoietic precursors, isolated before circulation, provide long-term multilineage reconstitution. *Immunity* **15**, 477-85.
- de Bruijn, M. F., Speck, N. A., Peeters, M. C. and Dzierzak, E.** (2000). Definitive hematopoietic stem cells first develop within the major arterial regions of the mouse embryo. *Embo J* **19**, 2465-74.
- Derynck, R., Akhurst, R. J. and Balmain, A.** (2001). TGF-beta signaling in tumor suppression and cancer progression. *Nat Genet* **29**, 117-29.
- Dickson, M. C., Martin, J. S., Cousins, F. M., Kulkarni, A. B., Karlsson, S. and Akhurst, R. J.** (1995). Defective haematopoiesis and vasculogenesis in transforming growth factor-beta 1 knock out mice. *Development* **121**, 1845-54.
- Drissen, R., von Lindern, M., Kolbus, A., Driegen, S., Steinlein, P., Beug, H., Grosveld, F. and Philippsen, S.** (2005). The erythroid phenotype of EKLF-null mice: defects in hemoglobin metabolism and membrane stability. *Mol Cell Biol* **25**, 5205-14.
- Dufresne-Zacharia, M. C., Dahmane, N., Theophile, D., Orti, R., Chettouh, Z., Sinet, P. M. and Delabar, J. M.** (1994). 3.6-Mb genomic and YAC physical map of the Down syndrome chromosome region on chromosome 21. *Genomics* **19**, 462-9.
- Faloon, P., Arentson, E., Kazarov, A., Deng, C. X., Porcher, C., Orkin, S. and Choi, K.** (2000). Basic fibroblast growth factor positively regulates hematopoietic development. *Development* **127**, 1931-41.
- Fraser, S. T., Isern, J. and Baron, M. H.** (2007). Maturation and enucleation of primitive erythroblasts during mouse embryogenesis is accompanied by changes in cell-surface antigen expression. *Blood* **109**, 343-52.
- Fujii, M., Takeda, K., Imamura, T., Aoki, H., Sampath, T. K., Enomoto, S., Kawabata, M., Kato, M., Ichijo, H. and Miyazono, K.** (1999). Roles of bone

morphogenetic protein type I receptors and Smad proteins in osteoblast and chondroblast differentiation. *Mol Biol Cell* **10**, 3801-13.

Gallea, S., Lallemand, F., Atfi, A., Rawadi, G., Ramez, V., Spinella-Jaegle, S., Kawai, S., Faucheu, C., Huet, L., Baron, R. et al. (2001). Activation of mitogen-activated protein kinase cascades is involved in regulation of bone morphogenetic protein-2-induced osteoblast differentiation in pluripotent C2C12 cells. *Bone* **28**, 491-8.

Goumans, M. J., Valdimarsdottir, G., Itoh, S., Rosendahl, A., Sideras, P. and ten Dijke, P. (2002). Balancing the activation state of the endothelium via two distinct TGF-beta type I receptors. *Embo J* **21**, 1743-53.

Grignani, F., Kinsella, T., Mencarelli, A., Valtieri, M., Riganelli, D., Grignani, F., Lanfrancone, L., Peschle, C., Nolan, G. P. and Pelicci, P. G. (1998). High-efficiency gene transfer and selection of human hematopoietic progenitor cells with a hybrid EBV/retroviral vector expressing the green fluorescence protein. *Cancer Res* **58**, 14-9.

Gurbuxani, S., Vyas, P. and Crispino, J. D. (2004). Recent insights into the mechanisms of myeloid leukemogenesis in Down syndrome. *Blood* **103**, 399-406.

Hanafusa, H., Ninomiya-Tsuji, J., Masuyama, N., Nishita, M., Fujisawa, J., Shibuya, H., Matsumoto, K. and Nishida, E. (1999). Involvement of the p38 mitogen-activated protein kinase pathway in transforming growth factor-beta-induced gene expression. *J Biol Chem* **274**, 27161-7.

Hanai, J., Chen, L. F., Kanno, T., Ohtani-Fujita, N., Kim, W. Y., Guo, W. H., Imamura, T., Ishidou, Y., Fukuchi, M., Shi, M. J. et al. (1999). Interaction and functional cooperation of PEBP2/CBF with Smads. Synergistic induction of the immunoglobulin germline Calpha promoter. *J Biol Chem* **274**, 31577-82.

Hodge, D., Coghill, E., Keys, J., Maguire, T., Hartmann, B., McDowall, A., Weiss, M., Grimmond, S. and Perkins, A. (2006). A global role for EKLF in definitive and primitive erythropoiesis. *Blood* **107**, 3359-70.

Iacovino, M., Hernandez, C., Xu, Z., Bajwa, G., Prather, M. and Kyba, M. (2009). A conserved role for Hox paralog group 4 in regulation of hematopoietic progenitors. *Stem Cells Dev* **18**, 783-92.

Inman, G. J., Nicolas, F. J., Callahan, J. F., Harling, J. D., Gaster, L. M., Reith, A. D., Laping, N. J. and Hill, C. S. (2002). SB-431542 is a potent and specific inhibitor of transforming growth factor-beta superfamily type I activin receptor-like kinase (ALK) receptors ALK4, ALK5, and ALK7. *Mol Pharmacol* **62**, 65-74.

Ito, Y. (2004). Oncogenic potential of the RUNX gene family: 'overview'. *Oncogene* **23**, 4198-208.

Ito, Y. and Miyazono, K. (2003). RUNX transcription factors as key targets of TGF-beta superfamily signaling. *Curr Opin Genet Dev* **13**, 43-7.

Kalev-Zylinska, M. L., Horsfield, J. A., Flores, M. V., Postlethwait, J. H., Vitas, M. R., Baas, A. M., Crosier, P. S. and Crosier, K. E. (2002). Runx1 is required for zebrafish blood and vessel development and expression of a human RUNX1-CBF2T1 transgene advances a model for studies of leukemogenesis. *Development* **129**, 2015-30.

Kingsley, P. D., Malik, J., Emerson, R. L., Bushnell, T. P., McGrath, K. E., Bloedorn, L. A., Bulger, M. and Palis, J. (2006). "Maturational" globin switching in primary primitive erythroid cells. *Blood* **107**, 1665-72.

Kingsley, P. D., Malik, J., Fantauzzo, K. A. and Palis, J. (2004). Yolk sac-derived primitive erythroblasts enucleate during mammalian embryogenesis. *Blood* **104**, 19-25.

Kitabayashi, I., Yokoyama, A., Shimizu, K. and Ohki, M. (1998). Interaction and functional cooperation of the leukemia-associated factors AML1 and p300 in myeloid cell differentiation. *Embo J* **17**, 2994-3004.

Kyba, M., Perlingeiro, R. C. and Daley, G. Q. (2002). HoxB4 confers definitive lymphoid-myeloid engraftment potential on embryonic stem cell and yolk sac hematopoietic progenitors. *Cell* **109**, 29-37.

Lacaud, G., Gore, L., Kennedy, M., Kouskoff, V., Kingsley, P., Hogan, C., Carlsson, L., Speck, N., Palis, J. and Keller, G. (2002). Runx1 is essential for hematopoietic commitment at the hemangioblast stage of development in vitro. *Blood* **100**, 458-66.

Landry, J. R., Kinston, S., Knezevic, K., de Bruijn, M. F., Wilson, N., Nottingham, W. T., Peitz, M., Edenhofer, F., Pimanda, J. E., Ottersbach, K. et al. (2008). Runx genes are direct targets of Scl/Tal1 in the yolk sac and fetal liver. *Blood* **111**, 3005-14.

Larsson, J., Goumans, M. J., Sjostrand, L. J., van Rooijen, M. A., Ward, D., Leveen, P., Xu, X., ten Dijke, P., Mummery, C. L. and Karlsson, S. (2001). Abnormal angiogenesis but intact hematopoietic potential in TGF-beta type I receptor-deficient mice. *Embo J* **20**, 1663-73.

Larsson, J. and Karlsson, S. (2005). The role of Smad signaling in hematopoiesis. *Oncogene* **24**, 5676-92.

Lee, K. S., Hong, S. H. and Bae, S. C. (2002). Both the Smad and p38 MAPK pathways play a crucial role in Runx2 expression following induction by transforming growth factor-beta and bone morphogenetic protein. *Oncogene* **21**, 7156-63.

Lee, K. S., Kim, H. J., Li, Q. L., Chi, X. Z., Ueta, C., Komori, T., Wozney, J. M., Kim, E. G., Choi, J. Y., Ryoo, H. M. et al. (2000). Runx2 is a common target of transforming growth factor beta1 and bone morphogenetic protein 2, and cooperation between Runx2 and Smad5 induces osteoblast-specific gene expression in the pluripotent mesenchymal precursor cell line C2C12. *Mol Cell Biol* **20**, 8783-92.

Li, C. and Wong, W. H. (2001). Model-based analysis of oligonucleotide arrays: expression index computation and outlier detection. *Proc Natl Acad Sci U S A* **98**, 31-6.

Lorsbach, R. B., Moore, J., Ang, S. O., Sun, W., Lenny, N. and Downing, J. R. (2004). Role of RUNX1 in adult hematopoiesis: analysis of RUNX1-IRES-GFP knock-in mice reveals differential lineage expression. *Blood* **103**, 2522-9.

Lugus, J. J., Chung, Y. S., Mills, J. C., Kim, S. I., Grass, J., Kyba, M., Doherty, J. M., Bresnick, E. H. and Choi, K. (2007). GATA2 functions at multiple steps in hemangioblast development and differentiation. *Development* **134**, 393-405.

Lutterbach, B., Westendorf, J. J., Linggi, B., Isaac, S., Seto, E. and Hiebert, S. W. (2000). A mechanism of repression by acute myeloid leukemia-1, the target of multiple chromosomal translocations in acute leukemia. *J Biol Chem* **275**, 651-6.

Lux, A., Attisano, L. and Marchuk, D. A. (1999). Assignment of transforming growth factor beta1 and beta3 and a third new ligand to the type I receptor ALK-1. *J Biol Chem* **274**, 9984-92.

Lux, C. T., Yoshimoto, M., McGrath, K., Conway, S. J., Palis, J. and Yoder, M. C. (2008). All primitive and definitive hematopoietic progenitor cells emerging before E10 in the mouse embryo are products of the yolk sac. *Blood* **111**, 3435-8.

Ma, Y. D., Lugus, J. J., Park, C. and Choi, K. (2008). Differentiation of mouse embryonic stem cells into blood. *Curr Protoc Stem Cell Biol Chapter 1*, Unit 1F 4.

Matheny, C. J., Speck, M. E., Cushing, P. R., Zhou, Y., Corpora, T., Regan, M., Newman, M., Roudaia, L., Speck, C. L., Gu, T. L. et al. (2007). Disease mutations in RUNX1 and RUNX2 create nonfunctional, dominant-negative, or hypomorphic alleles. *Embo J* **26**, 1163-75.

Miyazono, K., Maeda, S. and Imamura, T. (2004). Coordinate regulation of cell growth and differentiation by TGF-beta superfamily and Runx proteins. *Oncogene* **23**, 4232-7.

Miyoshi, H., Shimizu, K., Kozu, T., Maseki, N., Kaneko, Y. and Ohki, M. (1991). t(8;21) breakpoints on chromosome 21 in acute myeloid leukemia are clustered within a limited region of a single gene, AML1. *Proc Natl Acad Sci U S A* **88**, 10431-4.

Mukouyama, Y., Chiba, N., Hara, T., Okada, H., Ito, Y., Kanamaru, R., Miyajima, A., Satake, M. and Watanabe, T. (2000). The AML1 transcription factor functions to develop and maintain hematogenic precursor cells in the embryonic aorta-gonad-mesonephros region. *Dev Biol* **220**, 27-36.

Nagata, T. and Werner, M. H. (2001). Functional mutagenesis of AML1/RUNX1 and PEBP2 beta/CBF beta define distinct, non-overlapping sites for DNA recognition and heterodimerization by the Runt domain. *J Mol Biol* **308**, 191-203.

Nishimura, R., Kato, Y., Chen, D., Harris, S. E., Mundy, G. R. and Yoneda, T. (1998). Smad5 and DPC4 are key molecules in mediating BMP-2-induced osteoblastic differentiation of the pluripotent mesenchymal precursor cell line C2C12. *J Biol Chem* **273**, 1872-9.

North, T., Gu, T. L., Stacy, T., Wang, Q., Howard, L., Binder, M., Marin-Padilla, M. and Speck, N. A. (1999). Cbfa2 is required for the formation of intra-aortic hematopoietic clusters. *Development* **126**, 2563-75.

North, T. E., de Bruijn, M. F., Stacy, T., Talebian, L., Lind, E., Robin, C., Binder, M., Dzierzak, E. and Speck, N. A. (2002). Runx1 expression marks long-term repopulating hematopoietic stem cells in the midgestation mouse embryo. *Immunity* **16**, 661-72.

Nottingham, W. T., Jarratt, A., Burgess, M., Speck, C. L., Cheng, J. F., Prabhakar, S., Rubin, E. M., Li, P. S., Sloane-Stanley, J., Kong, A. S. J. et al. (2007). Runx1-mediated hematopoietic stem-cell emergence is controlled by a Gata/Ets/SCL-regulated enhancer. *Blood* **110**, 4188-97.

Oh, S. P., Seki, T., Goss, K. A., Imamura, T., Yi, Y., Donahoe, P. K., Li, L., Miyazono, K., ten Dijke, P., Kim, S. et al. (2000). Activin receptor-like kinase 1 modulates transforming growth factor-beta 1 signaling in the regulation of angiogenesis. *Proc Natl Acad Sci U S A* **97**, 2626-31.

Okuda, T., van Deursen, J., Hiebert, S. W., Grosveld, G. and Downing, J. R. (1996). AML1, the target of multiple chromosomal translocations in human leukemia, is essential for normal fetal liver hematopoiesis. *Cell* **84**, 321-30.

Oshima, M., Oshima, H. and Taketo, M. M. (1996). TGF-beta receptor type II deficiency results in defects of yolk sac hematopoiesis and vasculogenesis. *Dev Biol* **179**, 297-302.

Palis, J., Robertson, S., Kennedy, M., Wall, C. and Keller, G. (1999). Development of erythroid and myeloid progenitors in the yolk sac and embryo proper of the mouse. *Development* **126**, 5073-84.

Palstra, R. J., de Laat, W. and Grosveld, F. (2008). Beta-globin regulation and long-range interactions. *Adv Genet* **61**, 107-42.

Park, C., Afrikanova, I., Chung, Y. S., Zhang, W. J., Arentson, E., Fong Gh, G., Rosendahl, A. and Choi, K. (2004). A hierarchical order of factors in the generation of FLK1- and SCL-expressing hematopoietic and endothelial progenitors from embryonic stem cells. *Development* **131**, 2749-62.

Pevny, L., Simon, M. C., Robertson, E., Klein, W. H., Tsai, S. F., D'Agati, V., Orkin, S. H. and Costantini, F. (1991). Erythroid differentiation in chimaeric mice blocked by a targeted mutation in the gene for transcription factor GATA-1. *Nature* **349**, 257-60.

Rhodes, K. E., Gekas, C., Wang, Y., Lux, C. T., Francis, C. S., Chan, D. N., Conway, S., Orkin, S. H., Yoder, M. C. and Mikkola, H. K. (2008). The emergence of hematopoietic stem cells is initiated in the placental vasculature in the absence of circulation. *Cell Stem Cell* **2**, 252-63.

Samokhvalov, I. M., Samokhvalova, N. I. and Nishikawa, S. (2007). Cell tracing shows the contribution of the yolk sac to adult haematopoiesis. *Nature* **446**, 1056-61.

Shi, Y. and Massague, J. (2003). Mechanisms of TGF-beta signaling from cell membrane to the nucleus. *Cell* **113**, 685-700.

Speck, N. A. and Gilliland, D. G. (2002). Core-binding factors in haematopoiesis and leukaemia. *Nat Rev Cancer* **2**, 502-13.

Tracey, W. D., Jr., Pepling, M. E., Horb, M. E., Thomsen, G. H. and Gergen, J. P. (1998). A *Xenopus* homologue of aml-1 reveals unexpected patterning mechanisms leading to the formation of embryonic blood. *Development* **125**, 1371-80.

Vakoc, C. R., Letting, D. L., Gheldof, N., Sawado, T., Bender, M. A., Groudine, M., Weiss, M. J., Dekker, J. and Blobel, G. A. (2005). Proximity among distant regulatory elements at the beta-globin locus requires GATA-1 and FOG-1. *Mol Cell* **17**, 453-62.

Wang, Q., Stacy, T., Binder, M., Marin-Padilla, M., Sharpe, A. H. and Speck, N. A. (1996). Disruption of the *Cbfa2* gene causes necrosis and hemorrhaging in the central nervous system and blocks definitive hematopoiesis. *Proc Natl Acad Sci U S A* **93**, 3444-9.

- Weiss, M. J., Keller, G. and Orkin, S. H.** (1994). Novel insights into erythroid development revealed through in vitro differentiation of GATA-1 embryonic stem cells. *Genes Dev* **8**, 1184-97.
- Whitelaw, E., Tsai, S. F., Hogben, P. and Orkin, S. H.** (1990). Regulated expression of globin chains and the erythroid transcription factor GATA-1 during erythropoiesis in the developing mouse. *Mol Cell Biol* **10**, 6596-606.
- Wildey, G. M. and Howe, P. H.** (2009). Runx1 is a co-activator with FOXO3 to mediate Transforming Growth Factor {beta} (TGF{beta})-induced Bim transcription in hepatic cells. *J Biol Chem*.
- Yamamoto, N., Akiyama, S., Katagiri, T., Namiki, M., Kurokawa, T. and Suda, T.** (1997). Smad1 and smad5 act downstream of intracellular signalings of BMP-2 that inhibits myogenic differentiation and induces osteoblast differentiation in C2C12 myoblasts. *Biochem Biophys Res Commun* **238**, 574-80.
- Yokomizo, T., Hasegawa, K., Ishitobi, H., Osato, M., Ema, M., Ito, Y., Yamamoto, M. and Takahashi, S.** (2008). Runx1 is involved in primitive erythropoiesis in the mouse. *Blood* **111**, 4075-80.
- Zhang, W. J., Park, C., Arentson, E. and Choi, K.** (2005). Modulation of hematopoietic and endothelial cell differentiation from mouse embryonic stem cells by different culture conditions. *Blood* **105**, 111-4.
- Zhang, Y. W., Yasui, N., Ito, K., Huang, G., Fujii, M., Hanai, J., Nogami, H., Ochi, T., Miyazono, K. and Ito, Y.** (2000). A RUNX2/PEBP2alpha A/CBFA1 mutation displaying impaired transactivation and Smad interaction in cleidocranial dysplasia. *Proc Natl Acad Sci U S A* **97**, 10549-54.
- Zhong, S., Li, C. and Wong, W. H.** (2003). ChipInfo: Software for extracting gene annotation and gene ontology information for microarray analysis. *Nucleic Acids Res* **31**, 3483-6.

Figure 1.2-1.

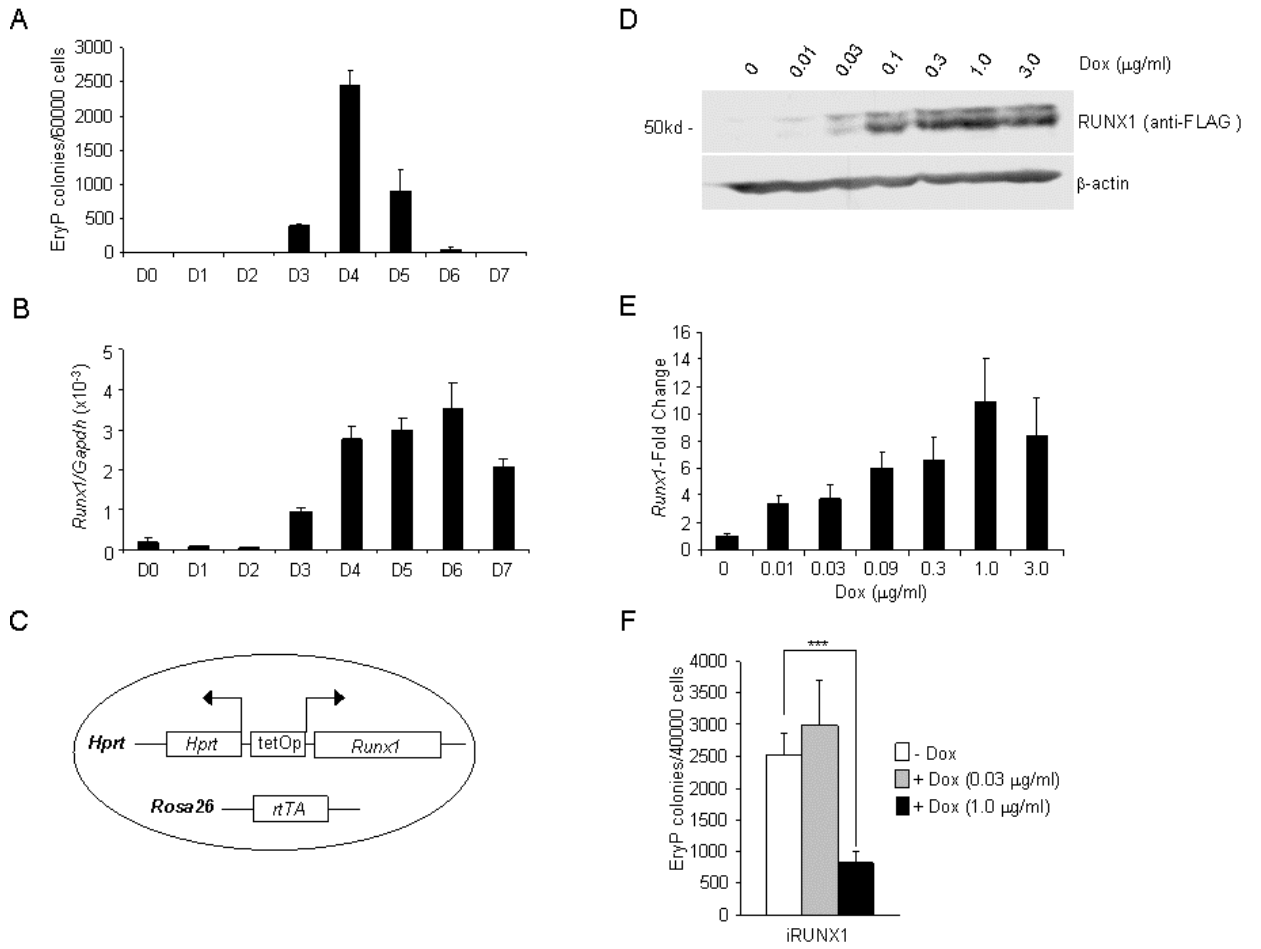


Figure Legends

Figure 1.2-1. Enforced RUNX1 expression during ES cell differentiation results in reduced EryP progenitors.

(A and B) A2Lox ES cells were differentiated in serum. EB cells were collected at indicated time points for EryP replating (A) and *Runx1* expression analysis (B).

EryP colonies were counted 4-5 days after replating. *Runx1* expression was analyzed and normalized to *Gapdh*. Values indicate mean \pm s.e.m. from three independent experiments.

(C) Schematic of the inducible RUNX1 (iRUNX1) ES cell lines with indicated loci containing modifications for production of rtTA and expression of *Runx1* cDNA.

(D) Western blot of the iRUNX1 ES cell lines. iRUNX1 ES cells differentiated in serum for three days were treated with the indicated concentrations of Dox for one additional day. Cells were collected on day 4 and subjected to SDS-PAGE followed by blotting with anti-FLAG and anti- β -actin antibodies.

(E) iRUNX1 ES cells were differentiated and treated with the indicated concentration of Dox on day 3. EB cells were harvested on day 4 for *Runx1* expression analysis by qRT-PCR. *Runx1* expression was analyzed and normalized to *Gapdh*. The expression level of *Runx1* in untreated cells was normalized as 1 and used to determine the *Runx1*-fold change in Dox-treated samples. Values indicate mean \pm s.e.m. from three independent experiments.

(F) iRUNX1 ES cells differentiated in serum were treated with Dox at 0.03 μ g/ml or at 1.0 μ g/ml on day 3 and harvested on day 4 for EryP replating. Values indicate mean \pm s.e.m. from three independent experiments; ***p<0.001.

Figure 1.2-2.

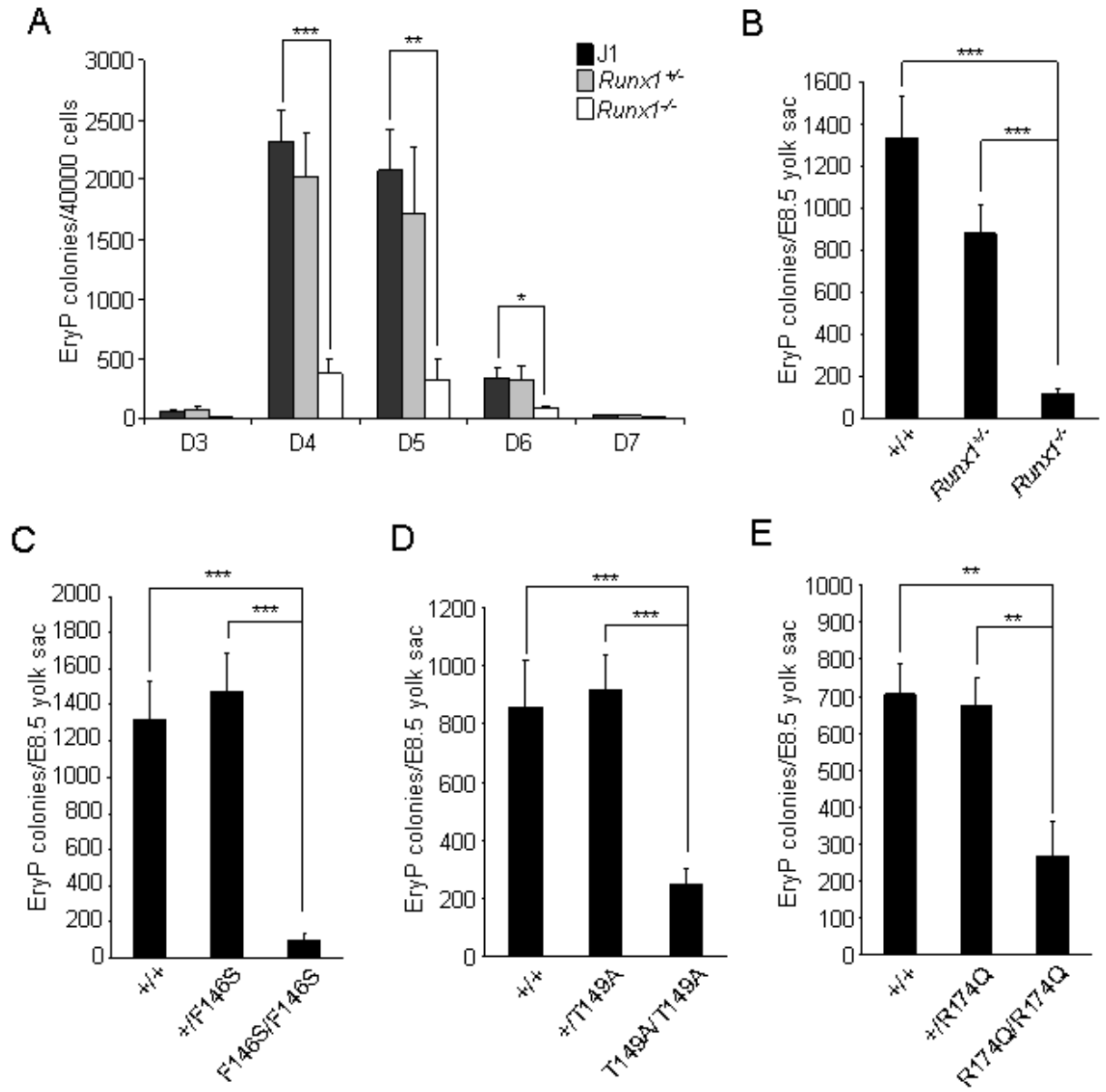


Figure 1.2-2. *Runx1* null and *Runx1* mutations resulted in decreased number of EryP progenitors in yolk sac.

(A) J1, *Runx1*^{+/-}, and *Runx1*^{-/-} ES cells differentiated in serum were harvested for EryP progenitor assay on the indicated day. Values are mean±s.e.m. of EryP colonies from four independent experiments.

(B) Primitive erythroid colonies from E8.5 yolk sacs (4-7 somite pair stage) of *Runx1*^{+/+} (n=9), *Runx1*^{+/-} (n=13), and *Runx1*^{-/-} (n=13).

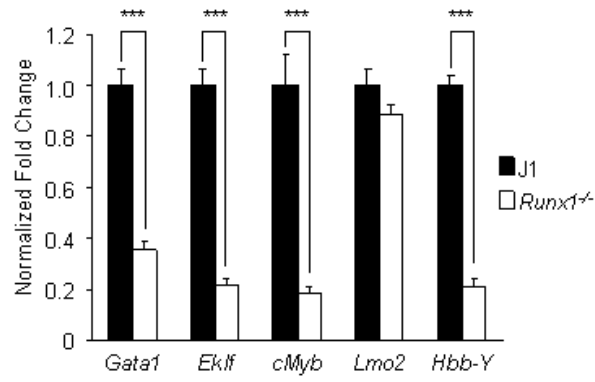
(C) EryP colonies of *Runx1-F146S* E8.5 yolk sacs (3-10 somite pair stage). n_{+/+} = 5; n_{+/F146S} = 12; n_{F146S/F146S} = 5.

(D) EryP colonies of *Runx1-T149A* E8.5 yolk sacs (3-8 somite pair stage). n_{+/+} = 8; n_{+/T149A} = 25; n_{T149A/T149A} = 18.

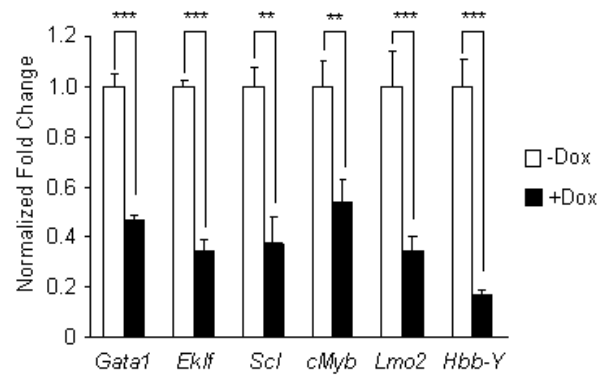
(E) EryP colonies of *Runx1-R174Q* E8.5 yolk sacs (3-9 somite pair stage). n_{+/+} = 10; n_{+/R174Q} = 16; n_{R174Q/R174Q} = 8. The results show mean±s.e.m. of EryP colonies. *p<0.05, **p<0.01, ***p<0.001.

Figure 1.2-3.

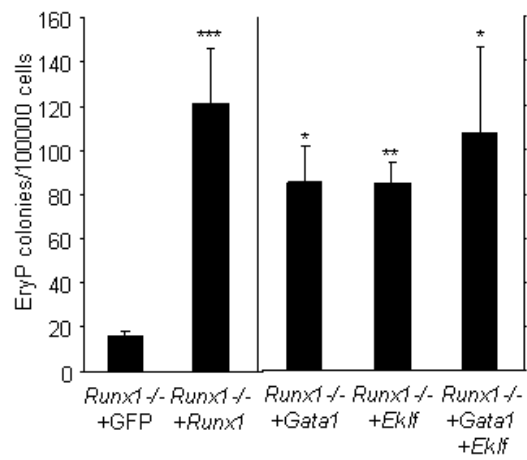
A



B



C



D

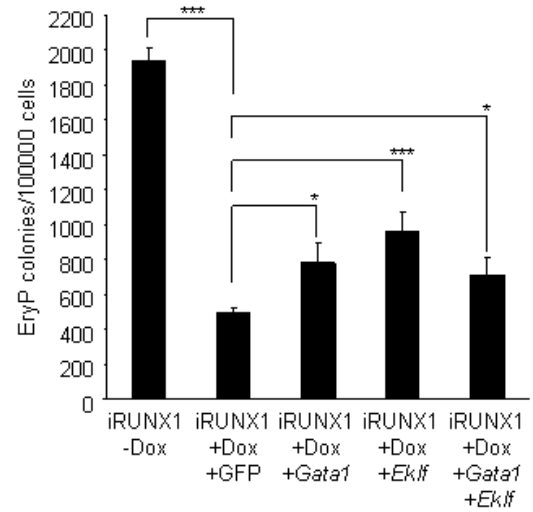


Figure 1.2-3. *Gata1* and *Eklf* rescue decreased EryP progenitor formation in *Runx1*^{-/-} and iRUNX1 EBs.

(A) J1 and *Runx1*^{-/-} ES cells were differentiated in serum, and EB cells were harvested on day 4. RNA was utilized for qRT-PCR analysis. Gene expressions were normalized against *Gapdh*, and then the ratio of the gene expression (*Runx1*^{-/-}) to gene expression (J1) was determined to generate normalized fold change. Values indicate mean±s.e.m. from three independent experiments.

(B) iRUNX1 ES cells were differentiated in serum, Dox (1.0 µg/ml) was added on day3, and EB cells were collected for qRT-PCR on day 4. Gene expressions were normalized against *Gapdh*, and then the normalized fold change was determined by calculating the ratio of the +Dox to -Dox. Values indicate mean±s.e.m. from two to three independent experiments.

(C and D) *Runx1*^{-/-} (C) and iRUNX1 (D) ES cells were differentiated for three days on OP9 cells, and cells were infected with MSCV-RUNX1-IRES-GFP, MSCV-GATA1-IRES-GFP, or MSCV-EKLF-IRES-GFP viral supernatants. One day later, the cells were collected for primitive erythroid replating. For the differentiation of iRUNX1 ES cell, Dox was added on day 3. Cells treated with MSCV-IRES-GFP viral supernatant were used as controls. Values are mean of EryP colonies±s.e.m. from three independent experiments. *p<0.05, **p<0.01, ***p<0.001.

Figure 1.2-4.

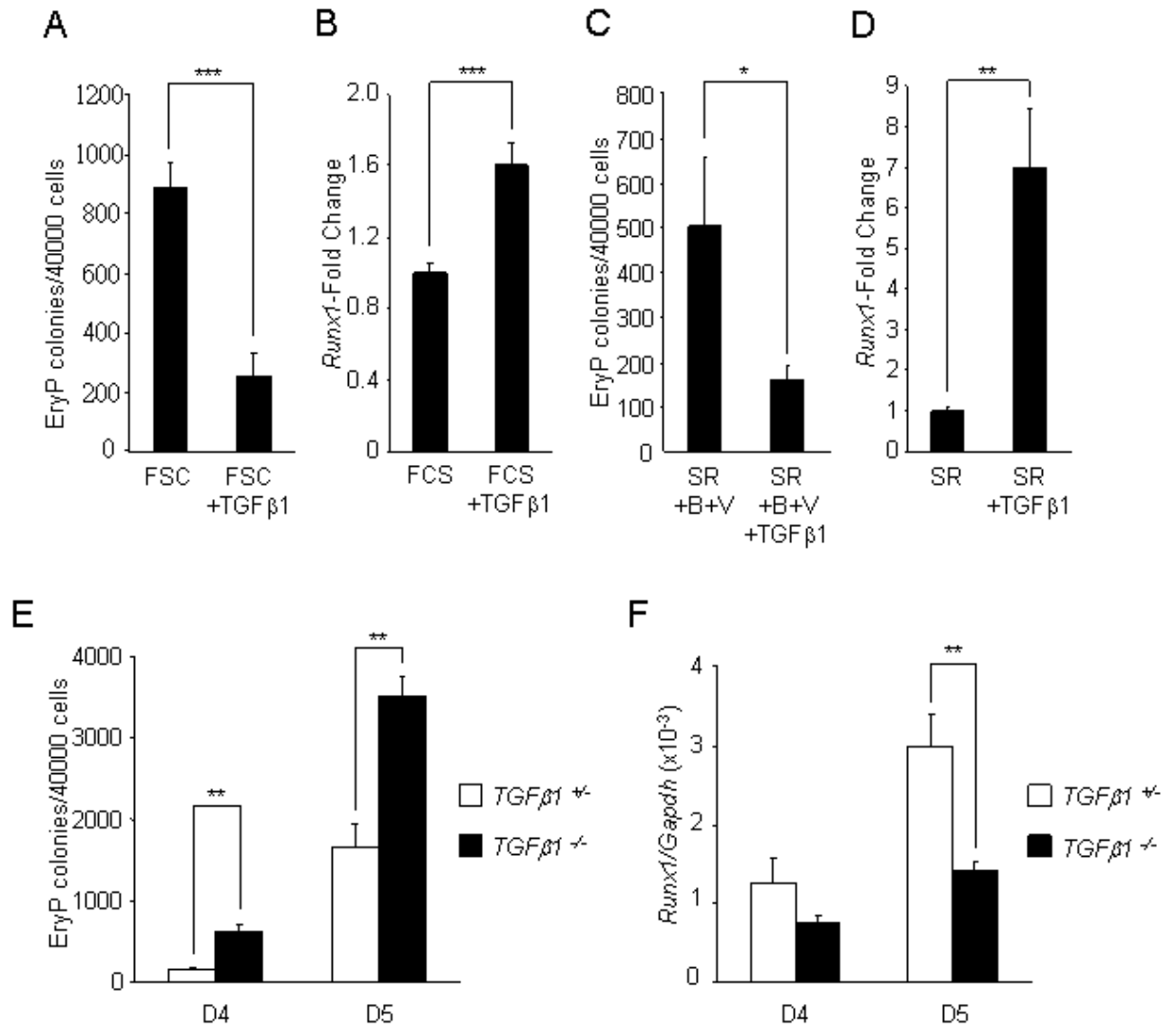


Figure 1.2-4. TGFβ1 inhibits EryP progenitor formation and induces *Runx1* expression.

(A and B) A2Lox ES cells were differentiated in serum, TGFβ1 (10 ng/ml) was added on day 3, and EB cells were collected on day 4 for EryP replating (A) and qRT-PCR (B). *Runx1* expression was normalized against *Gapdh*, and then the normalized fold change was determined by calculating the ratio of +TGFβ1 to -TGFβ1. Values are mean±s.e.m. from three independent experiments.

(C) TGFβ1 inhibits the number of EryP progenitors in serum free condition. A2Lox ES cells were differentiated in serum free (SR) media with BMP4 (5 ng/ml) and VEGF (10 ng/ml). TGFβ1 (10 ng/ml) was added on day 3, and day 4 EBs cells were collected for EryP replating. Values are mean±s.e.m. from three independent experiments.

(D) TGFβ1 induces *Runx1* expression in serum free conditions. A2Lox ES cells were differentiated for 2 days in SR and treated with TGFβ1 (10 ng/ml) for two more days. Day 4 EBs were harvested for qRT-PCR analysis. *Runx1* expression was normalized against *Gapdh* and the ratio of *Runx1* quantity (+TGFβ1) to *Runx1* quantity (SR) was determined to yield normalized fold change. Values are mean±s.e.m. from two independent experiments.

(E and F) Deficiency in *TGFβ1* leads to increased EryP colony formation with decreased *Runx1* expression. *Tgfβ1*^{+/-} and *Tgfβ1*^{-/-} ES cells were differentiated in serum free (SR) with BMP4 (5 ng/ml) and VEGF (10 ng/ml). Day 4 and day 5 EB cells were harvested for EryP replating (E) and *Runx1* expression analysis by qRT-PCR (F). *Runx1* expression was normalized against *Gapdh*. Values are

mean±s.e.m. from three independent experiments. * $p < 0.05$, ** $p < 0.01$, *** $p < 0.001$.

Figure 1.2-5.

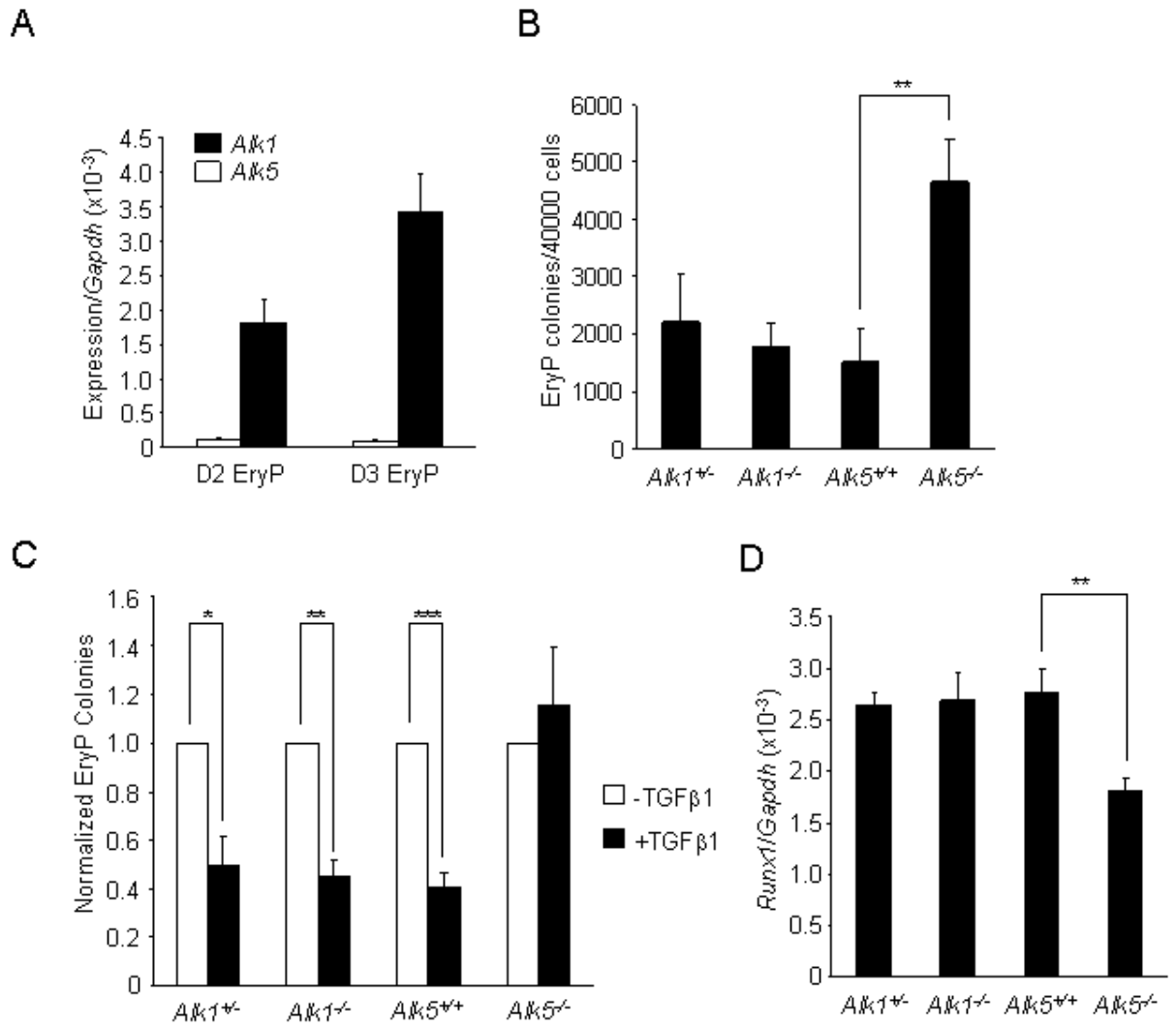


Figure 1.2-5. *Alk5* deficiency generates increased EryP progenitors.

(A) ALK5 is the major TGF β type I receptor in developing EryP colonies. A2Lox ES cells were differentiated in serum for 4 days and subjected to EryP colony assay. EryP cells harvested from 2 days and 3 days after replating were utilized for qRT-PCR analyses. Gene expressions were normalized against *Gapdh*. Values are mean \pm s.e.m. from two independent experiments.

(B) *Alk5*^{-/-} EB cells generate increased EryP colonies. *Alk1*^{+/-}, *Alk1*^{-/-}, *Alk5*^{+/+}, and *Alk5*^{-/-} ES cells differentiated in serum for 4 days were used for EryP progenitor assays. Values are mean \pm s.e.m. of EryP colonies from three independent experiments.

(C) TGF β 1 fails to suppress EryP progenitor formation in *Alk5*^{-/-} EBs. *Alk1*^{+/-}, *Alk1*^{-/-}, *Alk5*^{+/+}, and *Alk5*^{-/-} ES cells differentiated in serum free (SR) with BMP4 (5 ng/ml) and VEGF (10 ng/ml) were treated with TGF β 1 (10 ng/ml) on day 3 and were collected for EryP progenitor assay on day 4. The number of EryP colonies in untreated cells was normalized as 1 and used to determine the ratio of the EryP colonies in TGF β 1-treated samples. Values are mean \pm s.e.m. from three independent experiments.

(D) *Alk1*^{+/-}, *Alk1*^{-/-}, *Alk5*^{+/+}, and *Alk5*^{-/-} EB cells were harvested on day 4 and RNA samples were generated for qRT-PCR analyses. *Runx1* expression was normalized against *Gapdh*. Values are mean \pm s.e.m. from three independent experiments.

*p<0.05, **p<0.01, ***p <0.001.

Table 1.2-1. Viability of progeny from intercrosses of Runx1^{m/+} mice

	Biochemical Properties*		No. (%) of live mice at P21		
	DNA binding	CBF β binding	+/+	+/m	m/m
F146S	-	-	169 (40.8)	245 (59.2)	0
T149A	++	-	53 (32.1)	112 (67.9)	0
R174Q	-	++	109 (32.6)	225 (67.4)	0

-, loss of function

++, equivalent to wild-type

P: postnatal day

m: mutant allele

***(Nagata and Werner, 2001)**

Table 1.2-2. Common erythroid genes were downregulated in Runx1^{-/-} and iRUNX1+Dox EBs.

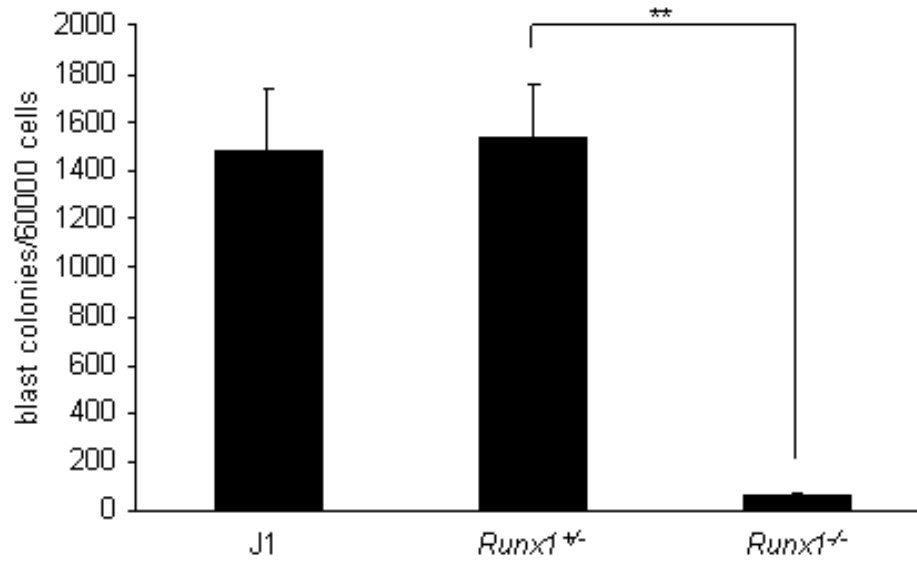
Microarray ID	EntrezGene ID	gene	Fold change of Runx1 ^{-/-} /J1	Fold change of +Dox/-Dox	
1452207_at	17684	<i>Cited2</i> : Cbp/p300-interacting transactivator, with Glu/Asp-rich carboxy-terminal domain, 2	-	-1.80	
1425400_a_at	56222	<i>Cited4</i> : Cbp/p300-interacting transactivator, with Glu/Asp-rich carboxy-terminal domain, 4	-	-6.43	
1423344_at	13857	<i>Epor</i> : erythropoietin receptor	-	-1.87	
1452514_a_at	16590	<i>Kit</i> : kit oncogene	-	-2.44	
1415855_at	17311	<i>Kitl</i> : kit ligand	-	-2.68	
1450736_a_at	15132	<i>Hbb-bh1</i> : hemoglobin Z, beta-like embryonic chain	-	-1.95	
1454086_a_at	16909	<i>Lmo2</i> : LIM domain only 2	-	-3.12	*
1449389_at	21349	<i>Tal1</i> : T-cell acute lymphocytic leukemia 1	-	-4.77	*
1449232_at	14460	<i>Gata1</i> : GATA binding protein 1	-1.45	-2.27	*
1418600_at	16596	<i>Klf1</i> : Kruppel-like factor 1 (erythroid)	-2.00	-3.80	*
1450194_a_at	17863	<i>Myb</i> : myeloblastosis oncogene	-1.59	-2.99	*
1436823_x_at	15135	<i>Hbb-y</i> : hemoglobin Y, beta-like embryonic chain	-5.88	-5.61	*
1417714_x_at	15122	<i>Hba-a1</i> : hemoglobin alpha, adult chain 1	-2.72	-1.57	
1425643_at	14934	<i>Gypa</i> : glycophorin A	-2.35	-	
1449077_at	170812	<i>Eraf</i> : erythroid associated factor	-5.90	-	

- indicates not applicable

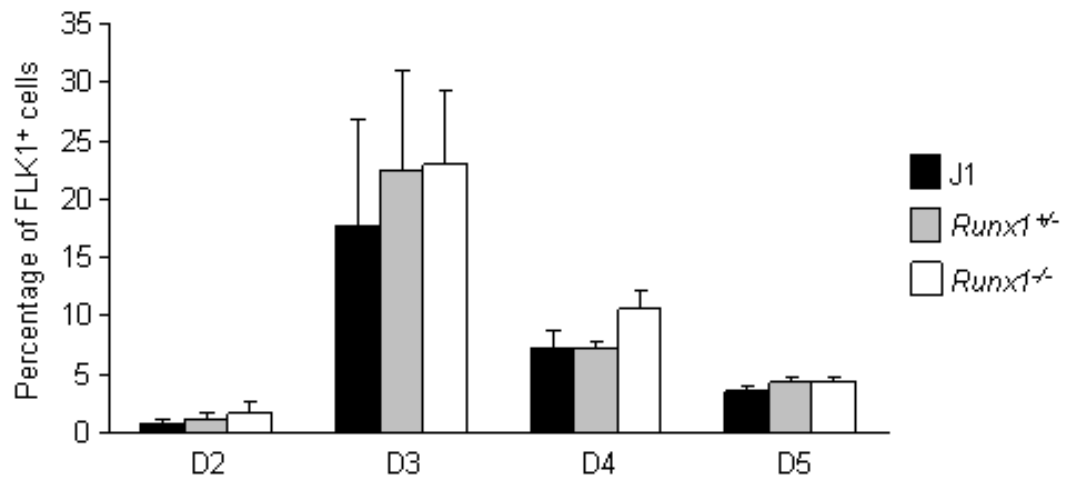
* gene expression subjected to qRT-PCR analysis

Supplementary Figure 1.2-1.

A



B

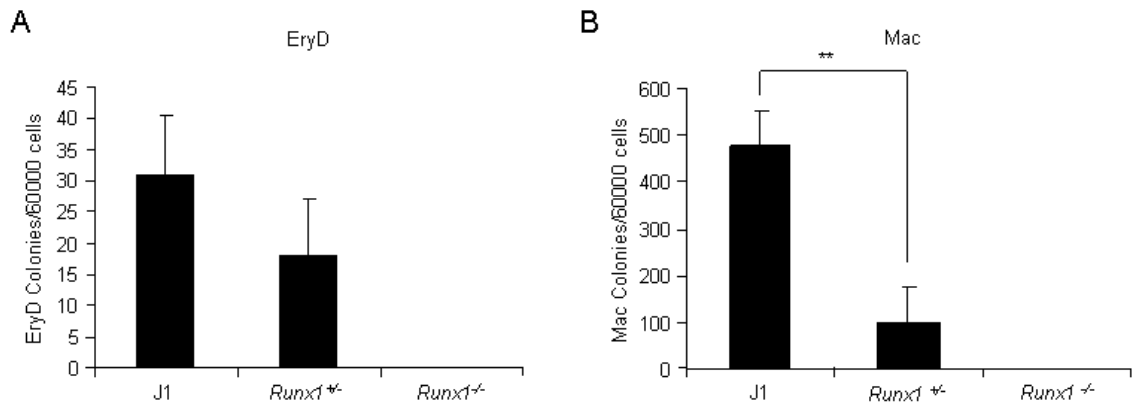


Supplementary Figure 1.2-1. *Runx1*^{-/-} EBs have reduced blast colonies and comparable FLK1⁺ differentiation kinetics compared to wild type EBs by FACS analysis.

(A) J1, *Runx1*^{+/-} and *Runx1*^{-/-} ES cells differentiated in serum were collected on day 2.75 for blast colony replating. Values are mean±s.e.m. from three independent experiments; ***p*<0.01.

(B) FACS analyses for FLK1 expression of J1, *Runx1*^{+/-}, and *Runx1*^{-/-} EBs. ES cells were differentiated in serum, and cells were collected for FLK1⁺ detection by FACS from day 2 to day 5. Values are mean±s.e.m. from three independent experiments.

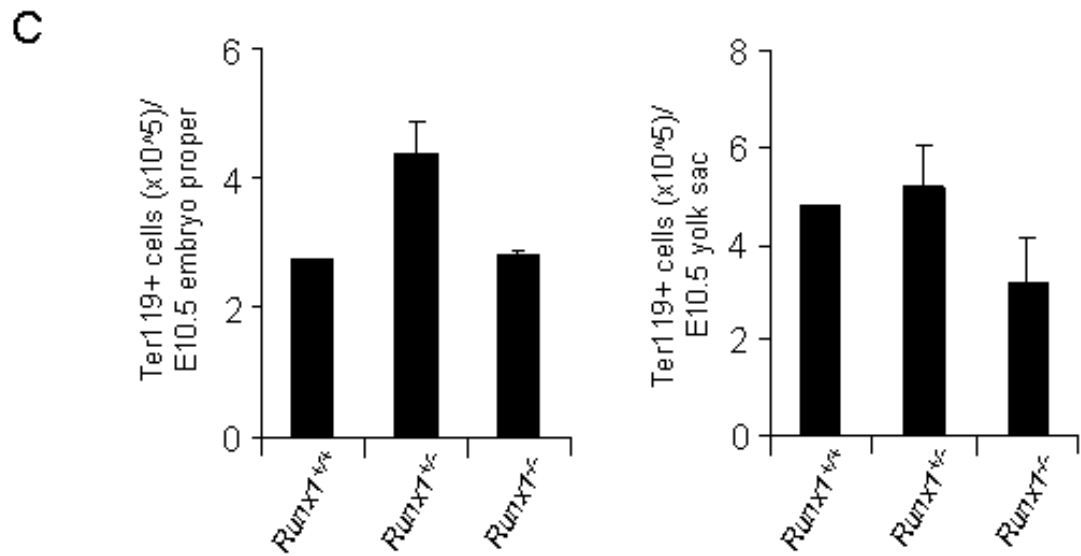
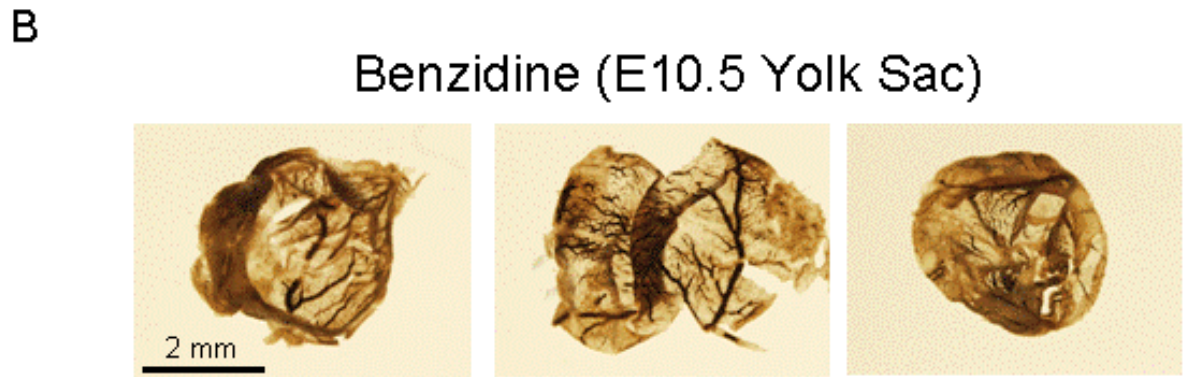
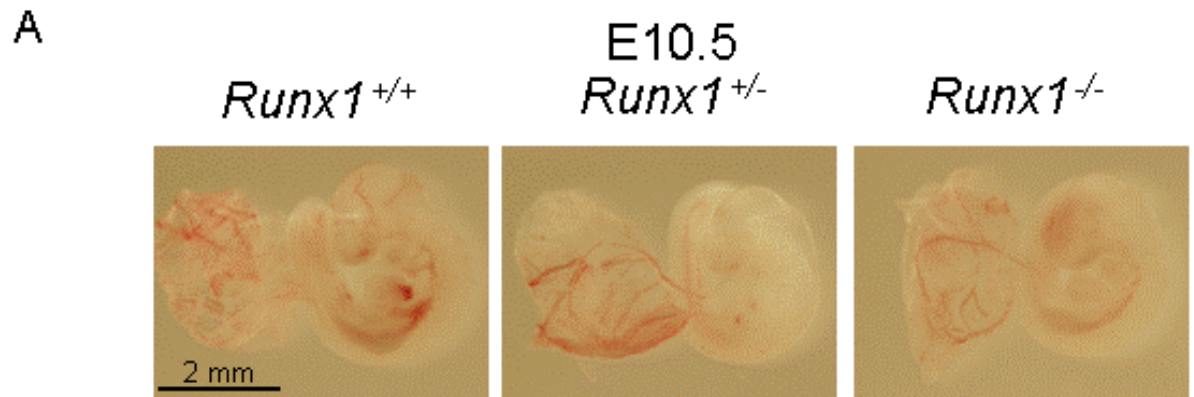
Supplementary Figure 1.2-2.



Supplementary Figure 1.2-2. *Runx1*^{-/-} EB cells have no definitive hematopoietic colonies.

J1, *Runx1*^{+/-}, and *Runx1*^{-/-} ES cells were differentiated in serum for six days. EB cells were harvested for definitive erythroid and myeloid replating. Colonies of EryD (A) and Mac (B) were counted 6-7 days after replating. Values are mean±s.e.m..from three independent experiments; ***p*<0.01. EryD: definitive erythroid colony, Mac: macrophage colony.

Supplementary Figure 1.2-3.

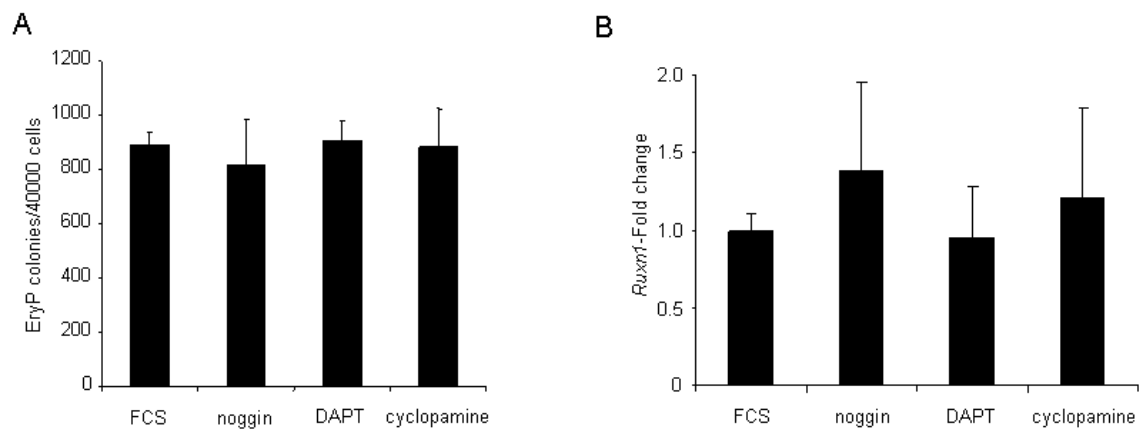


Supplementary Figure 1.2-3. E10.5 *Runx1*^{-/-} embryos have no gross abnormalities in blood cell generation.

(A) Morphology and (B) Benzidine staining of yolk sacs of *Runx1*^{+/+}, *Runx1*^{+/-}, and *Runx1*^{-/-} embryos at E10.5.

(C) FACS analysis on Ter119+ cells of the embryo proper (left) and the yolk sac (right) at E10.5. Values indicate mean±s.e.m. of total Ter119+ cells from *Runx1*^{+/+} (n=1), *Runx1*^{+/-} (n=4), and *Runx1*^{-/-} (n=2) embryos.

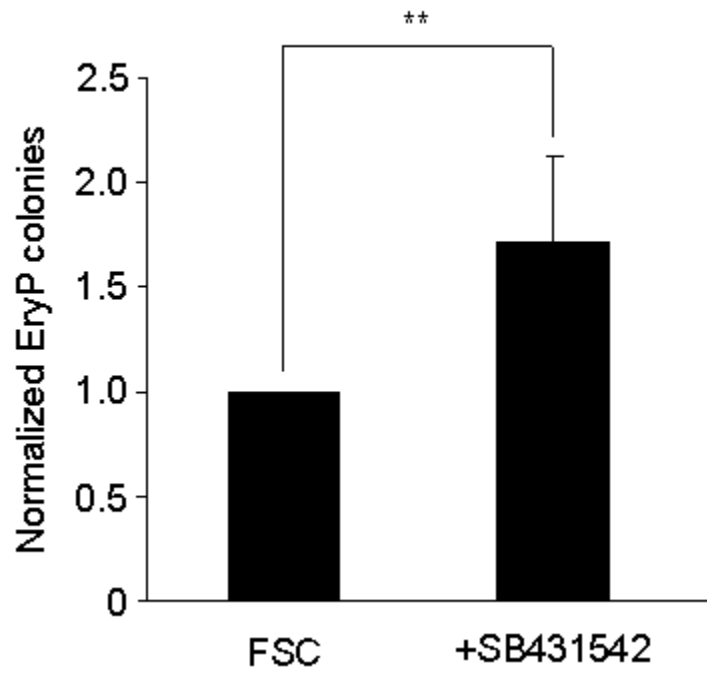
Supplementary Figure 1.2-4.



Supplementary Figure 1.2-4. Noggin, DAPT, and cyclopamine do not affect EryP progenitor formation and *Runx1* expression.

(A) A2Lox ES cells were differentiated in serum, Noggin (50 ng/ml), DAPT (2 μ M added 2 times/day), and Cyclopamine (3 μ M) were added on day 3 and EB cells were collected on day 4 for EryP replating (A) and qRT-PCR (B). *Runx1* expression was normalized against *Gapdh*. The quantity of *Runx1* expression in FSC was normalized as 1 and used to determine the *Runx1*-fold change in inhibitor-treated samples. Values indicate mean \pm s.e.m. of EryP colonies from three independent experiments.

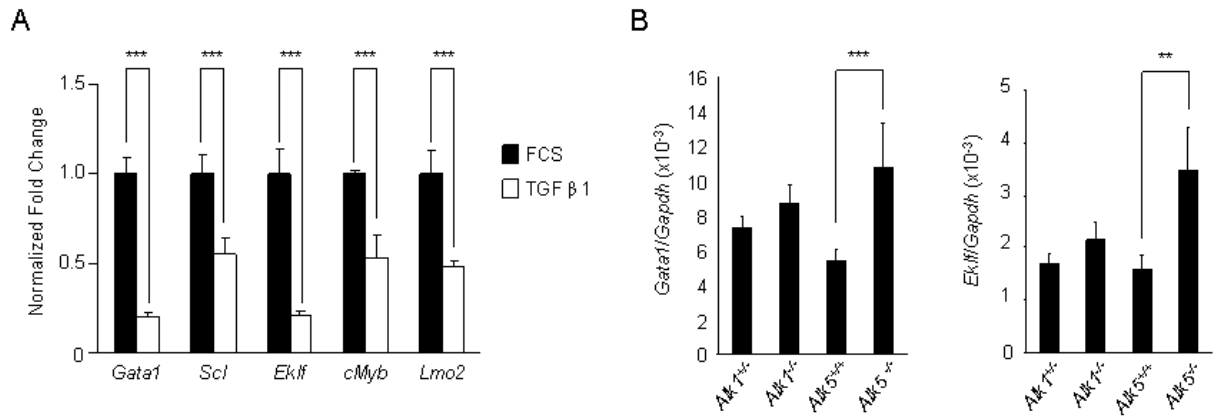
Supplementary Figure 1.2-5.



Supplementary Figure 1.2-5. SB431542 treated EB cells generate increased EryP colonies.

iRUNX1 ES cells differentiated in serum for 3 days were treated with SB431542 (2 μ M) on day 3. Cells were collected on day 4 for EryP replating. EryP colonies were counted, and the numbers of EryP colonies in SB431542-treated samples were normalized to that of FSC. Values are mean \pm s.e.m. from three independent experiments; **p<0.01.

Supplementary Figure 1.2-6.



Supplementary Figure 1.2-6. *Gata1* and *Eklf* expressions were decreased in TGFβ1 treated EBs but increased in *Alk5*^{-/-} EBs.

(A) A2Lox ES cells differentiated in serum were treated with and without TGFβ1 (10 ng/ml) on day 3. Cells were harvested on day 4 for qRT-PCR. Gene expressions were normalized against *Gapdh*, and then the normalized fold change was determined by calculating the ratio of the gene expression (+TGFβ1) to gene expression (-TGFβ1). Values are mean±s.e.m. from two to three independent experiments.

(B) *Alk1*^{+/-}, *Alk1*^{-/-}, *Alk5*^{+/+}, and *Alk5*^{-/-} EB cells were harvested on day 4 for qRT-PCR analyses. Gene expressions were normalized against *Gapdh*. Values are mean±s.e.m. from three independent experiments; **p<0.01, ***p<0.001.

Supplementary Table 1.2-1. Primer sequences for qRT-PCR.

Gene		Primer Sequence (5'-3')	Source
<i>Gapdh</i>	Forward	TGGCAAAGTGGAGATTGTTGCC	Lugus et al., 2007.
	Reverse	AAGATGGTGATGGGCTTCCCG	
<i>Runx1</i>	Forward	CTTCCTCTGCTCCGTGCTA	#Primer 3
	Reverse	CTGCCGAGTAGTTTTTCATCG	
<i>Gata1</i>	Forward	ATGGAATCCAGACGAGGAAC	Lugus et al., 2007.
	Reverse	CTCCCCACAATTCCCCTACTAC	
<i>Scl</i>	Forward	CAGCCTGATGCTAAGGCAAG	Lugus et al., 2007.
	Reverse	AGCCAACCTACCATGCACAC	
<i>Eklf</i>	Forward	ATGGGCTGCTGTCCGGATA	&PrimerBank ID: 6754454a3
	Reverse	TCTTAGGTGCCAAAGTTCGCC	
<i>c-myb</i>	Forward	GAGCACCCAACTGTTCTCG	PrimerBank ID: 19526473a1
	Reverse	CACCAGGGGCTGTTCTTAG	
<i>Lmo2</i>	Forward	AGGAGAGACTATCTCAGGCTTTT	PrimerBank ID: 6678702a3
	Reverse	TTGAAACACTCCAGGTGATACAC	
<i>Hbb-Y</i>	Forward	TGGCCTGTGGAGTAAGGTCAA	PrimerBank ID: 6680177a1
	Reverse	GAAGCAGAGGACAAGTTCCCA	
<i>Alk1</i>	Forward	GGGCCTTTTGATGCTGTCCG	PrimerBank ID: 6752958a1
	Reverse	TGGCAGAATGGTCTCTTGACAG	
<i>Alk5</i>	Forward	TCTGCATTGCACTTATGCTGA	PrimerBank ID: 2853637a1
	Reverse	AAAGGGCGATCTAGTGATGGA	

#Primer 3: <http://biotools.umassmed.edu/bioapps/primer3> www.cgi

&Primerbank: <http://pga.mgh.harvard.edu/primerbank/>

Chapter 1.3
Conclusion and Future Directions

Summary of Chapter One

During embryonic development, the appearance of red blood cells in the yolk sac marks the onset of hematopoiesis, known as primitive hematopoiesis. Primitive hematopoietic progenitors emerge exclusively in the yolk sac and are characterized by their transient nature. While the primitive hematopoiesis in the yolk sac declines, definitive hematopoiesis will begin to emerge in the yolk sac and/or in the embryo proper to take over blood cell production. The mechanisms regulating the transition from primitive to definitive hematopoiesis remain unclear. *Runx1* has been reported to be essential for the establishment of definitive hematopoiesis, but its expression can also be detected in the yolk sac blood islands where primitive erythroid (EryP) progenitors emerge, suggesting that *Runx1* might also play a role in primitive hematopoiesis. In chapter one, we have revealed novel roles of *Runx1* in primitive hematopoietic development, based on studies utilizing the embryonic stem (ES) cell differentiation system and *Runx1* mutant mice. We have found that inducing *Runx1* expression in the *in vitro* differentiation model of embryonic stem (ES) cells results in a decrease in EryP progenitor formation. A possible mechanism for this is related to the activity of transforming growth factor beta-1 (TGF β 1). We have demonstrated that TGF β 1 inhibits EryP progenitor formation and upregulates *Runx1* expression. *Tgf β 1*^{-/-} ES cells generate increased numbers of EryP progenitors with decreased *Runx1* expression levels. In addition, it was determined that ALK5 is the major type-I TGF β 1 receptor in EryP cells and *Alk5*-deficient ES cells produce higher numbers of EryP progenitors, relative to wild-type. Surprisingly, both *Runx1* null

animals and *Runx1*-deficient ES cells give rise to reduced numbers of EryP progenitors. However, despite generating fewer EryP progenitors during primitive hematopoiesis, *Runx1*-deficient mice can still survive during development until definitive hematopoiesis takes over blood formation. DNA binding and CBF β interaction of RUNX1 are needed for optimal generation of EryP progenitors *in vivo*. The decreased EryP progenitors in both *Runx1* null and overexpression systems coincide with decreased expressions of the transcription factors, *Gata1* and *Eklf*, and introduction of *Gata1* or *Eklf* partially rescue the EryP defects in both systems. Taken together, these studies suggest that RUNX1, likely in concert with TGF β 1, plays a critical role in the regulation of primitive hematopoiesis.

Possible Mechanisms for Runx1-Mediated Suppression of EryP

Development

Our studies have demonstrated that overexpression of *Runx1* between day 3 and day 4 of EB differentiation suppresses primitive erythroid progenitor formation in a dose-dependent manner. This observation leads to the intriguing question of how *Runx1* inhibits EryP generation. One possibility is that RUNX1 could directly modulate the expression of genes that are critical for EryP formation or development. The reduction of EryP progenitors coincides with the downregulation of multiple hematopoietic-related genes. One of the most downregulated genes is Hbb-y-globin (hemoglobin Y, beta-like embryonic chain), which reflects significantly reduced EryP levels. The β locus control region (β LCR)

is the most important regulatory element in the regulation of the expression of β -globin proteins (Noordermeer and de Laat, 2008). One hypothesis is that RUNX1 can regulate Hbb-y-globin expression by directly binding to the β LCR locus. However, RUNX1 binding to the β LCR region has not been detected by chromatin immunoprecipitation (ChIP) analysis (not shown). Therefore, the data suggest that RUNX1 more likely inhibits Hbb-y-globin expression through an indirect mechanism.

Gata1 and *Eklf* have been shown to be involved in both primitive and definitive erythropoiesis. Both *Gata1* and *Eklf* expression are decreased by induced *Runx1* expression. Rescue of either *Gata1* or *Eklf* by retroviral infection can partially reverse EryP defects seen in induced *Runx1* EB cells, suggesting that *Gata1* and *Eklf* might be directly regulated by *Runx1*. We have identified two conserved *Runx1* binding sites upstream of the transcriptional start sites of *Gata1* and one binding site upstream from the start site of *Eklf*. ChIP analysis did not reveal any direct binding of RUNX1 to these predicted sites (not shown) but these computationally-predicted binding sites may not include all of the biological RUNX1 binding sites in *Gata1* and *Eklf* locus. Based on this possibility, a genome-wide screening of RUNX1 binding targets in induced *Runx1* EBs is warranted. Chromatin immunoprecipitation-sequencing (ChIP-Seq) technology is well-suited for this purpose (Mikkelsen et al., 2007). Comparing the microarray data that is already on hand with the results from ChIP-Seq would provide valuable information about how RUNX1 carries out its inhibitory role in EryP progenitor formation.

Another possible mechanism by which RUNX1 may negatively regulate EryP generation would involve binding partners of RUNX1. RUNX1 can inhibit or activate target genes by interacting with transcriptional co-repressors or co-activators. For example, RUNX1 can interact cooperatively with p300, a transcriptional co-activator, to promote differentiation of a myeloid precursor cell line into mature neutrophils in response to granulocyte colony-stimulating factor (Kitabayashi et al., 1998). Conversely, RUNX1 interacts with the mSin3A co-repressor to repress *p21^{Waf1/Cip1}* promoter activity in NIH3T3 cells or to repress *c-Mpl* expression in hematopoietic progenitor cells (Lutterbach et al., 2000; Satoh et al., 2008). We have tested whether RUNX1 can interact with mSin3A to suppress EryP progenitor formation. We could not co-immunoprecipitate RUNX1 and mSin3A from induced *Runx1* EB cells, suggesting that Runx1 suppression of EryP progenitors may be not due to the interaction of RUNX1 and mSin3A in the ES/EB system. The suppression could, however, be due to RUNX1 interaction with other co-repressors such as Groucho/TLE and HDAC (histone deacetylase)(Durst and Hiebert, 2004; Durst et al., 2003; Imai et al., 1998). In support of this possibility, RUNX2, another member of the RUNX family, has been shown to interact with HDAC6, and the deacetylase activity of HDAC6 has been shown to repress RUNX2 target genes in osteoblast lineage cell lines (Westendorf et al., 2002). Additional studies, based on proteomics, designed to identify specific binding partners or co-repressors of RUNX1 in the ES/EB system should be undertaken in the future to clarify this mechanism.

The Relationship between TGFβ1 and Runx1 in Primitive Hematopoiesis

TGFβ acts as a negative regulator of the proliferation of adult hematopoietic progenitor cells in vitro (Keller et al., 1990; Ottmann and Pelus, 1988). Previous studies found that *Alk5*^{-/-} yolk sac cells generate significant increased number of erythroid colony-forming cells, suggesting TGFβ signaling could have an inhibitory effect on the formation and/or proliferation of erythroid progenitors in vivo (Larsson et al., 2001). Our results indicate that TGFβ1 inhibits EryP progenitor formation during ES cell differentiation. Importantly, TGFβ1-treated EBs also show increased *Runx1* expression. *Tgfβ1*^{-/-} and *Alk5*^{-/-} EB cells display larger EryP populations and decreased *Runx1* expression, relative to wild-type. These results suggest that TGFβ1 signaling negatively regulates EryP development, possibly through upregulation of *Runx1*. In agreement with this, overexpression of *Runx1* suppresses increased EryP production caused by inhibition of the interaction between TGFβ and ALK5. Based on these observations, generating inducible RUNX1 in *Alk5*^{-/-} ES cells would be a way to examine the negative role of the ALK5-RUNX1 axis in EryP development. Examining ectopic expression of *Runx1* in *Alk5*⁺ cells by generating *Alk5-cre*; *Rosa26 loxP-stop-loxP Runx1* mice would also provide important information.

It is worthwhile to note that when TGFβ1 was added to both wild-type, *Runx1*^{+/-} and *Runx1*^{-/-} EB cells, followed by EryP replating, a comparable reduction of EryP colonies was observed in both groups. It is likely, therefore, that TGFβ1 inhibits EryP development through other mechanisms, in addition to the *Runx1*-dependent pathway. This likelihood is supported by other recent studies.

TGF β 1 has, for instance, been shown to induce an epithelial-to-mesenchymal transition (EMT) by directly upregulating *Snail1* in cultured hepatocytes (Kaimori et al., 2007) or by indirectly upregulating *Zeb1* through a mechanism mediated by *Ets1* in epithelial cells (Shirakihara et al., 2007). Comparing the gene-expression profiles of wild-type and *Runx1*^{-/-} EBs after treatment with TGF β 1 would provide additional insight into the roles of other possible mediators of TGF β signaling in the suppression of EryP progenitor development, independent of *Runx1*.

References

- Durst, K. L. and Hiebert, S. W.** (2004). Role of RUNX family members in transcriptional repression and gene silencing. *Oncogene* **23**, 4220-4.
- Durst, K. L., Lutterbach, B., Kummalue, T., Friedman, A. D. and Hiebert, S. W.** (2003). The inv(16) fusion protein associates with corepressors via a smooth muscle myosin heavy-chain domain. *Mol Cell Biol* **23**, 607-19.
- Imai, Y., Kurokawa, M., Tanaka, K., Friedman, A. D., Ogawa, S., Mitani, K., Yazaki, Y. and Hirai, H.** (1998). TLE, the human homolog of groucho, interacts with AML1 and acts as a repressor of AML1-induced transactivation. *Biochem Biophys Res Commun* **252**, 582-9.
- Kaimori, A., Potter, J., Kaimori, J. Y., Wang, C., Mezey, E. and Koteish, A.** (2007). Transforming growth factor-beta1 induces an epithelial-to-mesenchymal transition state in mouse hepatocytes in vitro. *J Biol Chem* **282**, 22089-101.
- Keller, J. R., McNiece, I. K., Sill, K. T., Ellingsworth, L. R., Quesenberry, P. J., Sing, G. K. and Ruscetti, F. W.** (1990). Transforming growth factor beta directly regulates primitive murine hematopoietic cell proliferation. *Blood* **75**, 596-602.
- Kitabayashi, I., Yokoyama, A., Shimizu, K. and Ohki, M.** (1998). Interaction and functional cooperation of the leukemia-associated factors AML1 and p300 in myeloid cell differentiation. *Embo J* **17**, 2994-3004.
- Larsson, J., Goumans, M. J., Sjostrand, L. J., van Rooijen, M. A., Ward, D., Leveen, P., Xu, X., ten Dijke, P., Mummery, C. L. and Karlsson, S.** (2001). Abnormal angiogenesis but intact hematopoietic potential in TGF-beta type I receptor-deficient mice. *Embo J* **20**, 1663-73.
- Lutterbach, B., Westendorf, J. J., Linggi, B., Isaac, S., Seto, E. and Hiebert, S. W.** (2000). A mechanism of repression by acute myeloid leukemia-1, the target of multiple chromosomal translocations in acute leukemia. *J Biol Chem* **275**, 651-6.
- Mikkelsen, T. S., Ku, M., Jaffe, D. B., Issac, B., Lieberman, E., Giannoukos, G., Alvarez, P., Brockman, W., Kim, T. K., Koche, R. P. et al.** (2007). Genome-wide maps of chromatin state in pluripotent and lineage-committed cells. *Nature* **448**, 553-60.
- Noordermeer, D. and de Laat, W.** (2008). Joining the loops: beta-globin gene regulation. *IUBMB Life* **60**, 824-33.
- Ottmann, O. G. and Pelus, L. M.** (1988). Differential proliferative effects of transforming growth factor-beta on human hematopoietic progenitor cells. *J Immunol* **140**, 2661-5.
- Satoh, Y., Matsumura, I., Tanaka, H., Ezoe, S., Fukushima, K., Tokunaga, M., Yasumi, M., Shibayama, H., Mizuki, M., Era, T. et al.** (2008). AML1/RUNX1 works as a negative regulator of c-Mpl in hematopoietic stem cells. *J Biol Chem* **283**, 30045-56.
- Shirakihara, T., Saitoh, M. and Miyazono, K.** (2007). Differential regulation of epithelial and mesenchymal markers by deltaEF1 proteins in epithelial mesenchymal transition induced by TGF-beta. *Mol Biol Cell* **18**, 3533-44.
- Westendorf, J. J., Zaidi, S. K., Cascino, J. E., Kahler, R., van Wijnen, A. J., Lian, J. B., Yoshida, M., Stein, G. S. and Li, X.** (2002). Runx2 (Cbfa1, AML-3) interacts with histone deacetylase 6 and represses the p21(CIP1/WAF1) promoter. *Mol Cell Biol* **22**, 7982-92.

Chapter 2

Characterization of Hematopoietic Stem Cells in a Mouse Chronic Inflammatory Arthritis Model

Chapter 2.1

Introduction

Hematopoietic Stem Cell Niche

Hematopoietic stem cells (HSCs) are responsible for production of all blood cells. The bone marrow is the major site of hematopoiesis throughout adult life. HSCs reside mainly in the bone marrow and undergo well-controlled cell division to regenerate themselves while also producing progenitor cells that give rise to all types of mature blood cells. The maintenance of the identity and function of HSCs *in vivo* is thought to depend on a specific microenvironment of surrounding cells in the bone marrow known as the HSC niche (Wilson and Trumpp, 2006). The HSC niche microenvironment is thought to supply necessary factors that support specific aspects of hematopoiesis, such as HSC survival, self-renewal, and differentiation. The identification of the cellular components and mechanisms that comprise the HSC niche is an area of active investigation.

The endosteum is a thin layer of connective tissue that is located at the interface between bone and bone marrow. The endosteum surface, covered by bone-lining cells, contains a population of cells that can differentiate into bone-forming osteoblasts. A number of studies have shown that HSCs are commonly found at or near the endosteum in the bone marrow, in close proximity to osteoblasts, suggesting osteoblasts may serve as part of the HSC niche (Arai et al., 2004; Kiel et al., 2005; Nilsson et al., 2001; Suzuki et al., 2006; Zhang et al., 2003). Additionally, *in vitro* studies have demonstrated that human osteoblasts have the ability to produce important hematopoietic cytokines, such as granulocyte colony-stimulating factor (G-CSF) and hepatocyte growth factor (HGF), that support the proliferation of human hematopoietic progenitor cells

(CD34⁺ bone marrow cells) that were enriched in HSCs (Taichman et al., 2001; Taichman and Emerson, 1994; Taichman et al., 1996).

Parathyroid hormone (PTH) is a major regulator of calcium homeostasis, playing an important role in both the formation and resorption of bone. In a study by Calvi et al., transgenic mice (col1-caPPR) were generated which expressed constitutively activated PTH or the PTH-related protein (PTHrP) receptor (PPR) under control of the type-1 collagen $\alpha 1$ (*Col1 α 1*) promoter, which is active in osteoblastic cells (Calvi et al., 2003; Calvi et al., 2001). These transgenic mice displayed significant increases in the numbers of osteoblasts and functional HSCs in the bone marrow. PTH administered directly to wild-type animals also expanded the populations of both osteoblasts and HSCs (Calvi et al., 2003). In a separate study, mice engineered with a conditional inactivation of bone morphogenic protein receptor 1A (*Bmpr1a*), which is normally expressed in osteoblast cells but not in HSCs, showed a positive correlation between the number of osteoblasts and functional HSCs (Zhang et al., 2003). In the same study, it was also reported that HSCs were found in close contact with spindle-shaped, N-cadherin-positive osteoblasts on the endosteal surface (Zhang et al., 2003). Conversely, by using a transgenic mouse which allowed for the conditional destruction of osteoblasts, Visnjic et al. demonstrated that ablation of osteoblasts led to a decrease in the absolute number of HSCs in the bone marrow and a transfer of a substantial proportion of hematopoietic activity to the spleen and liver (Visnjic et al., 2004). These studies show that the number of osteoblasts in the bone marrow microenvironment is directly related to the

number of functional HSCs or hematopoietic progenitors, indicating that osteoblasts, or a subset of osteoblast cells, serve as important components of the HSC niche cells.

Bone homeostasis is tightly regulated not only by osteoblasts, but also by osteoclasts, which are specialized bone resorbing cells of hematopoietic origin. Osteoclasts have also been suggested to be components of the HSC microenvironment. Specifically, activation of osteoclasts promotes the mobilization of hematopoietic progenitors into circulation, suggesting that osteoclast activity may play a part in the regulation of the endosteal HSC niche (Kollet et al., 2006). Many studies have also proposed that osteoblasts and osteoclasts express a variety of factors, including osteopontin, angiopoietin-1, matrix metalloproteinase 9 (MMP9), and cathepsin K, which regulate the maintenance and localization of HSCs in the bone marrow (Arai et al., 2004; Kollet et al., 2006; Nilsson et al., 2005; Stier et al., 2005). In addition to the critical role of osteoblasts in supporting the maintenance of HSCs, osteoblasts have also been shown to influence B-lymphocyte commitment and differentiation (Visnjic et al., 2004; Wu et al., 2008; Zhu et al., 2007). Collectively, these studies suggest that there is a close relationship between bone homeostasis and hematopoiesis.

Other cellular components in the bone marrow have also been suggested to function in HSCs maintenance during adulthood. *In vivo* and tissue section images have shown HSCs are also located in close proximity to endothelial cells in the bone marrow, indicating that endothelial cells may also serve as important

components in the HSC niche (Kiel et al., 2005; Sipkins et al., 2005). *In vitro* experiments showed that vascular endothelial cells that were isolated either from embryonic tissues or from some adult non-hematopoietic tissues maintain the repopulating capacity of HSCs or support the expansion of hematopoietic progenitors (Li et al., 2003; Li et al., 2004; Ohneda et al., 1998). These studies suggest that endothelial cells express factors that promote the maintenance of HSCs *in vitro*. Moreover, perivascular reticular cells with high expression of CXCL12, a cytokine required for the maintenance of HSCs, have also been found in close contact with HSCs in the bone marrow suggesting a possible role of reticular cells in supporting HSCs (Sugiyama et al., 2006). Recently, Naveiras et al. demonstrated that bone-marrow adipocytes act as negative regulators in HSC maintenance (Naveiras et al., 2009). Together, these studies demonstrated that, in addition to the important role of bone homeostasis in HSC maintenance, the HSC niche in bone marrow could be influenced by multiple cell types found either at or near the endosteum, each of which may have different functions in the regulation or maintenance of HSCs.

However, the correlation between bone homeostasis and HSC maintenance were found in physiological states; whether the relationship between these two systems in pathological conditions would be disturbed remains uncertain.

The K/BxN Mouse Model of Inflammatory Arthritis

Rheumatoid arthritis (RA) is a chronic inflammatory disease which affects

approximately 1% of the world's population (Weinblatt and Kuritzky, 2007). A hallmark of this disease is the progressive destruction of peri-articular bone (bone near the joints) which leads to bone erosion and functional disability. In addition to joint destruction, human RA patients also display systemic osteoporosis (Haugeberg et al., 2000; Spector et al., 1993). The etiology and pathogenesis of RA remain poorly understood. In RA research, animal models have been used as important tools for studying pathways and mechanisms involved in inflammatory arthritis. One of the most-studied models is the KRNxNOD (herein K/BxN) mouse model. K/BxN mice develop an inflammatory joint disease that is very similar to human rheumatoid and inflammatory arthritis (reviewed in Mandik-Nayak and Allen, 2005).

This model was developed as follows: the KRN-C57BL/6 (herein KRN) transgenic mouse was originally designed to study the specificity of T-cell receptors (TCRs) recognizing an epitope of bovine RNase (Kouskoff et al., 1996; Kouskoff et al., 1995). KRN transgenic mice display a normal phenotype under the C57BL/6 background. Intriguingly, when those KRN mice are crossed with non-obese, diabetic (NOD) mice, all of the F1 progeny (K/BxN) spontaneously exhibit a rapid, symmetrical onset of joint inflammation, primarily restricted to the joints of the front and rear limbs at around 30 ± 5 days of age (Kouskoff et al., 1996). Many characteristics of the inflammation in K/BxN mice are similar to human rheumatoid arthritis, including pannus formation, synovial hyperplasia, increased synovial volume, massive leukocyte infiltration, cartilage destruction, and bone erosion, followed by remodeling in the distal joints in the later stages

(Kouskoff et al., 1996). When KRN mice and C57BL/6 mice that were congenic for the NOD MHC H-2^{g7} (C57BL/6.H-2^{g7}; herein G7) were crossed, the offspring (KRNxG7) all developed inflammatory symptoms which were indistinguishable from those seen in K/BxN mice, indicating that MHC class II molecule I-A^{g7} was responsible for promoting arthritis in K/BxN mice (Kouskoff et al., 1996).

Subsequent studies found that the autoimmune response that is responsible for the inflammation seen in K/BxN mice is initiated by TCR recognition of a ubiquitously-expressed self-peptide derived from the glycolytic enzyme glucose-6-phosphate isomerase (GPI) presented by the I-A^{g7} MHC molecule on B-cells, resulting in production of high titers of autoantibodies against GPI (Matsumoto et al., 1999). Arthritic symptoms can be transferred to wild-type recipients by injecting them with serum from K/BxN or KRNxG7 mice, which contains a high level of GPI autoantibodies (serum-transfer model), but the serum-induced disease resolves within a few weeks (Korganow et al., 1999; Maccioni et al., 2002; Matsumoto et al., 1999). Thus, the serum-transfer model serves as an acute inflammation model, whereas the K/BxN transgenic mice serve as a chronic inflammatory model.

Many studies have demonstrated that joint destruction in rheumatoid arthritis in humans is linked to the activation of osteoclasts in the joints (Gravallese et al., 1998; Gravallese et al., 2000; Shigeyama et al., 2000). Receptor activator of nuclear factor- κ B ligand (RANKL) is a cytokine that regulates the completion of the final steps of osteoclast differentiation, as well as for their bone resorbing activity (Kong et al., 1999; Lacey et al., 1998). Several

pro-inflammatory cytokines, such as interleukin (IL)-1, IL-6, IL-17 and especially tumor necrosis factor (TNF)- α , can induce and enhance RANKL expression (Kotake et al., 1999; Lam et al., 2000; Wei et al., 2005; Wong et al., 2006). It has been demonstrated that RA patients produce excessive TNF- α and RANKL (Chu et al., 1991; Gravallesse et al., 2000; Takayanagi et al., 2000). K/BxN mice also display high levels of TNF- α and IL-6 in their joints (Kouskoff et al., 1996). Mice with defective osteoclasts or limited osteoclastogenesis are resistant to both K/BxN serum-induced and TNF- α -mediated joint destruction (Pettit et al., 2001; Redlich et al., 2002).

Most studies using K/BxN mouse model have focused on identifying cellular components and pathogenic mechanisms involved in the initiation of joint-specific inflammation and destruction of joints (Akilesh et al., 2004; Corr and Crain, 2002; Ji et al., 2002a; Ji et al., 2002b; Lee et al., 2002; Pettit et al., 2001; Watts et al., 2005; Wipke and Allen, 2001), whereas associated conditions, such as systemic osteoporosis, have not been carefully characterized in the mouse model.

Overall Goals of Chapter Two

Hematopoietic stem cells (HSCs) reside mainly in the bone marrow and undergo well-controlled cell division to regenerate themselves while also producing progenitor cells that differentiate to all types of mature blood cells throughout adult life. The maintenance of HSCs in the bone marrow has been suggested to have a close association with bone homeostasis in normal physiological states, but little is known about their relationship in pathological conditions. The objective of chapter two is to investigate the relationship between hematopoiesis and bone homeostasis in pathological conditions using a mouse model of chronic inflammatory arthritis.

References

- Akilesh, S., Petkova, S., Sproule, T. J., Shaffer, D. J., Christianson, G. J. and Roopenian, D.** (2004). The MHC class I-like Fc receptor promotes humorally mediated autoimmune disease. *J Clin Invest* **113**, 1328-33.
- Arai, F., Hirao, A., Ohmura, M., Sato, H., Matsuoka, S., Takubo, K., Ito, K., Koh, G. Y. and Suda, T.** (2004). Tie2/angiopoietin-1 signaling regulates hematopoietic stem cell quiescence in the bone marrow niche. *Cell* **118**, 149-61.
- Calvi, L. M., Adams, G. B., Weibrecht, K. W., Weber, J. M., Olson, D. P., Knight, M. C., Martin, R. P., Schipani, E., Divieti, P., Bringham, F. R. et al.** (2003). Osteoblastic cells regulate the haematopoietic stem cell niche. *Nature* **425**, 841-6.
- Calvi, L. M., Sims, N. A., Hunzelman, J. L., Knight, M. C., Giovannetti, A., Saxton, J. M., Kronenberg, H. M., Baron, R. and Schipani, E.** (2001). Activated parathyroid hormone/parathyroid hormone-related protein receptor in osteoblastic cells differentially affects cortical and trabecular bone. *J Clin Invest* **107**, 277-86.
- Chu, C. Q., Field, M., Feldmann, M. and Maini, R. N.** (1991). Localization of tumor necrosis factor alpha in synovial tissues and at the cartilage-pannus junction in patients with rheumatoid arthritis. *Arthritis Rheum* **34**, 1125-32.
- Corr, M. and Crain, B.** (2002). The role of FcγR signaling in the K/B x N serum transfer model of arthritis. *J Immunol* **169**, 6604-9.
- Gravallese, E. M., Harada, Y., Wang, J. T., Gorn, A. H., Thornhill, T. S. and Goldring, S. R.** (1998). Identification of cell types responsible for bone resorption in rheumatoid arthritis and juvenile rheumatoid arthritis. *Am J Pathol* **152**, 943-51.
- Gravallese, E. M., Manning, C., Tsay, A., Naito, A., Pan, C., Amento, E. and Goldring, S. R.** (2000). Synovial tissue in rheumatoid arthritis is a source of osteoclast differentiation factor. *Arthritis Rheum* **43**, 250-8.
- Haugeberg, G., Uhlig, T., Falch, J. A., Halse, J. I. and Kvien, T. K.** (2000). Bone mineral density and frequency of osteoporosis in female patients with rheumatoid arthritis: results from 394 patients in the Oslo County Rheumatoid Arthritis register. *Arthritis Rheum* **43**, 522-30.
- Ji, H., Ohmura, K., Mahmood, U., Lee, D. M., Hofhuis, F. M., Boackle, S. A., Takahashi, K., Holers, V. M., Walport, M., Gerard, C. et al.** (2002a). Arthritis critically dependent on innate immune system players. *Immunity* **16**, 157-68.
- Ji, H., Pettit, A., Ohmura, K., Ortiz-Lopez, A., Duchatelle, V., Degott, C., Gravallese, E., Mathis, D. and Benoist, C.** (2002b). Critical roles for interleukin 1 and tumor necrosis factor alpha in antibody-induced arthritis. *J Exp Med* **196**, 77-85.
- Kiel, M. J., Yilmaz, O. H., Iwashita, T., Yilmaz, O. H., Terhorst, C. and Morrison, S. J.** (2005). SLAM family receptors distinguish hematopoietic stem and progenitor cells and reveal endothelial niches for stem cells. *Cell* **121**, 1109-21.
- Kollet, O., Dar, A., Shivtiel, S., Kalinkovich, A., Lapid, K., Sztainberg, Y., Tesio, M., Samstein, R. M., Goichberg, P., Spiegel, A. et al.** (2006). Osteoclasts degrade endosteal components and promote mobilization of hematopoietic progenitor cells. *Nat Med* **12**, 657-64.
- Kong, Y. Y., Yoshida, H., Sarosi, I., Tan, H. L., Timms, E., Capparelli, C., Morony, S., Oliveira-dos-Santos, A. J., Van, G., Itie, A. et al.** (1999). OPGL is a key regulator of osteoclastogenesis, lymphocyte development and lymph-node organogenesis. *Nature*

397, 315-23.

Korganow, A. S., Ji, H., Mangialaio, S., Duchatelle, V., Pelanda, R., Martin, T., Degott, C., Kikutani, H., Rajewsky, K., Pasquali, J. L. et al. (1999). From systemic T cell self-reactivity to organ-specific autoimmune disease via immunoglobulins. *Immunity* **10**, 451-61.

Kotake, S., Udagawa, N., Takahashi, N., Matsuzaki, K., Itoh, K., Ishiyama, S., Saito, S., Inoue, K., Kamatani, N., Gillespie, M. T. et al. (1999). IL-17 in synovial fluids from patients with rheumatoid arthritis is a potent stimulator of osteoclastogenesis. *J Clin Invest* **103**, 1345-52.

Kouskoff, V., Korganow, A. S., Duchatelle, V., Degott, C., Benoist, C. and Mathis, D. (1996). Organ-specific disease provoked by systemic autoimmunity. *Cell* **87**, 811-22.

Kouskoff, V., Signorelli, K., Benoist, C. and Mathis, D. (1995). Cassette vectors directing expression of T cell receptor genes in transgenic mice. *J Immunol Methods* **180**, 273-80.

Lacey, D. L., Timms, E., Tan, H. L., Kelley, M. J., Dunstan, C. R., Burgess, T., Elliott, R., Colombero, A., Elliott, G., Scully, S. et al. (1998). Osteoprotegerin ligand is a cytokine that regulates osteoclast differentiation and activation. *Cell* **93**, 165-76.

Lam, J., Takeshita, S., Barker, J. E., Kanagawa, O., Ross, F. P. and Teitelbaum, S. L. (2000). TNF-alpha induces osteoclastogenesis by direct stimulation of macrophages exposed to permissive levels of RANK ligand. *J Clin Invest* **106**, 1481-8.

Lee, D. M., Friend, D. S., Gurish, M. F., Benoist, C., Mathis, D. and Brenner, M. B. (2002). Mast cells: a cellular link between autoantibodies and inflammatory arthritis. *Science* **297**, 1689-92.

Li, W., Johnson, S. A., Shelley, W. C., Ferkowicz, M., Morrison, P., Li, Y. and Yoder, M. C. (2003). Primary endothelial cells isolated from the yolk sac and para-aortic splanchnopleura support the expansion of adult marrow stem cells in vitro. *Blood* **102**, 4345-53.

Li, W., Johnson, S. A., Shelley, W. C. and Yoder, M. C. (2004). Hematopoietic stem cell repopulating ability can be maintained in vitro by some primary endothelial cells. *Exp Hematol* **32**, 1226-37.

Maccioni, M., Zeder-Lutz, G., Huang, H., Ebel, C., Gerber, P., Hergueux, J., Marchal, P., Duchatelle, V., Degott, C., van Regenmortel, M. et al. (2002). Arthritogenic monoclonal antibodies from K/BxN mice. *J Exp Med* **195**, 1071-7.

Mandik-Nayak, L. and Allen, P. M. (2005). Initiation of an autoimmune response: insights from a transgenic model of rheumatoid arthritis. *Immunol Res* **32**, 5-13.

Matsumoto, I., Staub, A., Benoist, C. and Mathis, D. (1999). Arthritis provoked by linked T and B cell recognition of a glycolytic enzyme. *Science* **286**, 1732-5.

Naveiras, O., Nardi, V., Wenzel, P. L., Hauschka, P. V., Fahey, F. and Daley, G. Q. (2009). Bone-marrow adipocytes as negative regulators of the haematopoietic microenvironment. *Nature*.

Nilsson, S. K., Johnston, H. M. and Coverdale, J. A. (2001). Spatial localization of transplanted hemopoietic stem cells: inferences for the localization of stem cell niches. *Blood* **97**, 2293-9.

Nilsson, S. K., Johnston, H. M., Whitty, G. A., Williams, B., Webb, R. J., Denhardt, D. T., Bertonecello, I., Bendall, L. J., Simmons, P. J. and Haylock, D. N. (2005). Osteopontin, a key component of the hematopoietic stem cell niche and regulator of

primitive hematopoietic progenitor cells. *Blood* **106**, 1232-9.

Ohneda, O., Fennie, C., Zheng, Z., Donahue, C., La, H., Villacorta, R., Cairns, B. and Lasky, L. A. (1998). Hematopoietic stem cell maintenance and differentiation are supported by embryonic aorta-gonad-mesonephros region-derived endothelium. *Blood* **92**, 908-19.

Pettit, A. R., Ji, H., von Stechow, D., Muller, R., Goldring, S. R., Choi, Y., Benoist, C. and Gravallesse, E. M. (2001). TRANCE/RANKL knockout mice are protected from bone erosion in a serum transfer model of arthritis. *Am J Pathol* **159**, 1689-99.

Redlich, K., Hayer, S., Ricci, R., David, J. P., Tohidast-Akrad, M., Kollias, G., Steiner, G., Smolen, J. S., Wagner, E. F. and Schett, G. (2002). Osteoclasts are essential for TNF-alpha-mediated joint destruction. *J Clin Invest* **110**, 1419-27.

Shigeyama, Y., Pap, T., Kunzler, P., Simmen, B. R., Gay, R. E. and Gay, S. (2000). Expression of osteoclast differentiation factor in rheumatoid arthritis. *Arthritis Rheum* **43**, 2523-30.

Sipkins, D. A., Wei, X., Wu, J. W., Runnels, J. M., Cote, D., Means, T. K., Luster, A. D., Scadden, D. T. and Lin, C. P. (2005). In vivo imaging of specialized bone marrow endothelial microdomains for tumour engraftment. *Nature* **435**, 969-73.

Spector, T. D., Hall, G. M., McCloskey, E. V. and Kanis, J. A. (1993). Risk of vertebral fracture in women with rheumatoid arthritis. *Bmj* **306**, 558.

Stier, S., Ko, Y., Forkert, R., Lutz, C., Neuhaus, T., Grunewald, E., Cheng, T., Dombkowski, D., Calvi, L. M., Rittling, S. R. et al. (2005). Osteopontin is a hematopoietic stem cell niche component that negatively regulates stem cell pool size. *J Exp Med* **201**, 1781-91.

Sugiyama, T., Kohara, H., Noda, M. and Nagasawa, T. (2006). Maintenance of the hematopoietic stem cell pool by CXCL12-CXCR4 chemokine signaling in bone marrow stromal cell niches. *Immunity* **25**, 977-88.

Suzuki, N., Ohneda, O., Minegishi, N., Nishikawa, M., Ohta, T., Takahashi, S., Engel, J. D. and Yamamoto, M. (2006). Combinatorial Gata2 and Sca1 expression defines hematopoietic stem cells in the bone marrow niche. *Proc Natl Acad Sci U S A* **103**, 2202-7.

Taichman, R., Reilly, M., Verma, R., Ehrenman, K. and Emerson, S. (2001). Hepatocyte growth factor is secreted by osteoblasts and cooperatively permits the survival of haematopoietic progenitors. *Br J Haematol* **112**, 438-48.

Taichman, R. S. and Emerson, S. G. (1994). Human osteoblasts support hematopoiesis through the production of granulocyte colony-stimulating factor. *J Exp Med* **179**, 1677-82.

Taichman, R. S., Reilly, M. J. and Emerson, S. G. (1996). Human osteoblasts support human hematopoietic progenitor cells in vitro bone marrow cultures. *Blood* **87**, 518-24.

Takayanagi, H., Iizuka, H., Juji, T., Nakagawa, T., Yamamoto, A., Miyazaki, T., Koshihara, Y., Oda, H., Nakamura, K. and Tanaka, S. (2000). Involvement of receptor activator of nuclear factor kappaB ligand/osteoclast differentiation factor in osteoclastogenesis from synoviocytes in rheumatoid arthritis. *Arthritis Rheum* **43**, 259-69.

Visnjic, D., Kalajzic, Z., Rowe, D. W., Katavic, V., Lorenzo, J. and Aguila, H. L. (2004). Hematopoiesis is severely altered in mice with an induced osteoblast deficiency. *Blood* **103**, 3258-64.

Watts, G. M., Beurskens, F. J., Martin-Padura, I., Ballantyne, C. M., Klickstein, L. B., Brenner, M. B. and Lee, D. M. (2005). Manifestations of inflammatory arthritis are

- critically dependent on LFA-1. *J Immunol* **174**, 3668-75.
- Wei, S., Kitaura, H., Zhou, P., Ross, F. P. and Teitelbaum, S. L.** (2005). IL-1 mediates TNF-induced osteoclastogenesis. *J Clin Invest* **115**, 282-90.
- Weinblatt, M. E. and Kuritzky, L.** (2007). RAPID: rheumatoid arthritis. *J Fam Pract* **56**, S1-7; quiz S8.
- Wilson, A. and Trumpp, A.** (2006). Bone-marrow haematopoietic-stem-cell niches. *Nat Rev Immunol* **6**, 93-106.
- Wipke, B. T. and Allen, P. M.** (2001). Essential role of neutrophils in the initiation and progression of a murine model of rheumatoid arthritis. *J Immunol* **167**, 1601-8.
- Wong, P. K., Quinn, J. M., Sims, N. A., van Nieuwenhuijze, A., Campbell, I. K. and Wicks, I. P.** (2006). Interleukin-6 modulates production of T lymphocyte-derived cytokines in antigen-induced arthritis and drives inflammation-induced osteoclastogenesis. *Arthritis Rheum* **54**, 158-68.
- Wu, J. Y., Purton, L. E., Rodda, S. J., Chen, M., Weinstein, L. S., McMahon, A. P., Scadden, D. T. and Kronenberg, H. M.** (2008). Osteoblastic regulation of B lymphopoiesis is mediated by Gs{alpha}-dependent signaling pathways. *Proc Natl Acad Sci U S A* **105**, 16976-81.
- Zhang, J., Niu, C., Ye, L., Huang, H., He, X., Tong, W. G., Ross, J., Haug, J., Johnson, T., Feng, J. Q. et al.** (2003). Identification of the haematopoietic stem cell niche and control of the niche size. *Nature* **425**, 836-41.
- Zhu, J., Garrett, R., Jung, Y., Zhang, Y., Kim, N., Wang, J., Joe, G. J., Hexner, E., Choi, Y., Taichman, R. S. et al.** (2007). Osteoblasts support B-lymphocyte commitment and differentiation from hematopoietic stem cells. *Blood* **109**, 3706-12.

Chapter 2.2

Results

This chapter has been accepted by *Blood* on July 28, 2009.

Defects in osteoblast function but no changes in long term repopulating potential of hematopoietic stem cells in a mouse chronic inflammatory arthritis model

Yunglin D. Ma^{1,2,§}, Changwon Park^{1,§}, Haibo Zhao¹, Kwadwo A. Oduro Jr^{1,2,3}, Xiaolin Tu⁴, Fanxin Long⁴, Paul M. Allen¹, Steven L. Teitelbaum¹ and Kyunghee Choi^{1,2,#}

¹Department of Pathology and Immunology, ²Developmental Biology Program, ³Medical Scientist Training Program, ⁴Department of Medicine
Washington University School of Medicine, St. Louis, MO

[§]These authors contributed equally

[#]Corresponding author, kchoi@wustl.edu

Running title: Hematopoietic Stem Cells and Bone Homeostasis

Key words: hematopoietic stem cell, osteoporosis, osteoblast, niche, inflammation, arthritis

Abstract

Recent studies support the notion that there is an intricate relationship between hematopoiesis and bone homeostasis in normal steady states. By utilizing mice undergoing chronic inflammatory arthritis, we investigated the relationship between hematopoiesis and bone homeostasis in pathologic conditions. We demonstrate that mice undergoing chronic inflammatory arthritis displayed osteoporosis due to a severe defect in osteoblast function. Despite the defective osteoblast function, however, the hematopoietic stem cells from these mice exhibited normal properties in either long-term repopulation or cell cycling. Therefore, the bone forming capacity of osteoblasts is distinct from their ability to maintain hematopoietic stem cells in chronic inflammatory conditions.

Introduction

Under normal physiologic conditions, hematopoietic stem cells (HSCs) residing within the specialized bone marrow (BM) niche maintain a balance between self-renewal and differentiation and provide continuous supply of circulating mature immune cells with a limited life span. An intricate relationship exists between hematopoiesis and bone homeostasis. As such, osteoblasts serve as a HSC niche, while osteoclasts mediate HSC and progenitor egress from the BM (Kollet et al., 2007; Purton and Scadden, 2006). Specifically, an increase in osteoblast number and/or activation through conditional Alk3 deletion or parathyroid hormone administration augments the HSC frequency in BM (Calvi et al., 2003; Zhang et al., 2003). Conversely, ablation of osteoblasts results in a decrease in absolute number of phenotypic primitive hematopoietic progenitors (Visnjic et al., 2004).

Rheumatoid arthritis (RA) is a chronic systemic inflammatory autoimmune disease of unknown etiology afflicting 1% of the population. It leads to destruction of cartilage and bone at multiple joints with a distal to proximal preference. RA is also attended by systemic osteoporosis. However, the mechanisms of RA-associated osteoporosis are less appreciated than how joints are destroyed. The KRNxNOD (herein K/BxN) mouse model of inflammatory arthritis recapitulates many of the features of human RA (Kyburz and Corr, 2003; Monach et al., 2007). These mice were generated fortuitously when mice transgenic for a T cell receptor recognizing an epitope of bovine RNase

(C57BL/6.KRN, herein KRN) were bred onto a NOD background (Kouskoff et al., 1996). They developed spontaneous chronic and severely destructive arthritis with 100% penetrance that resembled human RA (Kouskoff et al., 1996). KRN with a C57BL/6 line congenic for the NOD MHC H-2^{g7} (C57BL/6.H-2^{g7}; herein G7) was used to distinguish the contribution of MHC from non-MHC NOD-derived genes to disease development. The KRNxC57BL/6.H-2^{g7} (herein KRNxG7) offspring all develop overt joint swelling and the histological hallmarks of arthritis of K/BxN mice, indicating that H-2^{g7} is sufficient for RA development (Kouskoff et al., 1996).

By utilizing a KRNxG7 mouse model, we investigated the relationship between HSCs and bone homeostasis in chronic inflammatory conditions. We demonstrate that similar to patients with RA, mice with inflammatory arthritis develop osteoporosis. However, unlike the osteolysis of inflamed joints, which reflects accelerated osteoclast activity, the systemic bone loss of arthritic mice is the result of arrested osteoblast function. This conclusion is consistent with the decrease in generation of mature osteoclasts in vivo. Unexpectedly, the osteoblast deficiency in bone formation did not affect the long term repopulating potential of HSCs in these arthritic mice. Collectively, we provide evidence that marrow HSCs can be maintained in the absence of functional osteoblasts in chronic inflammatory environments.

Materials and Methods

Mice

KRN (TCR transgenic) mice on a C57BL/6 background were crossed with G7 (I-A^{g7}) to generate KRNxG7 mice. C57BL/6J (CD45.2 allele) and B6.SJL-*Ptprc^aPep3^b*/BoyJ (CD45.1 allele) mice were obtained from The Jackson Laboratory (Bar Harbor, ME). All animals were housed in accordance with National Institutes of Health and American Association for Accreditation of Laboratory Animal Care regulations, and animal protocols were reviewed and approved by the Washington University animal studies committee.

Cell preparation and Flow Cytometric Analyses (FACS)

Bone marrow cells were prepared by vigorously flushing femur and tibia 6-8 times. Peripheral blood was obtained by retro-orbital collection. Spleen cells were prepared by gently crushing the tissue and filtering through a 40µm cell strainer (BD Falcon). Liver cells were obtained by gently crushing the tissue and filtering through a 70µm cell strainer (BD Falcon). All collected cells were treated with RBC lysis buffer (Roche) before analyses.

FACS analyses were performed as described previously (Park et al., 2004). For KSL analysis we used FITC-conjugated antibodies against CD4, CD8, Mac-1, Gr-1, Ter119, and B220 (lineage marker antibodies, BD Biosciences or eBioscience), PE-conjugated anti-Sca-1, PerCP/Cy5.5-conjugated anti-CD45, and APC-conjugated anti-c-Kit (eBioscience). For some experiments anti-CD45

APC-Alexa 750 (eBioscience) or anti-c-Kit PerCP/Cy5.5 (Biolegend) were used. SLAM analysis was performed using anti-CD150 PE (Biolegend), anti-CD48 FITC (eBioscience) and anti-CD41 FITC (BD Biosciences). Mature lineage analysis was performed with FITC and PE conjugated antibodies to the lineage markers mentioned above as well as Alexa 647 conjugated anti-Mac-1 (BD Biosciences) and APC conjugated F4/80 (eBioscience).

LMPP (Lymphoid Primed Multipotential Progenitor; Kit+Sca1+Lin-Flk2^{hi}CD34+) and CLP (Common Lymphoid Progenitor; Lin-Flk2+IL-7R α +) analyses were performed with the following fluorophore conjugated antibodies: α -Sca1-FITC, α -IL-7R α -biotin, α -cKit-APC-Alexa 750 (eBioscience), α -Flk2-PE, α -CD34-Alexa647, α -Lineage-APC cocktail, Streptavidin-PerCP/Cy5.5 (BD Biosciences) and α -Lineage-biotin cocktail (Miltenyi). PreproB analysis was performed with α -IgM-FITC, α -CD43-PE, α -NK1.1 PerCP/Cy5.5, α -CD11c PE-Cy7, α -B220-biotin (BD Bioscience), α -CD19-Alexa647, Streptavidin APC-eFluor 708 (eBioscience). Other antibodies used for B cell precursor analysis were α -B220-PerCP/Cy5.5 (eBioscience) and α -AA4.1-FITC (BD Bioscience). Cells were analyzed using a Facscalibur (4-color), a FACScan adapted for 5 color analysis, or FACScanto (6 color) and data analyzed with Cell Quest (BD) or Flow Jo softwares (Tree Star).

BrdU labeling

KRNxG7 and control mice (6-8 week old) were injected with a single dose (1mg per 6g of body mass) of sterile-filtered BrdU (Sigma) dissolved in PBS. Mice

were sacrificed 2-3 hours later and bone marrow cells harvested as described earlier. Harvested bone marrow cells were subjected to lineage cell depletion by magnetic separation using the lineage cell depletion kit (Miltenyi). Lineage depleted cells were stained with α -cKit-FITC (eBioscience), α -Sca1-PE and Streptavidin-PerCP-Cy5.5 (BD Pharmingen). Cells were subsequently fixed and intracellularly stained with APC conjugated α -BrdU antibody using the APC-BrdU flow kit (BD Pharmingen). Cells were analyzed using the BD FACScalibur and data analyzed using BD Cell Quest software.

Ki67/Hoechst Analysis

Lin⁺ cells were depleted from bone marrow by magnetic sorting as described above using biotin-conjugated anti-Lin antibodies (Miltenyi). Cells were surface stained with α -Sca1 PE, Streptavidin PerCP/Cy5.5 (BD Bioscience) and α -cKit APC (eBioscience). Ki67/Hoechst staining has previously been used to assess KSL cycling and our method was adapted from this previous study (Wilson et al., 2004). Surface stained cells were fixed and permeabilized using BD Cytotfix/Cytoperm buffer followed by intracellular staining with α -Ki67 FITC for 30 minutes followed by a 5 minute Hoechst incubation (20 μ g/ml). 5-color flow cytometry was performed with a MoFlo (Dako), which has UV excitation capability. Data analysis was performed with Summit or FlowJo softwares. Doublets were excluded in the gated populations that were analyzed for Ki67 expression. The Ki67 negative population was defined based on staining a

control population of cells with a FITC conjugated isotype control antibody (BD Biosciences).

Progenitor assay

Cells from bone marrow and spleen were replated in Methocult M3434 (Stemcell Tech, CA). Colonies were counted 7-10 days later.

Cell transplantation

For serial bone marrow transplantation, lethally irradiated (1,000Rads) B6xG7 (CD45.1xCD45.2) recipients were injected (i.v.) with unfractionated 1×10^6 BM cells from 6 week old KRNxG7 (CD45.2xCD45.2) or B6xG7 (CD45.2xCD45.2) mice (five recipients for each group). PB samples were analyzed for CD45.1 and CD45.2 every 4 weeks. Seven months after transplantation, bone marrow suspensions were prepared from primary recipients and 1×10^6 nucleated cells were injected into new lethally irradiated B6xG7 (CD45.1xCD45.2) recipient mice (8 for control and 9 for KRNxG7). The tertiary transplantation was performed seven months after secondary transplantation (7 for control and 9 for KRNxG7). The recipients of serial bone marrow transplantation were subjected to lineage analyses for donor contributions 6 or 7 months after transplantations.

Competitive repopulation assay has been described previously (Stier et al., 2005). Briefly, 6-week old B6xG7 (CD45.2xCD45.2) or KRNxG7 (CD45.2xCD45.2) bone marrow cells, 2×10^5 , were mixed with 2×10^5 B6xG7 (CD45.1xCD45.2) competitor

bone marrow cells and injected (i.v.) into lethally irradiated (1000 Rads) B6xG7 (CD45.1xCD45.2) recipient mice. Peripheral blood (PB) samples were collected retro-orbitally three and five months after transplantation and analyzed for CD45.1 and CD45.2.

Lineage negative (Lin⁻) spleen cells from 6-week old B6xG7 (CD45.2xCD45.2) or KRNxG7 (CD45.2xCD45.2) mice were isolated using MACS Lineage Cell Depletion Kit (Miltenyi Biotec). One x 10⁵ sorted Lin⁻ cells were injected into lethally irradiated (1,000Rads) B6xG7 (CD45.1xCD45.2) recipients. Reconstitution of donor-derived cells (CD45.2) was monitored by staining retro-orbitally obtained peripheral blood cells with monoclonal antibodies against CD45.2 and CD45.1 (eBioscience) followed by FACS analysis.

Serum TRAP5b activity and serum osteocalcin activity

Blood was collected retro-orbitally under anesthesia prior to sacrifice. The serum TRACP5b activities of 6 week old G7 and KRNxG7 mice were measured by MouseTRAPTM Assay ELISA kit (Immunodiagnostic Systems Inc.). Serum Osteocalcin levels of 6 week old G7 and KRNxG7 mice were measured by Mouse Osteocalcin ELISA kit (Biomedical Technologies Inc.).

Histology and Histomorphometry

The tibiae of 6-week old B6xG7 and KRNxG7 mice were fixed with 70% ethanol followed by plastic embedding and Goldner staining, or with 10% neutral buffered

formalin followed by the decalcification in 14% EDTA for 4-5 days, paraffin embedding, and TRAP staining. Calcein (Sigma) (7.5 mg/kg, i.p) was injected on day 7 and 12. Mice were sacrificed on day 14. Osteoclastic and osteoblastic perimeters were measured and analyzed using Osteomeasure (OsteoMetrics, Atlanta, GA) in a blinded fashion.

μCT

The trabecular volume in the distal femoral metaphysis was measured using a Scanco μCT40 scanner (Scanco Medical AG, Basserdorf, Switzerland). A threshold of 300 was used for evaluation of all scans. 30 slices were analyzed, starting with the first slice in which condyles and primary spongiosa were no longer visible.

qRT-PCR

RNA preparation and cDNA synthesis were previously described (Lee et al., 2008). Primer sequences used in this study are provided in supplementary Table 2.2-1.

Statistical Analyses

Statistical significance was assessed by two-tailed Student's *t* test. Values of $P < 0.05$ were considered statistically significant.

Total bone marrow cell isolation

Bone marrow isolation by crushing and enzymatic digestion was performed as done previously (Haylock et al., 2007) using the Hematopoietic Stem Cell Isolation Kit (Millipore). Briefly, one femur and one tibia were collected and ground in a mortar and pestle in PBS with 4% FCS. The cells and small bone fragments were washed with PBS with 4% FCS and filtered through a 40 μ m cell strainer. Small bone fragments were incubated with 3 mg/ml Collagenase I and 4 mg/ml Dispase II (Stem Cell Isolation Kit, Millipore) for 5 minutes at 37°C in an orbital shaker. The fragments were washed and cells were collected by filtered through 40 μ m cell strainer. Bone marrow from the contralateral femur and tibia were obtained by vigorous flushing as described in Methods. Cells retrieved by both isolation methods were RBC lysed, count on a hemocytometer and FACS analysed for KSL frequency.

Alkaline Phosphatase (AP) expression assay

The details of AP expression assay on bone marrow stromal cells (BMSCs) are previously described (Tu et al., 2007). Briefly, Cells were harvested 3 days later after 100% confluence and tested by a biochemical assay using p-nitrophenyl phosphate (Sigma, St. Louis, MO) as a substrate; for mineralization assays, cells were switched to mineralization medium containing 50 μ g/ml ascorbic acid + 50 mM β -glycerophosphate for 2 weeks and changed medium every 3 days. The nodule formation was verified by von Kossa staining.

Osteoblast differentiation assays

Mineralization assays on BMSCs were performed as previously described (Tu et al., 2007) with a slight modification. Basically, femurs and tibia were aseptically removed from 6-weeks-old G7 and KRNxG7 mice. After the ephyseal ends of each bone were cut off, bone marrow was flushed out with 1 ml of alpha-MEM using a 25-gauge needle. Cells were treated with 1 ml of red blood cell lysis buffer (Roche, Indianapolis, IN) for 5 min at room temperature, rinsed and resuspended in alpha-MEM containing 20% fetal bovine serum. After filtered through a 70 μ m cell strainer, the cells were seeded at 2×10^6 /well in 12-well plates. Half of medium was changed at day 3 and all medium at day 6.

Results

KRNxG7 mice are osteoporotic due to diminished bone formation

K/BxN and KRNxG7 mice develop arthritic symptoms including ankle swelling shortly after 3 weeks of age (Kouskoff et al., 1996). The ankle thickness increases up to 5-6 weeks of age reaching a maximum of 4-5mm and remaining constant at a slightly lower level thereafter (Kouskoff et al., 1996). Typically, 6 week-old KRNxG7 mice in C57BL/6 genetic background were used in this study, as they show overt inflammation at this time point. As expected, KRNxG7 mice develop rheumatoid joint pannus and lysis of peri-articular bone (Figure 2.2-1A, B). Since human inflammatory arthritis is also attended by systemic bone loss, we asked if the same holds true in this murine model. Radiographs of KRNxG7 tibiae showed destruction of epiphyseal bone as well as metaphyseal demineralization. Histomorphometric and μ CT analysis of the same bones established a marked reduction of trabecular bone volume and consequently increased trabecular spacing (Figure 2.2-1C,D, F). A DEXA analysis exhibited decreased bone mineral density in arthritic mice (Figure 2.2-1E). Despite the profound metaphyseal osteoporosis, however, the number of mature resorptive cells was decreased in the marrow of endosteal bone (Figure 2.2-1G). This observation was confirmed by diminished serum levels of the global osteoclast marker TRAP5b (Figure 2.2-1H) and impaired expression of osteoclast specific genes in whole bone marrow (Figure 2.2-1I).

The chemokine SDF-1 plays a critical role in osteoclastogenesis by promoting osteoclast differentiation and the cell's longevity (Wright et al., 2005; Zannettino et al., 2005). In addition, inhibition of BM SDF-1 expression promotes osteoclast progenitor cell mobilization to the periphery (Zhang et al., 2008). We found that SDF-1 BM mRNA levels were decreased in KRNxG7 mice and thus its suppression likely mediates, at least in part, the noted in vivo arrest of terminal osteoclast differentiation (Figure 2.2-1J). Because TNF- α , which accelerates osteoclast progenitor mobilization in inflammatory erosive arthritis, also suppresses SDF-1 expression (Zhang et al., 2008), we posited that TNF- α level is increased in KRNxG7 mice. We indeed found that TNF- α mRNA and protein are increased in KRNxG7 BM and serum, respectively (Figure 2.2-1J & data not shown). Thus, although a direct link between TNF- α and SDF-1 in KRNxG7 mice needs to be established, in face of suppressed *Sdf-1* expression, osteoclast progenitor cells most likely do not readily assume the full resorptive phenotype but are mobilized to the periphery and migrate to the inflamed joint, which they degrade upon maturation.

Osteoporosis may reflect stimulated osteoclast or diminished osteoblast activity. KRNxG7 mice have reduced marrow osteoclasts in face of systemic osteoporosis suggesting that the paucity of bone extant in these animals reflects suppressed bone formation. To address this issue, we first histomorphometrically determined the number of trabecular osteoblasts/mm bone surface, which we found indistinguishable in KRNxG7 and G7 mice (Figure 2.2-2A). Moreover, *in*

in vitro osteoblast formation and bone nodule formation assessed by alkaline phosphatase activity and mineralization assays, respectively, were indistinguishable between KRNxG7 and controls (Supplementary Figure 2.2-1a, b). However, the percentage of metaphyseal bone surface covered by osteoid was reduced in the arthritic mice suggesting that the bone synthesizing population was diminished (Figure 2.2-2B). This posture was confirmed by dynamic histomorphometry, which established that the rate of metaphyseal bone formation is less than 1/3 of control (Figure 2.2-2C). Similarly, serum Osteocalcin as well as *Osteocalcin* mRNA, a marker of global bone formation, was reduced in KRNxG7 mice (Figure 2.2-2D, E). Additionally, mRNA expression of osteoblast specific genes, receptor activator of NFkappaB ligand (*Rankl*), *Osteoprotegerin* and *Runx2* was all markedly diminished (Figure 2.2-2E). Thus, the systemic osteoporosis attending the inflammatory arthritis of KRNxG7 mice reflects diminished bone formation and not accelerated bone resorption.

Systemic increase in Gr1+ cells and decrease in B220+ cells accompanied by impaired KRNxG7 marrow B lymphopoiesis

Our data so far shows that osteoblasts are functionally defective in KRNxG7 mice. In addition to bone formation, osteoblasts have been reported to play crucial roles in hematopoiesis by providing a niche to maintain HSCs and supporting B lymphopoiesis (Arai et al., 2004; Calvi et al., 2003; Visnjic et al., 2004; Wu et al., 2008; Zhang et al., 2003; Zhu et al., 2007). We noticed that KRNxG7 bone marrow cellularity was higher (~50% more) compared to that of

controls irrespective of the method of bone marrow collection (Supplementary Figure 2.2-2a). To investigate the specific hematopoietic changes occurring in chronic inflammation, we examined mature hematopoietic cell lineages in BM, spleen, liver and peripheral blood (Figure 2.2-3A). There was an increase in myeloid cells, specifically Gr1⁺, cells in all KRNxG7 tissues analyzed. Myeloid cells including neutrophils are abundant in the joint inflammation of human RA patients (Haynes, 2007) and are critical for the disease, as depletion of neutrophils or macrophages ameliorates inflammatory joint disease in a serum transfer model of RA (Solomon et al., 2005; Wipke and Allen, 2001). In KRNxG7 mice, T cells (detected by CD3, CD4 or CD8) bearing T cell receptor (TCR) transgene undergo negative selection (Kouskoff et al., 1996). Thus, as expected, T cells were reduced.

A decrease was also seen in B220⁺ cells in KRNxG7 mice for all tissues analyzed (Figure 2.2-3A) and this indeed reflects a decrease in B lineage cells not merely a decrease in B220 expression (Supplementary Figure 2.2-3a). To determine if defective marrow B lymphopoiesis in KRNxG7 mice could at least in part explain the diminution in B220⁺ frequency we examined the frequency of marrow B cell precursors. We found that a majority of the residual B220⁺ cells in KRNxG7 marrow were B cells (B220^{hi}IgM⁺) cells with almost complete depletion of B cell precursors (B220^{lo}AA4.1⁺)(Figure 2.2-3B & data not shown)(Hardy et al., 1991; Li et al., 1996). Further analysis revealed that not only were B cell committed, pre-proB, proB and preB, precursors absent but common lymphoid

progenitors (Karsunky et al., 2008) were also absent from KRNxG7 marrow (Figure 2.2-3C & Supplementary Figure 2.2-3b). Analysis of whole bone marrow gene expression also revealed a downregulation in several marrow B lymphopoiesis promoting factors including SDF-1, IL-7 and Flt3-L (Figure 2.2-1J & 2.2-3D). Therefore, KRNxG7 mice have impaired marrow B lymphopoiesis attending the defective osteoblasts.

The frequency of c-Kit+Sca1+Lin- cells is not changed in KRNxG7 bone marrow

Based on the current understanding that endosteal osteoblasts serve as a HSC niche and maintain the quiescence of the HSCs (Arai et al., 2004; Calvi et al., 2003; Zhang et al., 2003), the impairment of osteoblast bone forming capacity in KRNxG7 mice raised the possibility that its role in the HSC niche was also compromised. To determine if HSC and progenitor cell homeostasis was affected in the absence of functional osteoblasts in chronic inflammatory arthritic environments, we subjected KRNxG7 and control BM, spleen, liver and peripheral blood cells to CD45 (pan hematopoietic marker), c-Kit, Sca-1 and Lineage (Lin) marker staining. The frequency of HSC enriched KSL cells in the bone marrow was similar between the control and KRNxG7 mice when examined at 3 weeks of age, just prior to the onset of joint swelling (Figure 2.2-4A). There was no increase in BM cellularity at this age (not shown). The KSL frequency was also similar at 6 weeks of age, when all KRNxG7 mice show overt arthritis, irrespective of the method of marrow isolation (Figure 2.2-4A & Supplementary

Figure 2.2-2b). The frequency of CD150+CD48-CD41- (SLAM) cells, also enriched for HSCs (Kiel et al., 2005), in the bone marrow was also similar (Figure 2.2-4A). As the total bone marrow cellularity was increased (Supplementary Figure 2.2-2a), there was a net increase in absolute KSL number in KRNxG7 bone marrow despite osteoblast deficiency (Supplementary Figure 2.2-2c).

c-Kit+Sca1+Lin- cells in KRNxG7 bone marrow cycle normally

It has been suggested that quiescence and restricted proliferation of HSCs is important in maintaining stem cell properties and that osteoblasts maintain HSCs by promoting their quiescence (Arai et al., 2004; Orford and Scadden, 2008; Wilson and Trumpp, 2006). We therefore next investigated if KRNxG7 HSCs displayed altered proliferation and/or cell cycling. To this end, KRNxG7 arthritic as well as B6 control mice were subjected to 5-bromodeoxyuridine (BrdU) incorporation and cell cycle analyses. Specifically, mice were injected with a single dose of BrdU, sacrificed 2-3 hours later and BM cells were harvested and subjected to BrdU staining. There was no difference in BrdU labeling in KSL cell populations between control and KRNxG7 BM at 6-8wks, nor at earlier or later time points (Figure 2.2-4B & Supplementary Figure 2.2-4). We were also unable to detect a decrease in quiescence of KSL cells assessed by Ki67 and Hoechst staining (Ki67^{neg}Hoechst^{low}, Figure 2.2-4C & Supplementary Figure 2.2-5). For unknown reasons, however, more mature progenitor fractions (i.e. Lin-c-Kit+Sca1- or Lin-) had reduced BrdU positive fraction and increased Ki67^{neg}Hoechst^{low} suggesting an overall decrease in cycling (Figure 2.2-4B, C).

We also compared the expression of several cell cycle regulators including the “stemness” gene Bmi in arthritic and control KSL cells but failed to detect any differences for most genes (Supplementary Figure 2.2-6). Expression of the cell cycle inhibitors, p21 and p27 (Supplementary Figure 2.2-6), was decreased in arthritic KSL cells, however, it has previously been shown that complete deletion of these genes does not alter HSC function and/or pool size or cycling (Cheng et al., 2000; van Os et al., 2007). KRNxG7 KSL cells did not show any significant differences in Annexin V staining pattern from controls (not shown), suggesting that the KRNxG7 KSL cell survival/longevity is not changed. Collectively, these data suggest that KRNxG7 KSL cell cycle is unaltered.

The long term repopulating potential of KRNxG7 hematopoietic stem cells is not impaired

To assess if the properties of HSCs are altered in the defective bone forming osteoblast environments, lethally irradiated B6xG7 (CD45.1xCD45.2) recipients were transplanted with 1×10^6 whole BM cells from 6-week old KRNxG7 (CD45.2xCD45.2) mice. Age matched B6xG7 (CD45.2xCD45.2) BM cells served as controls. The donor contribution from KRNxG7 (CD45.2xCD45.2) BM was similar to that from B6xG7 (CD45.2xCD45.2) donor cells (Figure 2.2-4D). As expected, all blood cell lineages of donor origin were found as evidenced by lineage analyses of peripheral blood at 7 months after transplantation, although T cell generation was deficient due to negative selection (Supplementary Figure 2.2-7).

Subsequent secondary and tertiary transplantation studies indicated that KRNxG7 HSCs displayed no obvious defects in self-renewal potential (Supplementary Figure 2.2-7). To rule out the possibility that the long-term repopulation potential of HSCs is diminished in older animals, BM transplantation from 4 months old KRNxG7 mice was performed. Again, there was no compromise in hematopoietic reconstitution potential of KRNxG7 HSCs from old animals (Supplementary Figure 2.2-8).

To further confirm that HSC function was not compromised in these mice, we next subjected KRNxG7 HSCs to competitive repopulation studies. (Purton and Scadden, 2007) Specifically, B6xG7 (CD45.2xCD45.2) or KRNxG7 (CD45.2xCD45.2) bone marrow cells were mixed with equal number of B6xG7 (CD45.1xCD45.2) competitor bone marrow cells (2×10^5 cells each) and injected (i.v.) into lethally irradiated (1000 Rads) B6xG7 (CD45.1xCD45.2) recipient mice. Peripheral blood cells were collected and analyzed for CD45.1 and CD45.2. The contribution from KRNxG7 bone marrow cells was indistinguishable from that of the controls (Figure 2.2-4E). Collectively, we conclude that despite the severe defects in osteoblast bone-forming function in KRNxG7 mice, KRNxG7 BM HSC cycling was similar to controls and long term repopulating potential of these HSCs was not impaired.

c-Kit+Sca1+Lin- cells are maintained in KRNxG7 spleen

We noticed that most of the KRNxG7 mice had splenomegaly with no obvious hepatomegaly (Supplementary Figure 2.2-9a,b & data not shown). Intriguingly, the frequency of KSL cells as well as absolute KSL number was much greater in KRNxG7 spleen compared to B6xG7 spleen at 6 weeks of age (Figure 2.2-5A, Supplementary Figure 2.2-9c & data not shown). Similar changes in the KSL frequency also occurred in K/BxN spleen (data not shown). To confirm that the apparently high frequency of phenotypic hematopoietic stem/progenitors in the spleen of arthritic mice indeed correlated with an actual increase in functional hematopoietic stem/progenitor cells, we performed hematopoietic replating and transplantation studies. Specifically, unfractionated bone marrow or spleen cells from 6 week old KRNxG7 and KRN controls were cultured in methylcellulose hematopoietic replating medium. KRNxG7 splenocytes generated a substantially higher number of hematopoietic colonies (Figure 2.2-5B). We further transplanted sorted Lin⁻ cells (1×10^5 cells/mouse) from KRNxG7 (CD45.2xCD45.2) and control B6xG7 (CD45.2xCD45.2) spleens into lethally irradiated B6xG7 (CD45.1xCD45.2) mice. A majority of the mice that received Lin⁻ cells from control spleen died within 2 weeks with 100% succumbing within 3 months. However, a significant number of mice that received Lin⁻ cells from KRNxG7 spleen were still survived past 6 months post transplantation (Figure 2.2-5C, left). A high donor chimerism was obvious when recipients of KRNxG7 splenic Lin⁻ cells were analyzed 3 months after transplantation (Figure 2.2-5C, right). These replating and transplantation studies corroborate FACS analyses

showing that functional hematopoietic progenitors are particularly abundant in KRNxG7 spleen.

The high frequency of hematopoietic stem and/or progenitor cells in the KRNxG7 spleen raised a possibility that hematopoietic stem/progenitor cells readily mobilized into the periphery in chronic inflammation. However, KSL cells in the peripheral blood and other organs such as the liver of KRNxG7 mice were hardly detectable and not significantly different from controls (data not shown).

Moreover, the KSL frequency in B6xG7 and KRNxG7 spleen was similar in young mice (1-2 weeks of age). While KSL cells were maintained in KRNxG7 spleen (6wks), they decreased greatly in age-matched mice (Figure 2.2-5A). We suggest that HSCs are sustained in the KRNxG7 spleen, although the possibility that hematopoietic stem/progenitor cells are continuously mobilized at very low levels to the spleen in chronic inflammatory environments cannot be ruled out at this moment.

Discussion

Inflammatory bone loss is associated with several chronic diseases in humans including RA (Romas and Gillespie, 2006). Such human inflammatory joint disease is generally complicated by systemic osteoporosis, which is particularly severe in KRNxG7 mice. While focal destruction of bone, within the rheumatoid joint, is the product of aggressive osteoclast recruitment, whether its attendant osteoporosis is the product of accelerated resorption or attenuated formation is less clear. Given the abundance of systemic inflammatory cytokines, the pathogenesis of rheumatoid-associated osteoporosis has been assumed to be primarily osteoclastic. We demonstrate, however, the number of endosteal osteoclasts and confirmatory markers of bone resorption are diminished. Although the osteoblast number per bone surface was similar, the absolute osteoblast number was reduced in KRNxG7 mice due to decreased trabecular bone volume. Given that osteoblast bone forming activity is also ablated, at least in the KRNxG7 model of RA, the attendant osteoporosis reflects retarded osteogenesis.

Our results extend a growing body of work, examining the relationship between bone homeostasis and hematopoiesis, to a disease model. Our findings that there was a net increase in absolute number of BM HSCs in osteoblast deficient KRNxG7 mice compared with controls seem to be at odds with the current view of the role of osteoblasts as HSC niche cells. Specifically, transgenic mice expressing a constitutively active PPR (PTH/PTHrP receptors) under the control

of the type1(I) collagen promoter (col1-caPPR) stimulated osteoblast and increased their number and stromal cells from these mice supported HSCs in culture. These transgenic mice as well as parathyroid hormone treatment of wild type mice also increased the frequency of KSL cells as well as functional HSCs (Calvi et al., 2003). Moreover, poly I:C treatment of *Mx1-Cre⁺Bmpr1a^{fl/fl}* mice resulted in about two fold increase in the percentage of KSL cells, which correlated with an increase in endosteal osteoblast number (Zhang et al., 2003). Conversely, ablation of osteoblasts by ganciclovir treatment of transgenic mice expressing herpesvirus thymidine kinase (TK) gene under the 2.3kb of the rat collagen α 1 type I promoter (Col2.3 Δ TK) resulted in a decrease in absolute number of KSL cells, although the frequency was increased in these mice due to reduced BM cellularity (Visnjic et al., 2004). These previous studies will predict that HSCs in KRNxG7 bones would be reduced which is contrary to what we observe.

We suggest several possible explanations for the apparent discrepancy. First, the remaining osteoblasts in the KRNxG7 mice, although reduced in numbers, may be sufficient to support the HSC maintenance. Second, osteoblast lineage cells are multifunctional. For example they not only manufacture bone, but stimulate osteoclastogenesis via expression of RANKL and M-CSF. In fact, there are circumstances of disassociation of these events as seen in multiple myeloma in which bone formation is arrested but osteoclastogenesis is exuberant, presumably reflecting altered Wnt signaling (Oshima et al., 2005). It is therefore

possible that KRNxG7 osteoblasts still support the HSC maintenance, although their bone forming ability is impaired. In this regard, it is important to note that Zhang et al determined histologically that HSCs in BMPR1a conditional knockout mice were located adjacent to spindle shaped bone lining cells that express N-cadherin (Zhang et al., 2003). Bone lining cells are classically regarded as quiescent non-functional osteoblasts (Aubin and Turksen, 1996) or immature osteoblasts (Zhang et al., 2003) and have distinguished morphology from the cuboidal osteoblasts that are responsible for bone formation (Aubin and Turksen, 1996). Lymperi et al have shown that increasing total osteoblasts without increasing N-cadherin⁺ osteoblasts enhances bone formation without increasing HSCs highlighting the dissociation between bone formation and HSC maintenance at the cellular level (Lymperi et al., 2008).

Even though HSCs were maintained normally in KRNxG7, B cells were greatly reduced in these mice. Previous studies have shown that conditional ablation of osteoblasts in Col2.3 Δ TK transgenic mice resulted in defects in B lymphopoiesis (Visnjic et al., 2004; Zhu et al., 2007). Furthermore, it has been shown that a cell autonomous defect of Gs α signaling in osteoblasts also impairs marrow B cell development (Wu et al., 2008). Our results are more similar to the effects of osteoblast depletion using the Col2.3 TK transgenic system. We find that similar to Zhu et al, preproB, proB and pre B precursors are all depleted in KRNxG7 mice in contrast with Wu et al, where preproB cells are intact. This more severe B cell depletion is also reflected by gene expression analysis which reveals a

decrease in not just IL-7 as obtained by Wu et al, but also of SDF-1 (which is not changed in Wu et al.) and of Flt3-L. Intriguingly CLPs are also absent from arthritic bone marrow, suggesting that importance of osteoblasts in marrow B lymphopoiesis occurs higher up in the developmental hierarchy than previously determined, prior to B cell commitment. It is possible that the decreased cycling of Kit+Sca-Lin- cells in KRNxG7 bone marrow is due to undefined progenitors in the lymphoid lineage. Previous studies have suggested that immunization, infection and inflammatory cytokines can mobilize B cell precursors into the periphery (Nagaoka et al., 2000; Ueda et al., 2005; Ueda et al., 2004). However it is at the moment unclear if and where B lymphopoiesis might be relocated to in the KRNxG7 mice.

Taken together, osteoblast determinants involved in bone formation vs B lymphopoiesis vs hematopoietic stem supporting activity could be distinct and uncoupled. Alternatively, while osteoblasts maybe obligatory for B cell development and bone formation, additional HSC niche cells, such as endothelial or reticular cells (Kiel and Morrison, 2006; Sugiyama et al., 2006), could compensate for the osteoblast defects in maintaining HSC integrity in inflammatory environments of KRNxG7 mice. To this end, previous studies demonstrate that endothelial cells of hematopoietic tissues, such as bone marrow or extramedullary organs, express cell surface molecules including E-selectin and VCAM-1. Intriguingly, these molecules are not expressed in quiescent endothelium of non-hematopoietic tissues, but become upregulated in

inflammation (Mazo et al., 1998; Schweitzer et al., 1996). Thus, it will be particularly important to know if the accumulation of HSCs and progenitors that we see in the spleens of arthritic mice is associated with changes in the endothelial niche in chronic inflammation. Moreover, studies distinguishing the requirements of osteoblast vs. endothelial niche in HSC maintenance in normal vs. pathologic conditions should be addressed thoroughly in the future.

Acknowledgements

This work was supported by grants from the National Institutes of Health, NIAMS AR055923-01 (F. L), AR032788 and AR046523 (S. L. T) and NHLBI HL63736 and HL55337 (K.C). The authors have no conflicting financial interests.

Author contributions

C.P., Y.D.M., and K.O., characterization of hematopoietic phenotype; H.Z., C.P., and Y.D.M., characterization of bone phenotype; X.T., in vitro osteoblast culture experiments; P.M.A., K/BxN and KRNxG7 mice; P.M.A., F.L. and S.L.T., discussion and manuscript editing; C.P., Y.D.M., K.O., H.Z., S.L.T. and K.C., project planning, data interpretation, figure preparation and manuscript writing.

References

- Arai, F., Hirao, A., Ohmura, M., Sato, H., Matsuoka, S., Takubo, K., Ito, K., Koh, G. Y. and Suda, T.** (2004). Tie2/angiopoietin-1 signaling regulates hematopoietic stem cell quiescence in the bone marrow niche. *Cell* **118**, 149-61.
- Aubin, J. E. and Turksen, K.** (1996). Monoclonal antibodies as tools for studying the osteoblast lineage. *Microsc Res Tech* **33**, 128-40.
- Calvi, L. M., Adams, G. B., Weibrecht, K. W., Weber, J. M., Olson, D. P., Knight, M. C., Martin, R. P., Schipani, E., Divieti, P., Bringhurst, F. R. et al.** (2003). Osteoblastic cells regulate the haematopoietic stem cell niche. *Nature* **425**, 841-6.
- Cheng, T., Rodrigues, N., Dombkowski, D., Stier, S. and Scadden, D. T.** (2000). Stem cell repopulation efficiency but not pool size is governed by p27(kip1). *Nat Med* **6**, 1235-40.
- Hardy, R. R., Carmack, C. E., Shinton, S. A., Kemp, J. D. and Hayakawa, K.** (1991). Resolution and characterization of pro-B and pre-pro-B cell stages in normal mouse bone marrow. *J Exp Med* **173**, 1213-25.
- Haylock, D. N., Williams, B., Johnston, H. M., Liu, M. C., Rutherford, K. E., Whitty, G. A., Simmons, P. J., Bertonecello, I. and Nilsson, S. K.** (2007). Hemopoietic stem cells with higher hemopoietic potential reside at the bone marrow endosteum. *Stem Cells* **25**, 1062-9.
- Haynes, D. R.** (2007). Inflammatory cells and bone loss in rheumatoid arthritis. *Arthritis Res Ther* **9**, 104.
- Karsunky, H., Inlay, M. A., Serwold, T., Bhattacharya, D. and Weissman, I. L.** (2008). Flk2+ common lymphoid progenitors possess equivalent differentiation potential for the B and T lineages. *Blood* **111**, 5562-70.
- Kiel, M. J. and Morrison, S. J.** (2006). Maintaining hematopoietic stem cells in the vascular niche. *Immunity* **25**, 862-4.
- Kiel, M. J., Yilmaz, O. H., Iwashita, T., Yilmaz, O. H., Terhorst, C. and Morrison, S. J.** (2005). SLAM family receptors distinguish hematopoietic stem and progenitor cells and reveal endothelial niches for stem cells. *Cell* **121**, 1109-21.
- Kollet, O., Dar, A. and Lapidot, T.** (2007). The multiple roles of osteoclasts in host defense: bone remodeling and hematopoietic stem cell mobilization. *Annu Rev Immunol* **25**, 51-69.
- Kondo, M., Weissman, I. L. and Akashi, K.** (1997). Identification of clonogenic common lymphoid progenitors in mouse bone marrow. *Cell* **91**, 661-72.
- Kouskoff, V., Korganow, A. S., Duchatelle, V., Degott, C., Benoist, C. and Mathis, D.** (1996). Organ-specific disease provoked by systemic autoimmunity. *Cell* **87**, 811-22.
- Kyburz, D. and Corr, M.** (2003). The KRN mouse model of inflammatory arthritis. *Springer Semin Immunopathol* **25**, 79-90.
- Lee, D., Park, C., Lee, H., Lugus, J. J., Kim, S. H., Arentson, E., Chung, Y. S., Gomez, G., Kyba, M., Lin, S. et al.** (2008). ER71 acts downstream of BMP, Notch, and Wnt signaling in blood and vessel progenitor specification. *Cell Stem Cell* **2**, 497-507.
- Li, Y. S., Wasserman, R., Hayakawa, K. and Hardy, R. R.** (1996). Identification of the earliest B lineage stage in mouse bone marrow. *Immunity* **5**, 527-35.

Lugus, J. J., Chung, Y. S., Mills, J. C., Kim, S. I., Grass, J., Kyba, M., Doherty, J. M., Bresnick, E. H. and Choi, K. (2007). GATA2 functions at multiple steps in hemangioblast development and differentiation. *Development* **134**, 393-405.

Lymperi, S., Horwood, N., Marley, S., Gordon, M. Y., Cope, A. P. and Dazzi, F. (2008). Strontium can increase some osteoblasts without increasing hematopoietic stem cells. *Blood* **111**, 1173-81.

Mazo, I. B., Gutierrez-Ramos, J. C., Frenette, P. S., Hynes, R. O., Wagner, D. D. and von Andrian, U. H. (1998). Hematopoietic progenitor cell rolling in bone marrow microvessels: parallel contributions by endothelial selectins and vascular cell adhesion molecule 1. *J Exp Med* **188**, 465-74.

Monach, P., Hattori, K., Huang, H., Hyatt, E., Morse, J., Nguyen, L., Ortiz-Lopez, A., Wu, H. J., Mathis, D. and Benoist, C. (2007). The K/BxN mouse model of inflammatory arthritis: theory and practice. *Methods Mol Med* **136**, 269-82.

Nagaoka, H., Gonzalez-Aseguinolaza, G., Tsuji, M. and Nussenzweig, M. C. (2000). Immunization and infection change the number of recombination activating gene (RAG)-expressing B cells in the periphery by altering immature lymphocyte production. *J Exp Med* **191**, 2113-20.

Orford, K. W. and Scadden, D. T. (2008). Deconstructing stem cell self-renewal: genetic insights into cell-cycle regulation. *Nat Rev Genet* **9**, 115-28.

Oshima, T., Abe, M., Asano, J., Hara, T., Kitazoe, K., Sekimoto, E., Tanaka, Y., Shibata, H., Hashimoto, T., Ozaki, S. et al. (2005). Myeloma cells suppress bone formation by secreting a soluble Wnt inhibitor, sFRP-2. *Blood* **106**, 3160-5.

Park, C., Afrikanova, I., Chung, Y. S., Zhang, W. J., Arentson, E., Fong Gh, G., Rosendahl, A. and Choi, K. (2004). A hierarchical order of factors in the generation of FLK1- and SCL-expressing hematopoietic and endothelial progenitors from embryonic stem cells. *Development* **131**, 2749-62.

Passegue, E., Wagers, A. J., Giuriato, S., Anderson, W. C. and Weissman, I. L. (2005). Global analysis of proliferation and cell cycle gene expression in the regulation of hematopoietic stem and progenitor cell fates. *J Exp Med* **202**, 1599-611.

Purton, L. E. and Scadden, D. T. (2006). Osteoclasts eat stem cells out of house and home. *Nat Med* **12**, 610-1.

Purton, L. E. and Scadden, D. T. (2007). Limiting factors in murine hematopoietic stem cell assays. *Cell Stem Cell* **1**, 263-70.

Romas, E. and Gillespie, M. T. (2006). Inflammation-induced bone loss: can it be prevented? *Rheum Dis Clin North Am* **32**, 759-73.

Schweitzer, K. M., Drager, A. M., van der Valk, P., Thijsen, S. F., Zevenbergen, A., Theijsmeijer, A. P., van der Schoot, C. E. and Langenhuijsen, M. M. (1996). Constitutive expression of E-selectin and vascular cell adhesion molecule-1 on endothelial cells of hematopoietic tissues. *Am J Pathol* **148**, 165-75.

Solomon, S., Rajasekaran, N., Jeisy-Walder, E., Snapper, S. B. and Illges, H. (2005). A crucial role for macrophages in the pathology of K/B x N serum-induced arthritis. *Eur J Immunol* **35**, 3064-73.

Stier, S., Ko, Y., Forkert, R., Lutz, C., Neuhaus, T., Grunewald, E., Cheng, T., Dombkowski, D., Calvi, L. M., Rittling, S. R. et al. (2005). Osteopontin is a hematopoietic stem cell niche component that negatively regulates stem cell pool size. *J Exp Med* **201**, 1781-91.

- Sugiyama, T., Kohara, H., Noda, M. and Nagasawa, T.** (2006). Maintenance of the hematopoietic stem cell pool by CXCL12-CXCR4 chemokine signaling in bone marrow stromal cell niches. *Immunity* **25**, 977-88.
- Tu, X., Joeng, K. S., Nakayama, K. I., Nakayama, K., Rajagopal, J., Carroll, T. J., McMahon, A. P. and Long, F.** (2007). Noncanonical Wnt signaling through G protein-linked PKCdelta activation promotes bone formation. *Dev Cell* **12**, 113-27.
- Ueda, Y., Kondo, M. and Kelsoe, G.** (2005). Inflammation and the reciprocal production of granulocytes and lymphocytes in bone marrow. *J Exp Med* **201**, 1771-80.
- Ueda, Y., Yang, K., Foster, S. J., Kondo, M. and Kelsoe, G.** (2004). Inflammation controls B lymphopoiesis by regulating chemokine CXCL12 expression. *J Exp Med* **199**, 47-58.
- van Os, R., Kamminga, L. M., Ausema, A., Bystrykh, L. V., Draijer, D. P., van Pelt, K., Dontje, B. and de Haan, G.** (2007). A limited role for p21Cip1/Waf1 in maintaining normal hematopoietic stem cell functioning. *Stem Cells* **25**, 836-43.
- Visnjic, D., Kalajzic, Z., Rowe, D. W., Katavic, V., Lorenzo, J. and Aguila, H. L.** (2004). Hematopoiesis is severely altered in mice with an induced osteoblast deficiency. *Blood* **103**, 3258-64.
- Wilson, A., Murphy, M. J., Oskarsson, T., Kaloulis, K., Bettess, M. D., Oser, G. M., Pasche, A. C., Knabenhans, C., Macdonald, H. R. and Trumpp, A.** (2004). c-Myc controls the balance between hematopoietic stem cell self-renewal and differentiation. *Genes Dev* **18**, 2747-63.
- Wilson, A. and Trumpp, A.** (2006). Bone-marrow haematopoietic-stem-cell niches. *Nat Rev Immunol* **6**, 93-106.
- Wipke, B. T. and Allen, P. M.** (2001). Essential role of neutrophils in the initiation and progression of a murine model of rheumatoid arthritis. *J Immunol* **167**, 1601-8.
- Wright, L. M., Maloney, W., Yu, X., Kindle, L., Collin-Osdoby, P. and Osdoby, P.** (2005). Stromal cell-derived factor-1 binding to its chemokine receptor CXCR4 on precursor cells promotes the chemotactic recruitment, development and survival of human osteoclasts. *Bone* **36**, 840-53.
- Wu, J. Y., Purton, L. E., Rodda, S. J., Chen, M., Weinstein, L. S., McMahon, A. P., Scadden, D. T. and Kronenberg, H. M.** (2008). Osteoblastic regulation of B lymphopoiesis is mediated by Gs{alpha}-dependent signaling pathways. *Proc Natl Acad Sci U S A* **105**, 16976-81.
- Zannettino, A. C., Farrugia, A. N., Kortesisidis, A., Manavis, J., To, L. B., Martin, S. K., Diamond, P., Tamamura, H., Lapidot, T., Fujii, N. et al.** (2005). Elevated serum levels of stromal-derived factor-1alpha are associated with increased osteoclast activity and osteolytic bone disease in multiple myeloma patients. *Cancer Res* **65**, 1700-9.
- Zhang, J., Niu, C., Ye, L., Huang, H., He, X., Tong, W. G., Ross, J., Haug, J., Johnson, T., Feng, J. Q. et al.** (2003). Identification of the haematopoietic stem cell niche and control of the niche size. *Nature* **425**, 836-41.
- Zhang, Q., Guo, R., Schwarz, E. M., Boyce, B. F. and Xing, L.** (2008). TNF inhibits production of stromal cell-derived factor 1 by bone stromal cells and increases osteoclast precursor mobilization from bone marrow to peripheral blood. *Arthritis Res Ther* **10**, R37.
- Zhu, J., Garrett, R., Jung, Y., Zhang, Y., Kim, N., Wang, J., Joe, G. J., Hexner, E., Choi, Y., Taichman, R. S. et al.** (2007). Osteoblasts support B-lymphocyte commitment and differentiation from hematopoietic stem cells. *Blood* **109**, 3706-12.

Figure 2.2-1.

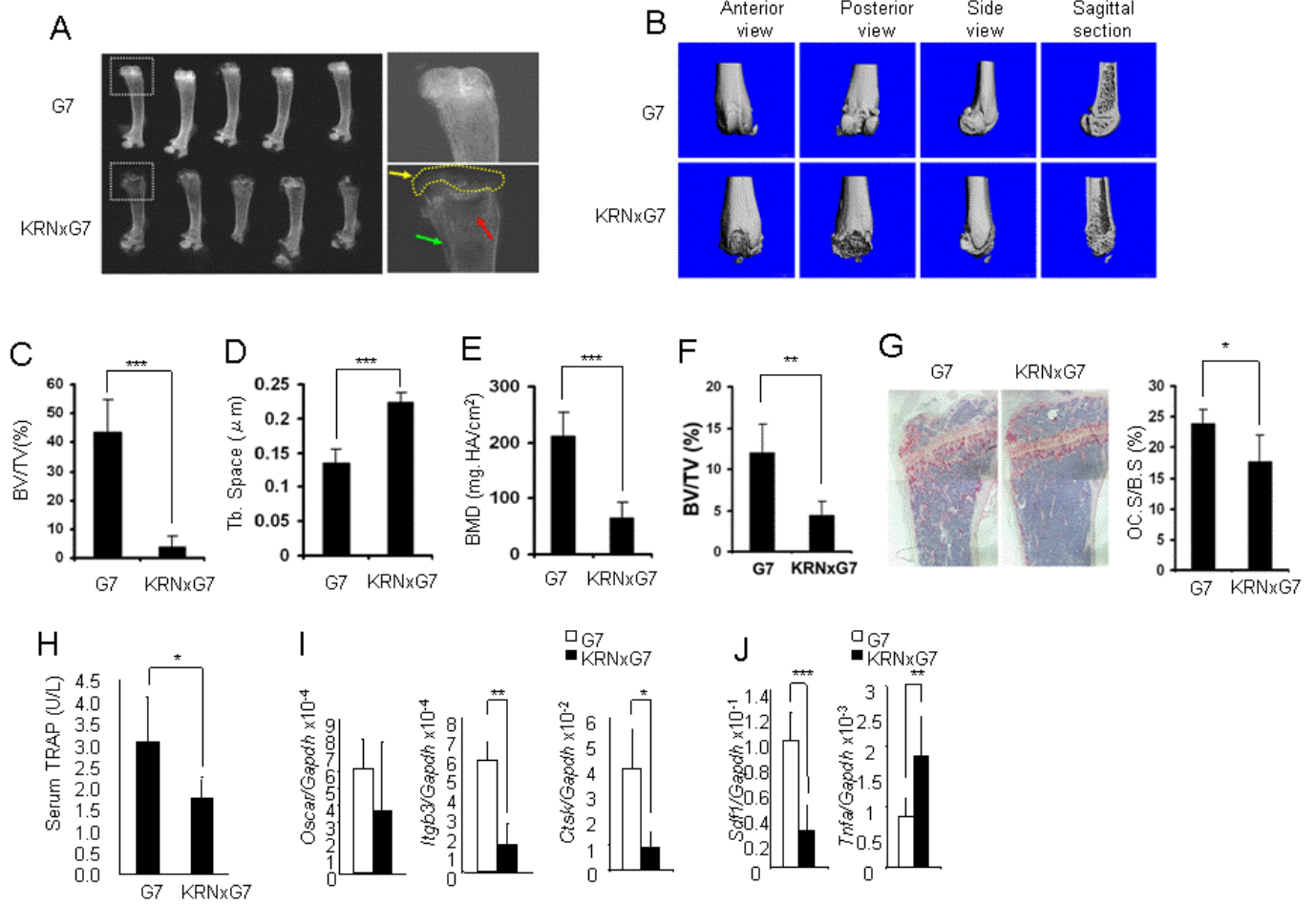


Figure legends

Figure 2.2-1. Severe joint destruction and osteoporosis in KRN/G7 mice.

(A) Radiographs of femurs of 6 week old G7 and KRNxG7 mice. Right panels are higher magnification images of boxed areas in the left panels. Yellow arrow and dashed circle in lower right panel denote destroyed articular surface and secondary ossification center. Red arrow points to trabecular bone region.

Green arrow indicates micro-fractures.

(B) Representative three-dimensional reconstruction of the femur by μ CT.

(C) The percentage of trabecular bone volume/tissue volume determined by μ CT (BV/TV).

(D) Trabecular separation determined by μ CT (Tb. space).

(E) DEXA determined bone mineral density (BMD). Data are presented as mean \pm SD, n=5 in each group of mice.

(F)) Histomorphometric determination of BV/TV. Trabecular bone volume normalized to total marrow space (BV/TV).

(G) TRAP (red reaction product) stained histological sections of G7 and KRNxG7 tibia. Data are expressed as % trabecular bone surface covered by osteoclasts. n=5.

(H) Global osteoclast number, in vivo, was quantified by serum TRAP5b ELISA.

(I) Oscar, integrin β 3 and cathepsin K expression was analyzed by quantitative PCR with RNA from G7 and KRNxG7 BM. Shown is the mean expression \pm SD for each gene normalized to GAPDH. n=3.

(J) SDF1 and TNF- α expression was analyzed by quantitative RT-PCR with RNA from G7 and KRNxG7 BM. Shown is the mean expression \pm SD for each gene normalized to GAPDH. n=3.

*p<0.05, **p<0.01, ***p<0.001

Figure 2.2-2.

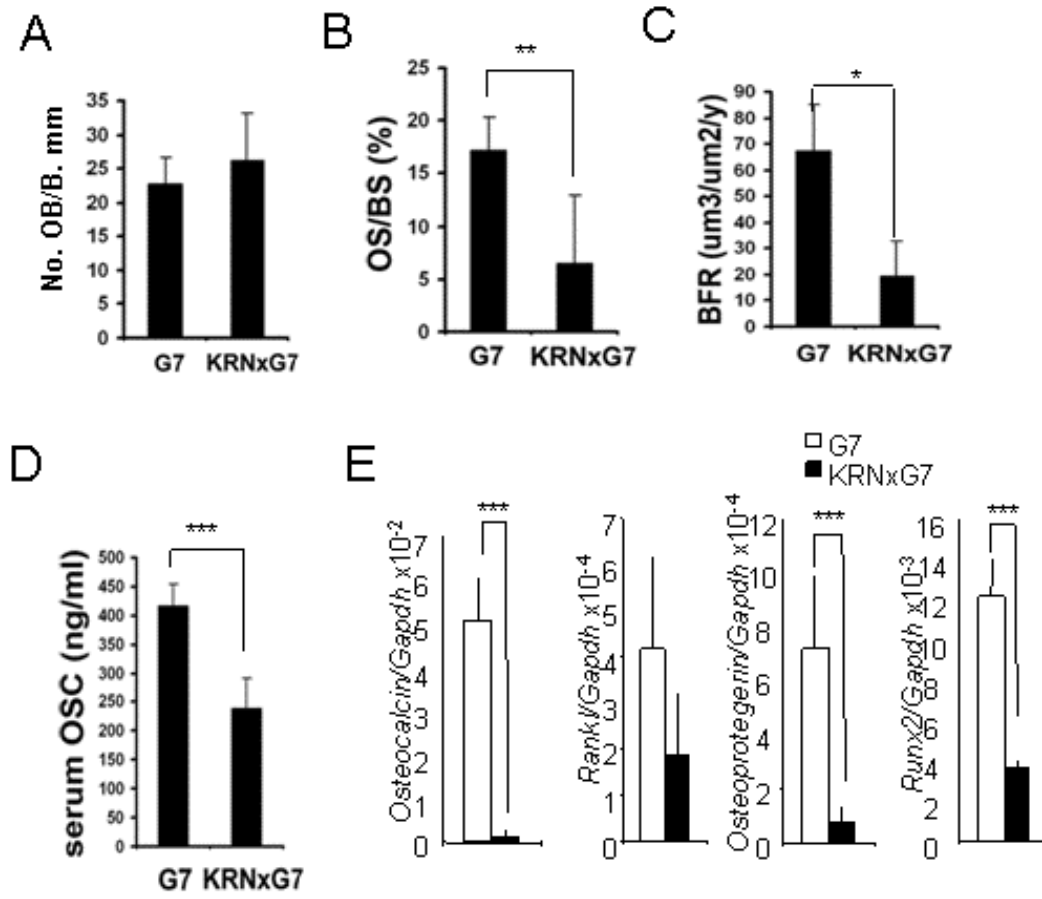


Figure 2.2-2. Impaired bone formation rate in KRN/G7 mice.

(A) Osteoblast number/mm bone perimeter (No. OB/B.mm).

(B) % trabecular surface covered by osteoid (OS.S/B.mm).

(C) Bone formation rate (BFR) histomorphometrically quantitated from double calcein labeled tibia.

(D) In vivo bone formation was quantified by serum osteocalcin (Osc) level at 6 weeks of age. n=5.

(E) RNA of KRN and KRNxG7 BM was analyzed for gene expression of osteoblast markers, receptor activator of NFkappaB ligand (*Rankl*), *Osteoprotegerin (Opg)*, *Runx2* and *Osteocalcin* by quantitative RT-PCR. Shown is the mean expression \pm SD for each gene normalized to GAPDH.

*p<0.05, **p<0.01, ***p<0.001

Figure 2.2-3.

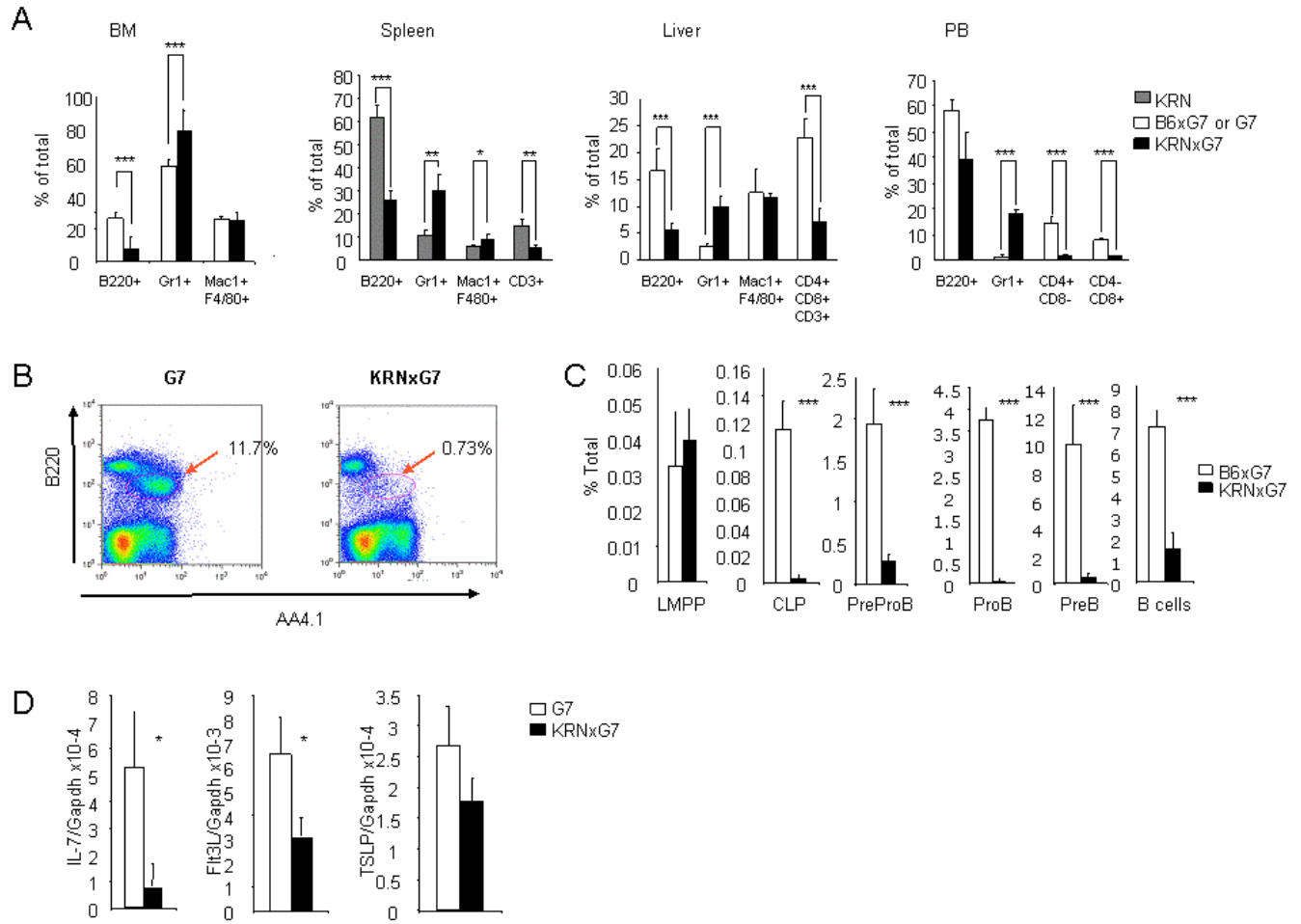


Figure 2.2-3. Characterization of mature cells and B cell development defect in KRNxG7 mice.

(A) Systemic increase in myeloid cells and decrease in lymphoid cells. BM, spleen, liver and peripheral Blood (PB) cells were harvested from 6 to 8 week old KRNxG7 and control (KRN, G7 or B6xG7) mice, stained for the indicated lineage markers and analyzed by flow cytometry. B220 is a B cell marker, Gr1 stains granulocytes and monocyte populations, Mac1 and F480 combination stains macrophages, CD3, CD4 and CD8 stain T cells. Shown is the mean for 3 to 11 mice analyzed per strain for each tissue.

(B) FACS plot for B cell precursors in bone marrow. Bone marrow cells from KRNxG7 or G7 controls are stained for B220 and AA4.1 (a marker for B cell precursors). B cell precursors (B220^{lo}AA4.1⁺; red arrow) are virtually depleted in KRNxG7 bone marrow while most of the residual cells are B220^{hi} and IgM⁺ (IgM staining not shown).

(C) Systematic analysis of bone marrow B cell development. FACS determined frequency of various B cell precursors from earliest (left) to the latest (right) are shown. LMPP (Lymphoid Primed Multipotential Progenitor; Kit⁺Sca1⁺Lin⁻Fli2^{hi}CD34⁺), CLP (Common Lymphoid Progenitor; Lin⁻Fli2⁺IL-7R α ⁺), PreproB (B220⁺IgM⁻CD19⁻CD43⁺NK1.1⁻CD11c⁻), ProB (B220⁺IgM⁻CD19⁺CD43⁺), PreB (B220⁺IgM⁻CD19⁺CD43⁻), B cells (B220⁺IgM⁺). We confirmed that Lin⁻Fli2⁺IL-7R α ⁺ CLPs were almost predominantly Kit^{lo}Sca1^{lo} (data not shown) as previously reported.(Karsunky et al., 2008; Kondo et al., 1997)

(D) Expression of various B lymphopoiesis promoting cytokines in whole marrow.

Expression was determined by quantitative real time PCR, followed by normalization to GAPDH. IL-7(Interleukin 7), Flt3-L(Ligand for Fik2), TSLP (Thymic Stromal Lymphopoietin).

* $p < 0.05$, ** $p < 0.01$, *** $p < 0.001$.

Figure 2.2-4.

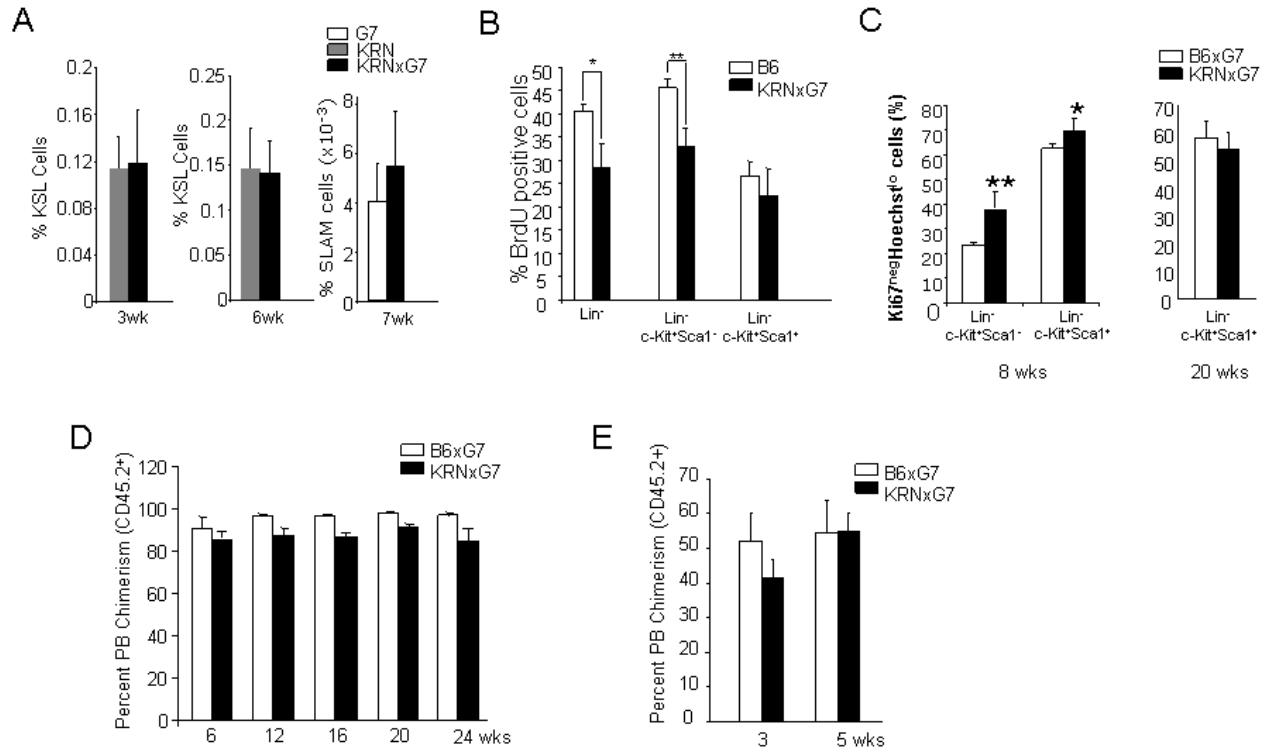


Figure 2.2-4. Hematopoietic stem cells are not impaired in KRNxG7 mice.

(A) Immunophenotypic analyses of HSC containing populations. BM from 3, 6 and 7 week old KRN, B6xG7 and KRNxG7 mice were subjected to FACS analyses for cKit, Sca1 and lineage or CD150, CD48 and CD41 markers. The frequency \pm SD of KSL or SLAM is shown on the Y-axis. (n \geq 4).

(B) Cell Cycle analysis of bone marrow sub-populations. 6-8 week old mice were injected with a single dose of bromodeoxy-uridine (BrdU) proportionate to body mass for 2-3 hours prior to sacrifice. Different bone marrow fractions were analyzed for BrdU incorporation by flow cytometry. Shown is the mean \pm SD of BrdU positive cells for each population for 2 independent experiments (n=4-5 total mice).

(C) Quiescent Fraction Analysis of Bone Marrow KSL cells. Bone marrow cells from KRNxG7 and B6xG7 mice (n=4-5) of different ages were lineage depleted, surface stained for c-Kit and Sca-1 and subjected to intracellular staining for Ki67 and Hoechst (see methods and Supplementary Figure 2.2-5). Quiescent cells do not express Ki67 (Ki67^{neg}) and stain low for Hoechst because of their 2N DNA content (versus 4N DNA content of S/G2/M phase cells). Ki67^{neg}Hoechst^{low} (quiescent cell) fraction of the stem cell enriched Lin-cKit+Sca1+ (KSL) population and the non-stem cell enriched Lin-cKit+Sca1- population are shown. As expected KSL cells are more quiescent than Lin-cKit+Sca1- progenitors. However there is no appreciable difference in quiescent fraction in KRNxG7 KSL cells compared with B6xG7 KSL cells.

(D) B6xG7 (CD45.2xCD45.2) or KRNxG7 (CD45.2xCD45.2) BM was transplanted into lethally irradiated B6xG7 (CD45.1xCD45.2) recipients. Peripheral blood was analyzed for donor contribution (CD45.2) every 6 weeks after BM transplantation for 6 months. The percentage \pm SD of CD45.2⁺ chimerism is shown on the Y-axis (n=4/genotype).

(E) B6xG7 (CD45.2+) or KRNxG7 (CD45.2+) bone marrow cells (2×10^5) were mixed with B6xG7 (CD45.1+; CD45.2+) competitor bone marrow cells (2×10^5) and injected (i.v.) into lethally irradiated (1000 Rads) B6xG7 (CD45.1xCD45.2) recipient mice. PB CD45.2+ cells were analyzed 3 months and 5 months post-transplantation. Data represent the average percentages peripheral blood chimerism \pm s.e.m.

*p<0.05, **p<0.01

Figure 2.2-5.

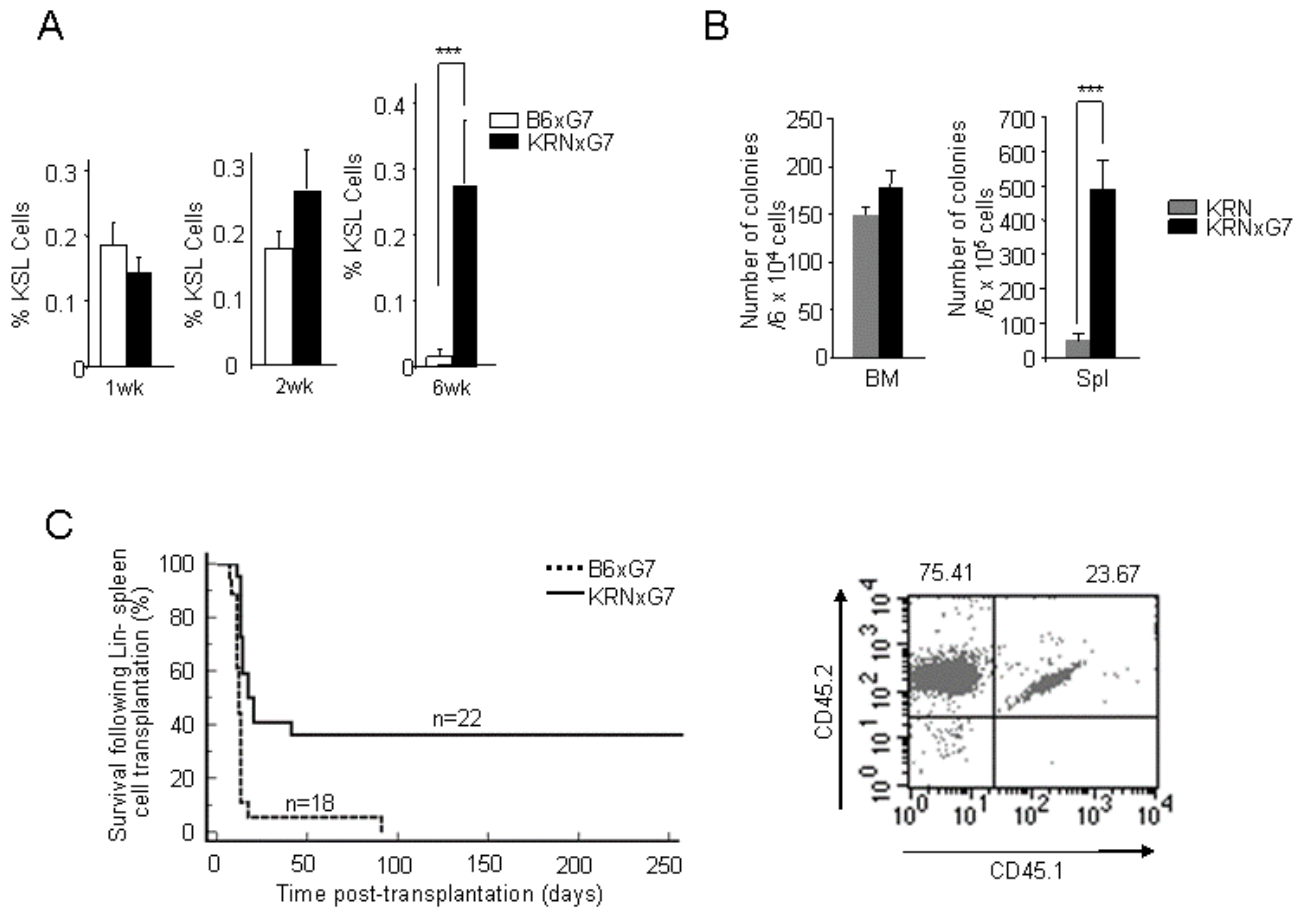


Figure 2.2-5. Characterization of HSCs and progenitors in KRNxG7 spleen.

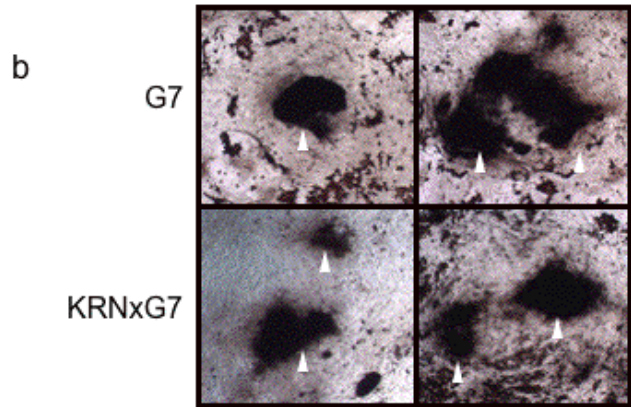
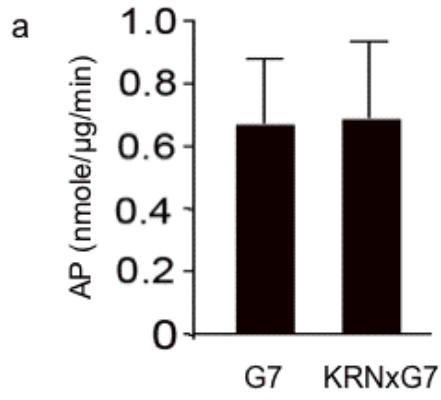
(A) Spleen from 1, 2 and 6 week old B6xG7, KRN and KRNxG7 mice were subjected to FACS analyses for cKit, Sca1 and lineage markers. The frequency \pm SD of CD45⁺KSL⁻ is shown on the Y-axis. (n \geq 5).

(B) BM and spleen cells from 6 week old KRN and KRNxG7 mice were subjected to hematopoietic replating assay (n = 3). Hematopoietic colonies were counted 7-10 days after replating.

(C) Lin⁻ spleen cells from B6xG7 (CD45.2xCD45.2) or KRNxG7 (CD45.2xCD45.2) were transplanted into lethally irradiated B6xG7 (CD45.1xCD45.2) mice. Survival rate of the recipients is shown on the left. CD45.2⁺ cells were analyzed 3 months after transplantation. One representative FASC data is shown on the right.

***p<0.001.

Supplementary Figures 2.2-1.



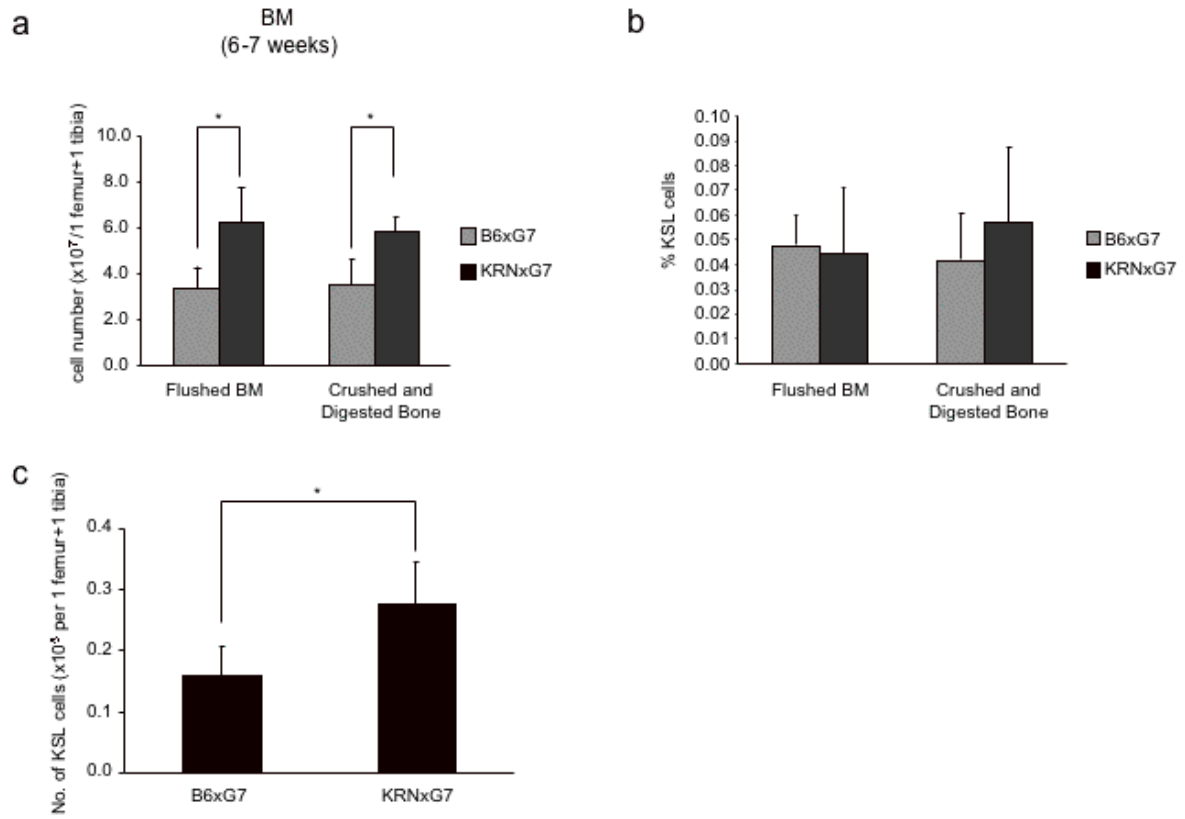
Supplementary Figures 2.2-1. *In vitro* osteoblasts differentiation from KRNxG7 bone marrow stromal cells is normal.

(a) AP quantitative assay for high-density BMSC cultures in osteogenic medium.

Data is presented as mean \pm SD, n=5 in each group of mice.

(b) Detection of bone nodule formation by von Kossa staining. The BMSC cells were incubated for 14 days in mineralization medium. (arrowhead denotes a nodule)

Supplementary Figures 2.2-2.



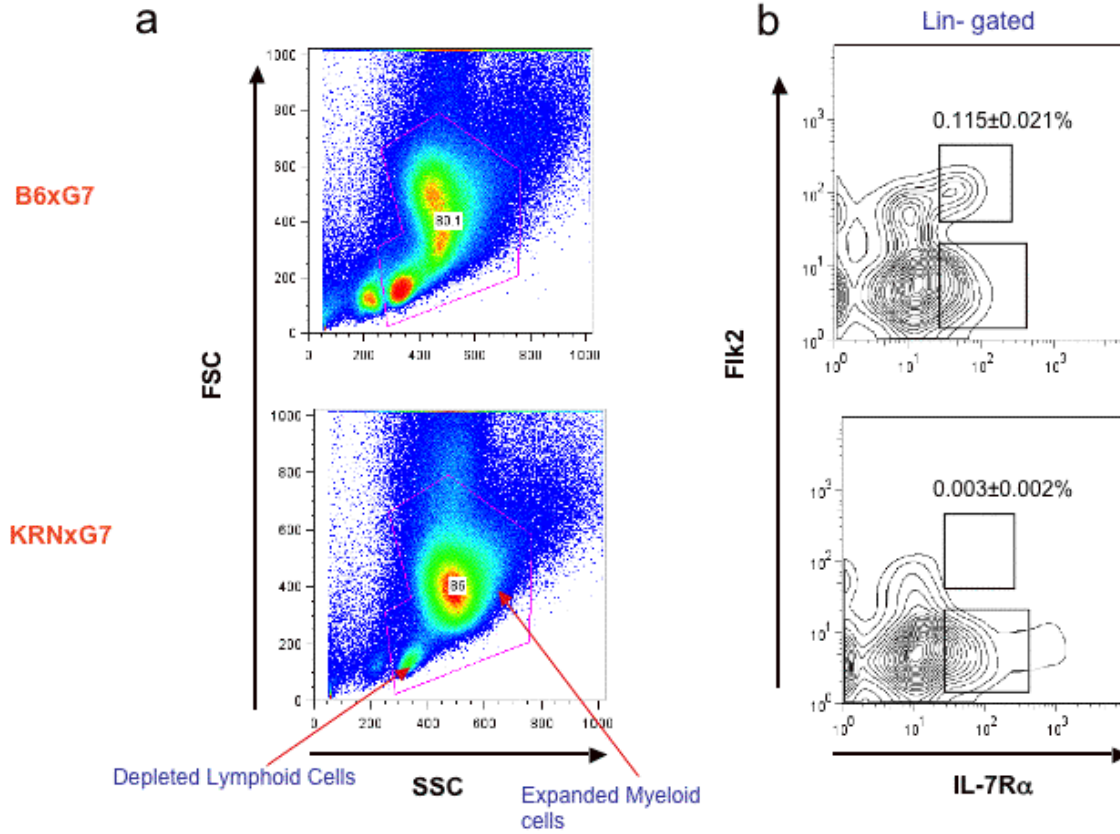
Supplementary Figures 2.2-2. Marrow cellularity and KSL frequency are independent of harvesting method.

(a) Number of bone marrow cells generated from flushing method and collagenase/dispase enzymatic digestion method of total bone. One femur and one tibia from 6 week old B6xG7 and KRNxG7 mice were examined. The values indicate cell number \pm SD from one femur plus one tibia on the Y-axis. n=4 for each group.

(b) Flushed BM and total BM from 6 week old B6xG7 and KRNxG7 mice were subjected to KSL FACS analyses. The values indicate frequency \pm SD of KSL on the Y-axis.

(c) Absolute number of KSL cells of one femur and one tibia of B6xG7 and KRNxG7. The values indicate cell number \pm SD on the Y-axis. n=4 for each group, *p<0.05.

Supplementary Figures 2.2-3.

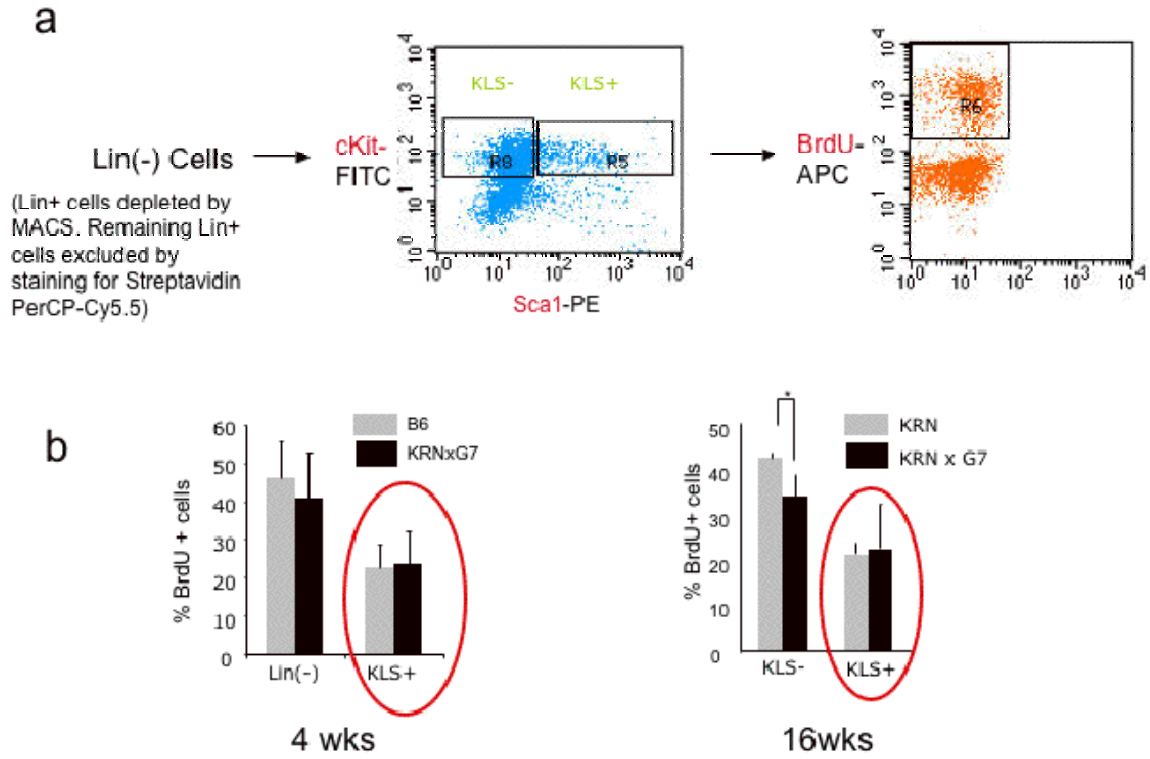


Supplementary Figures 2.2-3. Depleted lymphoid cells in KRNxG7 bone marrow.

(a) Representative FACS plot depicting depleted lymphoid cells and expanded myeloid cells in KRNxG7 bone marrow. Lymphoid cells have low forward scatter (FSC) and side scatter (SSC) as a result of the smaller size and less granularity. In bone marrow majority of lymphoid cells are B220+ (~30% of leukocytes). This reduced FSC^{lo}SSC^{lo} frequency in KRNxG7 mice is also reflected in B220+ frequency (see Figure 2.2-3A).

(b) Representative FACS plot depicting depleted CLP in KRNxG7 bone marrow. CLPs are Fli2+IL-7R α +Lin-. Indicated fractions are mean CLP frequency in total marrow \pm standard deviation.

Supplementary Figures 2.2-4.

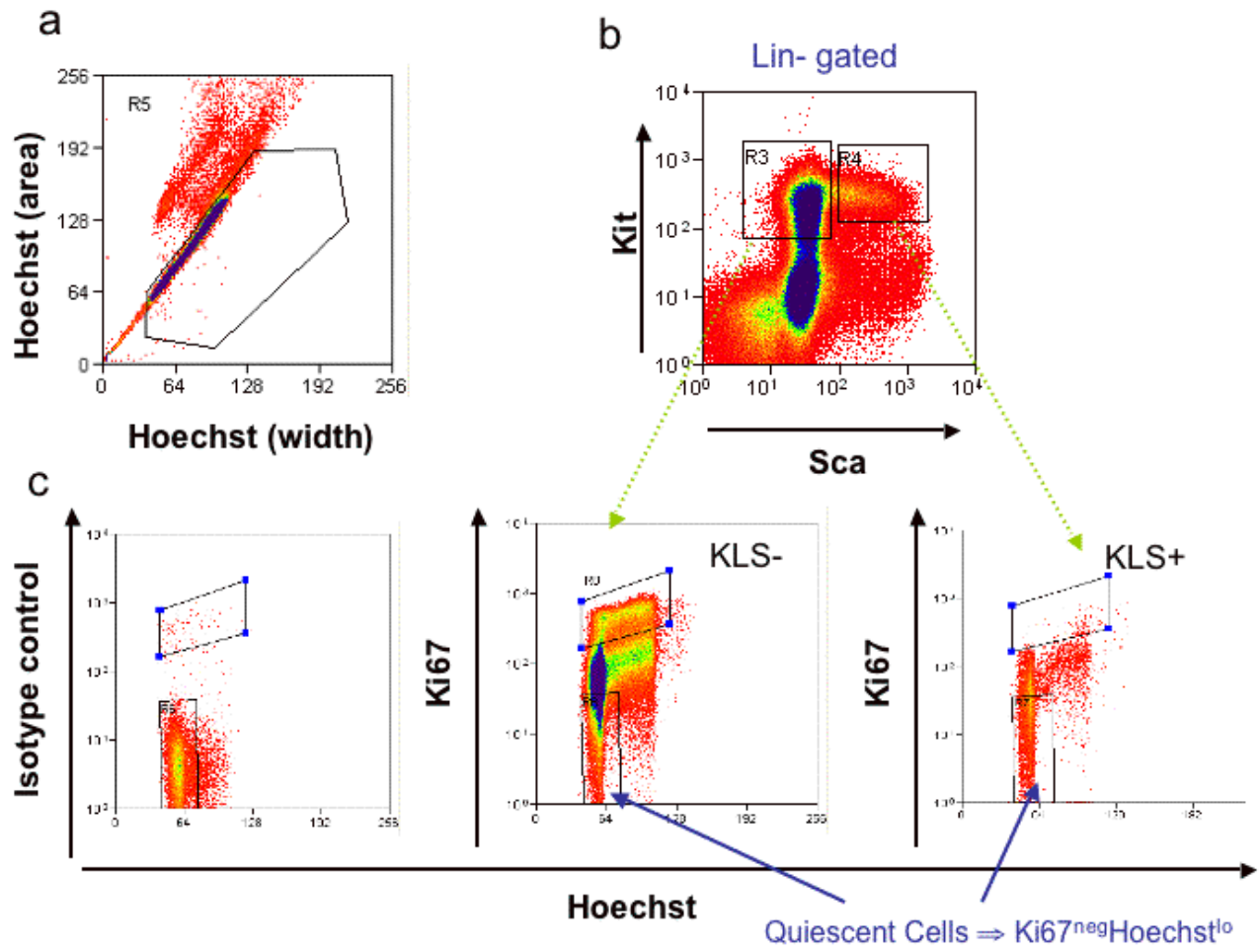


Supplementary Figures 2.2-4. BrdU analysis of progenitor populations.

(a) Schema for BrdU analysis. Lin⁺ cells are excluded by magnetic depletion using biotin conjugated anti-lineage marker antibodies and also by FACS gating by excluding Streptavidin-PerCP-Cy5.5 positive cells. Various gated progenitor fractions – Lin⁻, KSL⁺, KSL⁻ are subsequently analyzed for BrdU positive cells.

(b) BrdU analysis of bone marrow progenitor cells at early time point (4wks;) and later time point (16wks). N=2-4, *p<0.05.

Supplementary Figures 2.2-5.



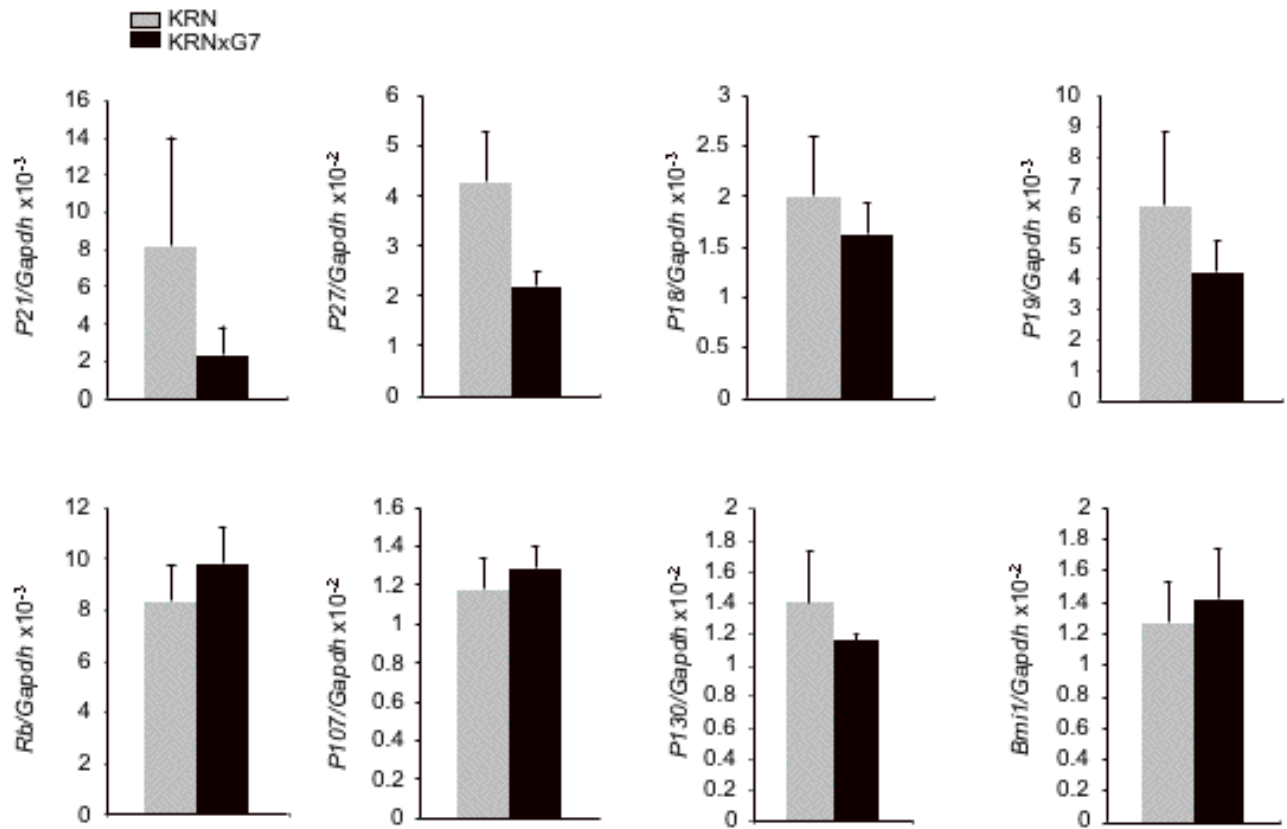
Supplementary Figures 2.2-5. Schema for Ki67/Hoechst analysis.

(a) Exclusion of Lin⁺ cells by magnetic depletion and flow cytometric gating (see methods & Supplementary Figure 2.2-4a) was performed. Lin⁻ cells were subjected to doublet discrimination.

(b) c-Kit and Sca-1 expression of doublet free and Lin⁻ gated cells to get KLS (KLS⁺) and KLS⁻ populations.

(c) Ki67 and Hoechst analysis of gated KLS⁺ and KLS⁻ cells. Quiescent cells are Ki67^{neg}Hoechst^{lo}. The more primitive KLS⁺ population conspicuously lack Ki67^{hi} cells, which are present in KLS⁻ population that are devoid of HSCs.

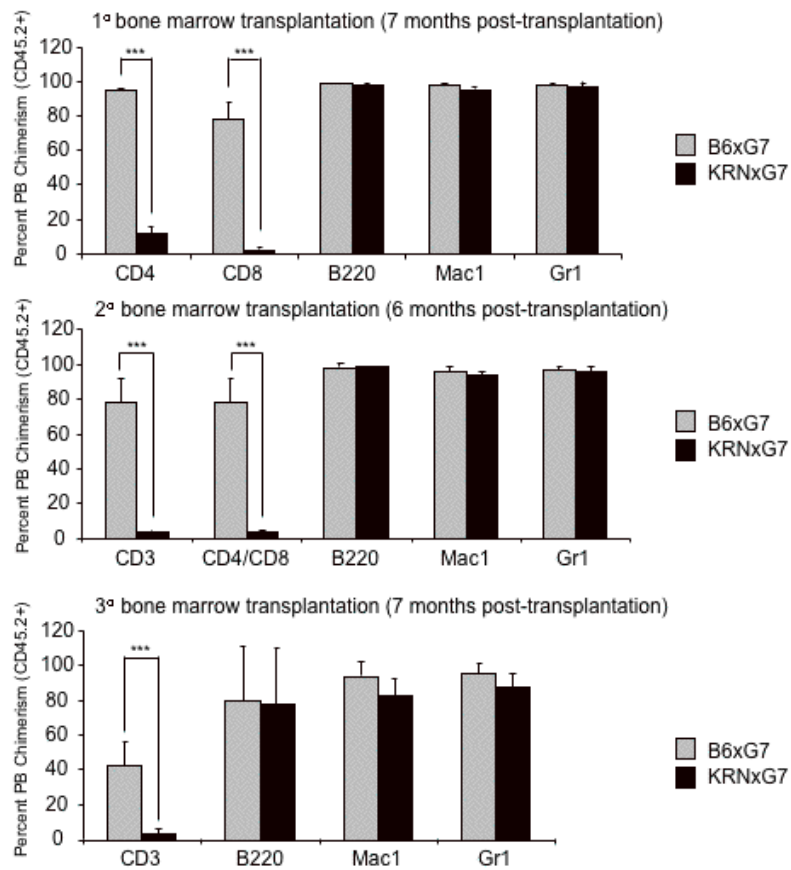
Supplementary Figures 2.2-6.



Supplementary Figures 2.2-6. Expression of cell cycle Regulators in BM derived KSL cells.

CD45+KSL cells were FACS sorted from 6 week old KRNxG7 and KRN control mice (10-11 mice for each). RNA was extracted and used for quantitative real-time PCR for various cell cycle regulators: p21 and p27 are cyclin dependent kinase (Cdk) inhibitors of the Cip/Kip family; p18 and p19 are Cdk inhibitors of the Ink4 family; Rb, p107 and p130 are retinoblastoma (Rb) family genes; Bmi is an epigenetic regulator of stem cell self renewal. Shown is the average of 2-4 experiments for each gene with error bars representing standard deviation. Each experiment was performed in duplicate.

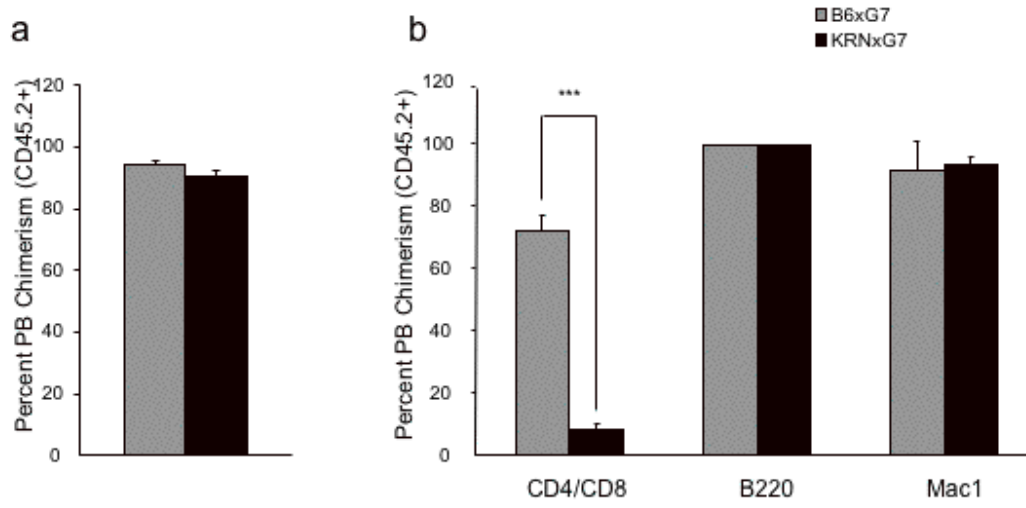
Supplementary Figures 2.2-7.



Supplementary Figures 2.2-7. Analyses for donor cell derived hematopoietic cell lineages in primary, secondary and tertiary recipients.

Peripheral blood was analyzed for the donor cell contribution (CD45.2) to individual hematopoietic cell lineages. The data shown is the mean percentage PB chimerism (CD45.2+) \pm SD of CD3+, CD4+, CD8+ (T cells), B220+ (B cells), Gr1+ (granulocytes), and Mac-1+ (macrophages) populations. ***p<0.001.

Supplementary Figures 2.2-8.

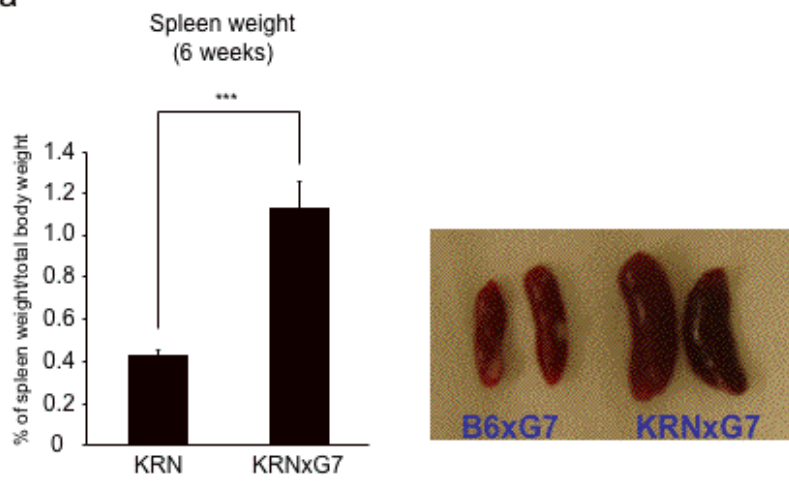


Supplementary Figures 2.2-8. HSCs from 4 month old KRNxG7 mice are not compromised.

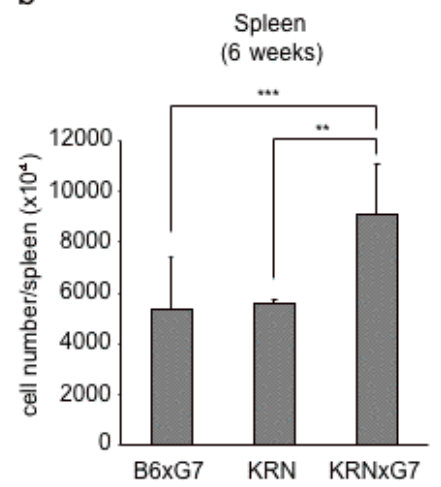
Lethally irradiated B6xG7 (CD45.1xCD45.2) recipient mice were transplanted with 1×10^6 BM cells from 4 months old B6xG7 (CD45.2xCD45.2) or KRNxG7 (CD45.2xCD45.2) mice. The figures shown are the mean percentage \pm SD of donor-derived cells in the peripheral blood (PB) 6 weeks after transplantation. (a) The percentage CD45.2+ donor derived cells is shown. (b) Donor derived mature hematopoietic cell populations are detected as CD4/CD8, B220, and Mac-1 positive populations. n=8, ***p<0.001

Supplementary Figures 2.2-9.

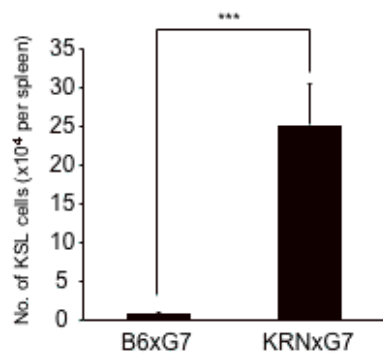
a



b



c



Supplementary Figures 2.2-9. Splenomegaly in KRNxG7 mice.

(a) KRNxG7 mice display splenomegaly. KRNxG7 spleen weight was compared to that of control mice. Left panel shows quantified mean spleen weight normalized to total body weight using KRN controls \pm SD. $n=5$. Right panel shows representative spleens from KRNxG7 and control B6xG7 to illustrate splenomegaly.

(b) The spleen of 6 week old KRN, B6xG7, and KRNxG7 were collected, treated with RBS lysis buffer and counted. The values indicate mean cell number \pm S.D. $n\geq 4$.

(c) Absolute number of KSL cells of spleen cells of B6xG7 and KRNxG7. The values indicate cell number \pm SD on the Y-axis. $n=8$ for each group, $**p<0.01$, $***p<0.001$.

Supplementary Table 2.2-1. Primer sequences used for qRT-PCR.

Gene	Forward Primer	Reverse Primer	Source
β 3 Integrin	CCACACGAGGCGTGAAGCTC	CTTCAGGTTACATCGGGGTGA	Primerbank 7949057a1
Bmi-1	ATCCCCACTTAATGTGTGCCT	CTTGCTGGTCTCCAAGTAACG	Primerbank 192203a1
Cathepsin K	GAAGAAGACTCACCAGAAGCAG	TCCAGGTTATGGGCAGAGATT	Primerbank 31982433a1
Fli3-L	AGATGCAAACGCTTCTGGAG	AGGTGGGAGATGTTGGTCTG	Primer 3
GAPDH	TGGCAAAGTGGAGATTGTTGCC	AAGATGGTGATGGGCTTCCCG	Ref (Lugus et al., 2007)
IL-7	TGAATTCCTCCACTGATCC	ACCAGTGTGGTGTGCCTTG	Ref (Ueda et al., 2005)
OPG	GGGCGTTACCTGGAGATCG	GAGAAGAACCCATCTGGACATTT	Primerbank 31543882a2
OSCAR	CCTAGCCTCATACCCCCAG	CAAACCGCCAGGCAGATTG	Primerbank 18376821a3 or 28274692a3
Osteocalcin	CTGACCTCACAGATCCCAAGC	TGGTCTGATAGCTCGTACAAG	Primerbank 13811695a1
p107	AGCTTCAGCCACTCAAAGTGTAAG	GCTCACTTGGTGCGCTTTTT	Ref (Passegue et al., 2005)
p130	TGATGGCAAAGGTCACAAAAGA	GGCCTGTGGCTGAGTCCTGTA	Ref (Passegue et al., 2005)
p18	CGAGCAGCACTCTGGACTAC	AGGCTCGGCCATTCTTTAG	Primer 3
p19	CTTCTTCACCGGGAGCTG	CAAAGCAACTGCTGGACTTC	Primer 3
p21	GTGGCCTTGTCGCTGTCTT	GCGCTTGAGTGATAGAAATCTG	Primerbank 6671726a3
p27	TCTCTTCGGCCCGGTCAAT	GGGGCTTATGATTCTGAAAGTCG	Primerbank 31542372a2
RANKL	CAGCATCGCTCTGTTCTGTA	CTGCGTTTTTCATGGAGTCTCA	Primerbank 8843823a1
Rb	TGACCTGGTAATCTCATTTTCAGC	GGGTGTTTCGAGGTGAACCAT	Primerbank 6677679a3
Runx2	TGTTCTCTGATCGCCTCAGTG	CCTGGGATCTGTAATCTGACTCT	Primerbank 20806530a2
TSLP	CTCCCCGACAAAACATTTGCC	GCCATTTCTGAGTACCGTCATT	Primerbank 10946698a3

- Primerbank: <http://pga.mgh.harvard.edu/primerbank/>
- Primer 3: <http://biotools.umassmed.edu/bioapps/primer3> www.cgi

Chapter 2.3

Conclusion and Future Directions

Summary of Chapter Two

During adulthood, hematopoietic stem cells (HSCs) are responsible for the generation of all blood cells. Under normal physiological conditions, HSCs reside mainly in specific microenvironments within bone marrow (BM) cavities, known as BM niches, where they maintain a balance between self-renewal and differentiation into more mature cells. Bone homeostasis has been proposed to have important effects on HSC maintenance under physiological states, but little is known about their relationship in pathological states. In this chapter, the relationship between HSCs and bone homeostasis in chronic inflammatory conditions is examined using the KRNxG7 transgenic mouse model. Using this model, it was found that mice with chronic inflammatory arthritis also develop osteoporosis. The overall systemic bone loss phenotype of these mice is not due to increased resorption of bone, but rather to decreased bone formation. Osteoblasts, bone forming cells, have been proposed to be one of the components that comprise the BM niches that maintain HSC homeostasis and supports B lymphopoiesis. In our studies, we have found that these arthritic mice display defective bone marrow B lymphopoiesis but, intriguingly, HSC frequency, cell cycling, and long-term functional repopulating ability were all unchanged, compared to normal mice. Our findings indicate that the bone-forming function of osteoblasts is disassociated from their ability to maintain HSCs in the bone marrow in a chronic inflammatory condition. These observations suggest that other cell types, such as endothelial cells in the bone marrow, might serve as niche cells to maintain HSC homeostasis under pathological conditions.

Hematopoietic Stem Cell Niche in KRNxG7 Mouse

We found that KRNxG7 mice, a mouse model to study human RA, exhibit an osteoporotic phenotype, due to diminished bone formation. The molecular mechanisms that affect the number and function of osteoblasts in the bone marrow of KRNxG7 mice remain unclear. Previous *in vitro* studies demonstrated that the pro-inflammatory cytokine, TNF α , inhibits the development and activity of osteoblastic cells by down-regulating bone-formation markers including alkaline phosphatase, type-I collagen, osteocalcin and *Runx2* (Centrella et al., 1988; Gilbert et al., 2002; Gilbert et al., 2005; Kuroki et al., 1994; Li and Stashenko, 1992; Nakase et al., 1997). We have found that KRNxG7 mice display a high level of TNF- α mRNA and protein in BM and serum. Thus, it is possible that high level of TNF α has an impact on the development and function of osteoblasts in the bone marrow. It will be important to assess the effects of TNF α on the osteoporotic phenotype in KRNxG7 mice. One experiment would be to use antibodies against TNF α to KRNxG7 mice before onset of the arthritic symptoms. For example, injection of antibodies to neonatal KRNxG7 mice or to pregnant female would determine if they can reduce the osteoblast defects that are seen in the tibias and femurs of adult KRNxG7 mice. Furthermore, deletion of TNF α signaling in KRNxG7 mice could give a detailed insight on the TNF α -mediated osteoporotic phenotype found in these arthritic mice.

Previous studies using genetically modified mice have demonstrated that osteoblast numbers and activity correlate positively with the number of functional

HSCs seen in the bone marrow (Calvi et al., 2003; Visnjic et al., 2004; Zhang et al., 2003). However, we revealed that, while the numbers and activity of osteoblasts in the bone marrow of KRNxG7 mice were reduced, the maintenance of the HSC population was intact. Those data do not, therefore, support the previous notion at least in this model of chronic inflammation. I propose two possibilities to explain our observations: first, the remaining osteoblasts in arthritic mice can sufficiently support the HSC maintenance; second, endothelial cells in the bone marrow could compensate the osteoblast defects and sufficiently support the HSC maintenance in KRNxG7 mice.

When we tracked green fluorescent protein (GFP) expression under the control of the osteoblast-specific Col2.3 promoter (Kalajzic et al., 2002), we found that some GFP+ cells were still present in KRNxG7 bone marrow (unpublished data). These Col2.3 GFP-expressing osteoblasts might be part of the HSC niche because conditional ablation of the population leads to a decrease in the total number of HSCs found in the bone marrow (Visnjic et al., 2004). Thus, it is possible that a limited population of osteoblast cells that remain active in KRNxG7 mice might still be sufficient to maintain HSC integrity in the bone marrow of arthritic mice. Another possibility is that osteoblast-lineage cells are multifunctional. It has been proposed in previous studies that a subset of osteoblasts, expressing N-cadherin, might serve as HSC niche cells (Arai et al., 2004; Zhang et al., 2003). Lyperi et al. showed that increasing the activity and total number of osteoblasts, without increasing the N-cadherin-expressing osteoblast subpopulation, results in excessive bone formation without increasing

the number of HSCs (Lymperi et al., 2008). This observation suggests that HSC number is correlated, not with the total number of osteoblasts, but with a subset of osteoblasts which may not be involved in bone formation. Therefore, it is possible that the remaining osteoblasts in KRNxG7 mice, possessing little or no bone-forming activity, could be sufficient to maintain HSCs in the bone marrow.

To test if the remaining osteoblasts have the ability to maintain HSCs, a possible experiment would be to cross KRNxG7 mice with Col2.3 Δ TK transgenic mice (Visnjic et al., 2004), which allows conditionally ablation of osteoblasts by ganciclovir. This cross could be used to assess whether or not HSC maintenance is disturbed by ablation of the remaining osteoblast population seen in KRNxG7 mice. If the functional HSCs are affected in KRNxG7;Col2.3 Δ TK mice, the result would suggest that the remaining osteoblasts are sufficient to serve as HSC niche cells. On the other hand, if HSC maintenance is not affected by the ablation, it would indicate that other cells play important roles in the HSC maintenance under conditions of chronic inflammation.

HSCs have been observed to closely attach to the endothelial cells in the BM and mobilized spleen, suggesting endothelial cells might serve as important components as HSC niche cells (Kiel et al., 2007; Kiel et al., 2005). It is possible that inflammatory environment might alter the ability of endothelial cells in the bone marrow of arthritic mice, and that the endothelial cells could sufficiently support HSC maintenance, compensating for the osteoblast-related defects in the KRNxG7 mice. Li et al. showed that endothelial cells, isolated from several adult, non-hematopoietic organs and co-cultured with various cytokines, supported the

expansion of hematopoietic progenitors, some of which maintained the repopulating capacity of HSCs (Li et al., 2004). Cell adhesion molecules (CAMs), such as E-selectin and vascular cell adhesion molecule-1 (VCAM-1), are involved in hematopoietic progenitor cells homing in to and repopulating the new bone marrow after bone marrow transplantation (Frenette et al., 1998; Papayannopoulou et al., 1995). These CAMs are constitutively expressed on the surfaces of endothelial cells in hematopoietically active tissues, such as adult bone marrow and fetal liver (Schweitzer et al., 1996), but not detectable on the endothelial cells of non-hematopoietic tissues under normal conditions. Interestingly, these molecules can be upregulated in conditions of inflammation or by various inflammatory cytokines (Haraldsen et al., 1996; Iademarco et al., 1995; Schweitzer et al., 1996; Strickland et al., 1997). We have found that KRNxG7 mice have enlarged spleens with accumulations of HSCs and hematopoietic progenitors, despite the fact that osteoblasts are not found in the spleen.

Therefore, it is critical to examine whether endothelial cells are responsible for the HSC maintenance in the bone marrow and for the accumulated HSCs in the spleens of arthritic mice. A possible approach to this question is to examine histological sections of spleen and tibia/femur from KRNxG7 and control mice (i.e. G7 or KRN mice), double-staining with HSC markers, such as CD150+CD41-CD48- (Kiel et al., 2005), and with endothelial cell markers, such as MECA-32 or VE-cadherin, to determine if HSCs reside in proximity to endothelial cells in these tissues. If HSCs reside more closely to the endothelial cells comparing to other cell types in KRNxG7 mice versus control mice, it would provide an insight that

the endothelial cells might play significant roles for the HSC maintenance in chronic inflammation conditions. Furthermore, determining the expression levels of CAMs such as E-selectin and VCAM-1 on the endothelial cells of the spleen and tibia/femur of KRNxG7 versus control mice would be warranted. Next, to disturb the assembly of BM endothelial cells in KRNxG7 and control mice by using VE-cadherin-specific antibody (Avecilla et al., 2004) followed by HSC analyses would further elucidate the roles of endothelial cells in HSC maintenance under normal vs. pathologic conditions. Future analyses comparing gene expressions of isolated endothelial cells from spleen and bone marrow between KRNxG7 and control mice would provide further understanding of how chronic inflammation might affect bone marrow and splenic endothelial cells to support HSC maintenance molecularly.

Moreover, the bone marrow microenvironment contains diverse populations of non-hematopoietic cells such as mesenchymal progenitors, osteoblasts, osteoclasts, fibroblasts, reticular cells, adipocytes, and endothelial cells. Future studies will require further determining the involvements of these cells or even unidentified cell types in supporting HSC maintenance in the bone marrow of KRNxG7 mice.

References

- Arai, F., Hirao, A., Ohmura, M., Sato, H., Matsuoka, S., Takubo, K., Ito, K., Koh, G. Y. and Suda, T. (2004). Tie2/angiopoietin-1 signaling regulates hematopoietic stem cell quiescence in the bone marrow niche. *Cell* **118**, 149-61.
- Avecilla, S. T., Hattori, K., Heissig, B., Tejada, R., Liao, F., Shido, K., Jin, D. K., Dias, S., Zhang, F., Hartman, T. E. et al. (2004). Chemokine-mediated interaction of hematopoietic progenitors with the bone marrow vascular niche is required for thrombopoiesis. *Nat Med* **10**, 64-71.
- Calvi, L. M., Adams, G. B., Weibrecht, K. W., Weber, J. M., Olson, D. P., Knight, M. C., Martin, R. P., Schipani, E., Divieti, P., Bringham, F. R. et al. (2003). Osteoblastic cells regulate the haematopoietic stem cell niche. *Nature* **425**, 841-6.
- Centrella, M., McCarthy, T. L. and Canalis, E. (1988). Tumor necrosis factor-alpha inhibits collagen synthesis and alkaline phosphatase activity independently of its effect on deoxyribonucleic acid synthesis in osteoblast-enriched bone cell cultures. *Endocrinology* **123**, 1442-8.
- Frenette, P. S., Subbarao, S., Mazo, I. B., von Andrian, U. H. and Wagner, D. D. (1998). Endothelial selectins and vascular cell adhesion molecule-1 promote hematopoietic progenitor homing to bone marrow. *Proc Natl Acad Sci U S A* **95**, 14423-8.
- Gilbert, L., He, X., Farmer, P., Rubin, J., Drissi, H., van Wijnen, A. J., Lian, J. B., Stein, G. S. and Nanes, M. S. (2002). Expression of the osteoblast differentiation factor RUNX2 (Cbfa1/AML3/PeBP2alpha A) is inhibited by tumor necrosis factor-alpha. *J Biol Chem* **277**, 2695-701.
- Gilbert, L. C., Rubin, J. and Nanes, M. S. (2005). The p55 TNF receptor mediates TNF inhibition of osteoblast differentiation independently of apoptosis. *Am J Physiol Endocrinol Metab* **288**, E1011-8.
- Haraldsen, G., Kvale, D., Lien, B., Farstad, I. N. and Brandtzaeg, P. (1996). Cytokine-regulated expression of E-selectin, intercellular adhesion molecule-1 (ICAM-1), and vascular cell adhesion molecule-1 (VCAM-1) in human microvascular endothelial cells. *J Immunol* **156**, 2558-65.
- Iademarco, M. F., Barks, J. L. and Dean, D. C. (1995). Regulation of vascular cell adhesion molecule-1 expression by IL-4 and TNF-alpha in cultured endothelial cells. *J Clin Invest* **95**, 264-71.
- Kalajzic, I., Kalajzic, Z., Kaliterna, M., Gronowicz, G., Clark, S. H., Lichtler, A. C. and Rowe, D. (2002). Use of type I collagen green fluorescent protein transgenes to identify subpopulations of cells at different stages of the osteoblast lineage. *J Bone Miner Res* **17**, 15-25.
- Kiel, M. J., Radice, G. L. and Morrison, S. J. (2007). Lack of evidence that hematopoietic stem cells depend on N-cadherin-mediated adhesion to osteoblasts for their maintenance. *Cell Stem Cell* **1**, 204-17.
- Kiel, M. J., Yilmaz, O. H., Iwashita, T., Yilmaz, O. H., Terhorst, C. and Morrison, S. J. (2005). SLAM family receptors distinguish hematopoietic stem and progenitor cells and reveal endothelial niches for stem cells. *Cell* **121**, 1109-21.
- Kuroki, T., Shingu, M., Koshihara, Y. and Nobunaga, M. (1994). Effects of cytokines on alkaline phosphatase and osteocalcin production, calcification and calcium release by human osteoblastic cells. *Br J Rheumatol* **33**, 224-30.

- Li, W., Johnson, S. A., Shelley, W. C. and Yoder, M. C.** (2004). Hematopoietic stem cell repopulating ability can be maintained in vitro by some primary endothelial cells. *Exp Hematol* **32**, 1226-37.
- Li, Y. P. and Stashenko, P.** (1992). Proinflammatory cytokines tumor necrosis factor-alpha and IL-6, but not IL-1, down-regulate the osteocalcin gene promoter. *J Immunol* **148**, 788-94.
- Lymperi, S., Horwood, N., Marley, S., Gordon, M. Y., Cope, A. P. and Dazzi, F.** (2008). Strontium can increase some osteoblasts without increasing hematopoietic stem cells. *Blood* **111**, 1173-81.
- Nakase, T., Takaoka, K., Masuhara, K., Shimizu, K., Yoshikawa, H. and Ochi, T.** (1997). Interleukin-1 beta enhances and tumor necrosis factor-alpha inhibits bone morphogenetic protein-2-induced alkaline phosphatase activity in MC3T3-E1 osteoblastic cells. *Bone* **21**, 17-21.
- Papayannopoulou, T., Craddock, C., Nakamoto, B., Priestley, G. V. and Wolf, N. S.** (1995). The VLA4/VCAM-1 adhesion pathway defines contrasting mechanisms of lodgement of transplanted murine hemopoietic progenitors between bone marrow and spleen. *Proc Natl Acad Sci U S A* **92**, 9647-51.
- Schweitzer, K. M., Drager, A. M., van der Valk, P., Thijsen, S. F., Zevenbergen, A., Theijssmeijer, A. P., van der Schoot, C. E. and Langenhuijsen, M. M.** (1996). Constitutive expression of E-selectin and vascular cell adhesion molecule-1 on endothelial cells of hematopoietic tissues. *Am J Pathol* **148**, 165-75.
- Strickland, I., Rhodes, L. E., Flanagan, B. F. and Friedmann, P. S.** (1997). TNF-alpha and IL-8 are upregulated in the epidermis of normal human skin after UVB exposure: correlation with neutrophil accumulation and E-selectin expression. *J Invest Dermatol* **108**, 763-8.
- Visnjic, D., Kalajzic, Z., Rowe, D. W., Katavic, V., Lorenzo, J. and Aguila, H. L.** (2004). Hematopoiesis is severely altered in mice with an induced osteoblast deficiency. *Blood* **103**, 3258-64.
- Zhang, J., Niu, C., Ye, L., Huang, H., He, X., Tong, W. G., Ross, J., Haug, J., Johnson, T., Feng, J. Q. et al.** (2003). Identification of the haematopoietic stem cell niche and control of the niche size. *Nature* **425**, 836-41.